The Pennsylvania State University

The Graduate School

Department or Energy and Mineral Engineering

PREDICTION OF WATER CONE FORMATION IN A NATURALLY FRACTURED RESERVOIR WITH AQUIFER DRIVE -AN ARTIFICIAL EXPERT APPLICATION

A Thesis in

Energy and Mineral Engineering

by

Chang Eon Bae

© 2015 Chang Eon Bae

Submitted in Partial Fulfillment
of the Requirements
for the Degree of

Master of Science

August 2015

The thesis of Chang Eon Bae was reviewed and approved* by the following:

Turgay Ertekin

Head, John and Willie Leone Family Department of Energy and Mineral Engineering
Professor of Petroleum and Natural Gas Engineering
George E. Trimble Chair in Earth and Mineral Sciences
Thesis Advisor

Zuleima T. Karpyn

Associate Professor of Petroleum and Natural Gas Engineering;
Quentin E. and Louise L. Wood Faculty Fellow in Petroleum and Natural Gas Engineering

Jeremy M. Gernand

Assistant Professor of Industrial Health and Safety

Luis F. Ayala H.

Associate Professor of Petroleum and Natural Gas Engineering;
Associate Department Head for Graduate Education

*Signatures are on file in the Graduate School

ABSTRACT

In the recent past, highly productive reservoirs found are naturally fractured and have a complex geologic setting. Typically in a geological situation where a nearby strong water drive exists, production performance and ultimate recoveries of the reservoir are comparatively higher. A strong water drive often results in high production, but may pose difficulties in production due to significant water influx. Hence, an accurate water influx predictive model helps in lowering the uncertainty and reducing the risk.

This study attempts to use Artificial Expert Systems to predict water coning behavior around horizontal wells in naturally fractured reservoirs with a strong water drive. By using a numerical simulator, various reservoir conditions and scenarios are simulated. With the help of these simulated datasets, an artificial expert system based tool is developed to enable engineers to predict water coning behavior in a given horizontal well instantaneously.

In the first part, a tool for predicting various production data is developed. Input datasets of reservoir properties, well data and output datasets are provided to Artificial Neural Network (ANN). Then, the ANN based model predicts outputs for testing datasets. The targets of this module are cumulative oil production, oil production rate, cumulative water production, and water production rate. Various architectures are tested and the optimum architecture with average error less than 20% is established.

In the second part, the module developed predicts water saturation data. For training the ANN, water saturation data from numerical simulator is used. Thereby the tool will be able to predict the water saturation in horizontal well-located planes. The targets are laterally arrayed water saturation in the center cross section of the reservoir. Neural network architectures are generated depending on depth of the reservoir and production time. Also, randomly generated input datasets of reservoir properties, well data are given to inputs of the ANN.

Lastly, a Graphical User Interface (GUI) is developed as a part of this study to incorporate all the above mentioned networks that will aid an engineer to predict water coning. There are two groups in GUI: single porosity model and dual porosity model. Each group has its subgroups: predicting oil production data, water production data, and water saturation data. Examples and input data criteria are presented at the end to help a user navigate through the GUI.

TABLE OF CONTENTS

LIST OF FIGURES

LIST OF TABLES

NONMENCLATURES

$acre$	Reservoir drainage area, acre
B_o	Oil formation volume factor, RB/STB
Φ	Porosity
Φ_m	Matrix porosity
Φ_f	Fracture porosity
r_o	Oil density, lb/ft^3
r_w	Water density, lb/ft^3
μ_w	Water viscosity, cp
d_f	Fracture spacing, ft
d_{owc}	Distance from well to oil-water contact, ft
F	Dimensionless function
k_h	Horizontal permeability, md
k_h	Vertical permeability, md
k_m	Matrix permeability, md
k_{hf}	Fracture horizontal permeability, md
k_{hf}	Fracture vertical permeability, md
k_{rw}	Water relative permeability, md
k_{row}	Oil relative permeability, md
l_{wp}	Length of well perforation, ft
L	Horizontal well length, ft
h_t	Reservoir thickness, ft
p_i	Initial reservoir pressure, psi
p_c	Capillary pressure, psi
p_{sf}	Bottom hole pressure, psi
psi	Pounds per square inch
q	Fluid flow rate, STB/day
q_o	Critical Rate, STB/day
S_w	Water saturation
y_e	Half drainage length(perpendicular to the well), ft
wd	Width of grid block (x-axis, y-axis)

ACKNOWLEDGEMENTS

Above all, I would like to express my sincere appreciation to my academic advisor, Dr. Turgay Ertekin for his invaluable guidance, patience, understanding, and support throughout my graduate study years. With his deep insight and knowledge, this work has been successful. I also thank my thesis committee members, Dr. Zuleima Karpyn, and Dr. Jeremy Gernand for their contributions in reviewing and recommending some suggestions on my thesis work.

I am very thankful to my friends in the Department of Energy and Mineral Engineering, Chong hyun Ahn, Kyoung Jae Im, Ju Hyun Cho, and Kyung Jin Yoo, Vaibhav Rajput and Sarath Ketineni for their support, guidance, and mentoring to keep up with my master study. Also, special gratitude goes to my company, Korea Gas Corporation for the financial support, and allowing me to study at the Pennsylvania State University.

Lastly, I always thank all of my family members for having done great job without any problems in U.S. They have been in hard times to get used to totally new environment here. Their well-being in U.S. makes my graduate study possible. In addition, I appreciate my wife, Hye suk Son who has been supportive to take good care of my family.

Chapter 1

Introduction

For years, significant amount of oil has been produced from naturally fractured reservoirs in many countries. The characteristics of these reservoirs are defined by high permeability in the fractures and low inter-granular porosity. Ultimate production from these reservoirs is sensitive to production rates. High production rates lead to water encroachment from the bottom water aquifers. In an extreme case, water influx results in formation of water cone, and hence early breakthrough into production wells.

In the past, highly productive petroleum reservoirs have exhibited strong water drive from aquifers. Water-drive reservoirs are considered beneficial in terms of enhanced oil recovery. Once reservoir is put on production, it typically loses its pressure, called depletion. It is expected that water-drive helps to improve oil recovery by providing pressure support to reservoirs.

However, water drive reservoirs have their drawbacks. When a high water cut is encountered, the productivity of the producing well significantly gets worse with time. Moreover, it is environmentally unviable and economically expensive to deal with water produced from the well. Thus, it is essential to know whether water cresting will take place or if it does, when would it affect the production.

Water coning is critically sensitive to production rate. More precisely, it can be referred to wellbore phenomenon. Pressure drawdown occurs significantly near the wellbore, then a highly water saturated distribution referred to as a water cone forms upward to the well perforation, depending on relative viscous and gravitational forces around the well. With this phenomenon related to pressure drawdown near wellbore, water tends to flow into the perforation.

To minimize the formation of water cones as well as maximize the production efficiency, the horizontal wells are drilled. Implementation of horizontal wells is expected to see lesser pressure drawdown than that of vertically drilled wells.

Chapter 3 presents a background of water coning in naturally fractured reservoirs, and explanation of ANN methodology. Chapter 4 has literature review of water coning in naturally fractured reservoirs. In chapter 5, problem statement of this study and work flow is presented. Chapter 6 discusses about the process of data generation for ANN based model for water cone prediction. Chapter 7 contains detailed explanation of ANN development procedures. Chapter 8 discusses the results from ANN predictions, and summarizes this study. Graphic User Interface (GUI) developed as a part of this study is presented in Appendix A.

To perform this study, CMG [1] IMEX [2] (version 2012, 10) is extensively used for generating working datasets through numerical reservoir simulation. MATLAB[3] (version 2013) Neural Network Toolbox is used to create the models for this study.

[1] CMG: **C**omputer **M**odeling **G**roup

[2] IMEX: Three Phase Black Oil Reservoir Simulator

[3] MATLAB: **MA**trix **LAB**oratory, a multi-paradigm numerical computing environment

Chapter 2

Background

2.1 Water Coning

It is highly likely in a condition of hydrocarbon reservoir with a strong water-drive, that the wells will exhibit water coning when subject to long period of production. Water coned curve is represented by the shape of high water saturation area. When producing at high production rates, water coning occurs in a more pronounced manner. With water coning, water production accelerates much faster than ever. In the end, water production cannot be controlled anymore. The term coning or cresting is used interchangeably. Typically coning is used in a vertical well, cresting in a horizontal well. Figure 2.1 is an example to demonstrate coning (or cresting) in reservoirs with water drive.

The following aspects are important in understanding the water coning behavior; good understanding of geological aspects of the reservoir, water cut history profile, reservoir pressure changes, GOR (gasoil ratio) data, and material balance analysis. Diagnostic approaches are necessary to identify possible water-drive, but they are time and cost intensive.

Mobility ratio and aspect ratio of the drainage area are some of the dominating features responsible for water coning phenomenon. Tendency of coning (for water and gas) originates from various petro physical properties. In general, coning is proportional to the fluid viscosity, but inversely proportional to density difference. And, the difference of densities between oil and gas is larger than that between water and oil. Thus, it can be implied that gas coning has less tendency than water coning. However, viscosity of gas is far lower than that of oil. Under the same pressure drawdown, gas flow rate is higher than water. Thus, it can be concluded that density and viscosity meet the equilibrium at some points.

In addition, high permeability reservoirs have less coning phenomenon than low permeability reservoirs. Usually, heavy oil reservoirs tend to have high permeability zones. Also, high permeability reservoirs have smaller pressure drops near the wellbore than low permeability reservoirs. To the contrary, naturally fractured reservoirs that have high vertical fractures show high tendency of water or gas coning. It is because water or gas flows through vertical fractured matrix, not through low matrix permeability that is hard for water to penetrate into. Thus, in a conventional oil reservoir with aquifer at the bottom, the perforation of wells should be in the center of the oil pay zone. It is because that once unwanted gas production begins, it is very hard to stop gas production and the gas production dominates the oil production. Even worse cases, producing well cease to produce oil.

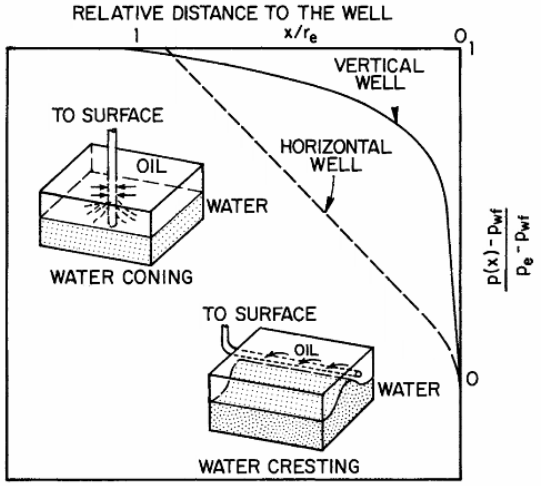

Figure-2.1 Comparison of Pressure drawdown of vertical wells and horizontal wells (Joshi.S.D, 2011)

Several works have concluded that low production rate can prevent coning behavior. Critical rate is the maximum rate of oil production that can avoid coning effect of water or gas. Using proper experimental analysis and analytical models, obtaining a critical rate is the key to

coning problem solution. Several researchers have come up with various correlations for coning problems. Those correlations have shown that critical rate mostly relies on those petro physical parameters; oil density disparity from water (or gas) density, oil viscosity, oil permeability (vertical or horizontal), ratio of well perforation to pay thickness, so called aspect ratio. The following three correlations are widely used to predict the critical oil flow rate in horizontal wells.

Table-2.1 Horizontal well critical rate correlations (Joshi, 2001)

Chaperon Method $q_o = 4.888 \times 10^4 \frac{L}{y_e} \Delta\rho \frac{(k_h h^2)}{\mu_o B_o} F \quad for\ 1 \leq \alpha'' < 70\ and\ 2y_e < 4L$ $\alpha'' = (\frac{ye}{h})\sqrt{k_v/k_h}$
Efros Method $q_o = \frac{4.888 \times 10^4\, \Delta\rho L}{[2y_e + \sqrt{(2y_e)^2 + \left(\frac{h^2}{3}\right)}\,]} \frac{(k_h h^2)}{\mu_o B_o}$
Giger and Karcher et al. Method $q_{o,v} = \frac{1.535 \times 10^{-3}(\rho_o - \rho_g)(k_h)(h^2 - (h - l_v)^2)}{\mu_o B_o \ln(\frac{r_e}{r_w})}$ $\frac{q_{o,h}}{q_{o,v}} = \frac{(h^2 - (h - l_h)^2)\ln(\frac{r_e}{r_w})}{(h^2 - (h - l_v)^2)\ln(\frac{r_e}{r_w'})}$

2.3 Horizontal Well

A horizontal well is a well that is horizontally drilled to the target location of the hydrocarbon reservoir. It is parallel to the reservoir's pay zone, so that lateral section of the well remains within the petroleum formation. It is known that horizontal wells extend horizontally up to 8,000 feet long. The horizontal well is beneficial in terms of increased wellbore surface area compared to vertically drilled wells. However, drawbacks are that a single horizontal well can cost about millions of dollars.

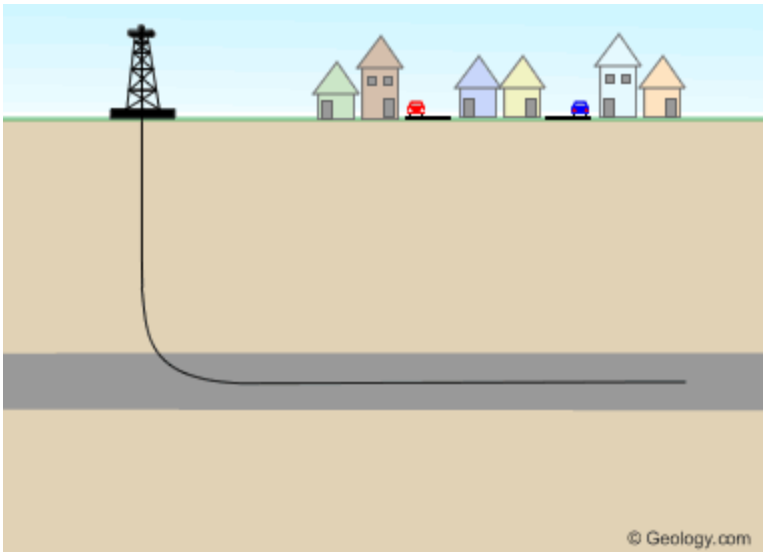

Figure-2.2 Schematic of a horizontal well (Geology.com, 2015)

2.2 Naturally Fractured Reservoir

Knebel et al. (1956) claims that until 1956, 41% of the hydrocarbon reserves belong to naturally fractured reservoirs. This indicated the relevance of studying naturally fractured reservoirs is in the petroleum industry. Naturally fractured reservoirs differ from conventional hydrocarbon reservoirs in terms of geometrical characteristics and deposition. Vugs and interconnecting channels exist in fractures and openings, in which the fine cracks create blocks that play a role of reservoirs. Low permeable porous media contribute to the storage, and transport of fluids is enabled via the fractures that have low storage capacity and high permeability. Regardless of how low average permeability is, naturally fractured reservoirs show higher effective permeability than matrix permeability. In other words, although matrix permeability is quite low, the fluid flows from matrix to fracture due to the characteristics of fracture to be able to act as conduit for flow.

Pirson (1953) coined two porosity systems presenting the pressure transient models for well test data of dual porosity systems. Barenblatt et al. and Zheltov (1960) developed analytical models for naturally fractured reservoirs to describe the fluid transport and storage in fractured reservoirs. Among those analytical models, the dual porosity model that has intermediate matrix permeability, is deemed as classic for naturally fractured reservoirs. To a large extent, the dual porosity system has two sub-domains: fracture and matrix system. One of the prominent analytical models for dual porosity systems is the model of Warren and Root (1963).

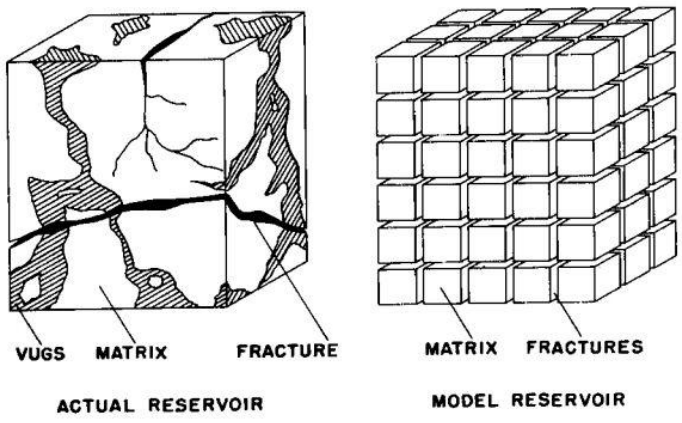

Figure-2.3 Model of a naturally fractured reservoir (WarrenRoot, 1963)

Warren and Root introduced two parameter definitions to explain fluid transport in naturally fracture reservoirs. Inter-porosity flow coefficient (or transmissivity,λ) and storativity ratio (ω). The coefficients are mathematically expressed as following:

$$\lambda = \alpha \frac{k_m}{k_f} \mathrm{r}_w{}^2, \text{ where, } \alpha = \frac{4j(j+2)}{L^2}$$

$$\omega = \frac{\phi_f C_f}{\phi_f C_f + \phi_m C_m}$$

The Inter-porosity flow coefficient is an indicator of how fluid flows from matrix to fracture. In α parameter, L is a characteristic dimension of a matrix block and j is the number of normal sets of planes limiting the less-permeable medium (Warren and Root, 1963). And the storativity is a ratio of how much fracture storage capacity is in the naturally fractured reservoir.

When production takes places, the fluid in the fractures is depleted. Then pressure difference is created between micropore and macropore structures. This pressure difference acts

as a driving force to draw the fluid from matrix to fracture. To explain fracture network models, it is categorized as dual porosity model and dual permeability model.

Dual porosity model is that assuming that matrix acts as fluid storage medium and fractures act as flow path of fluid into wellbore. Dual porosity models defined in literature comprise of standard dual porosity model, multiple interacting continua model, and vertical refinement model. Contrary to the dual porosity model, the dual permeability model has fluid flow and heat distribution both on matrix and fracture. In the dual permeability model, each matrix block is linked together with neighboring fractures. Figure 2.3 shows standard dual porosity and dual permeability models.

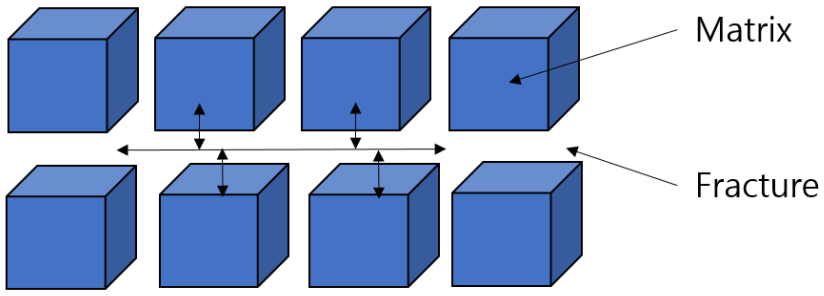

Dual Porosity Model

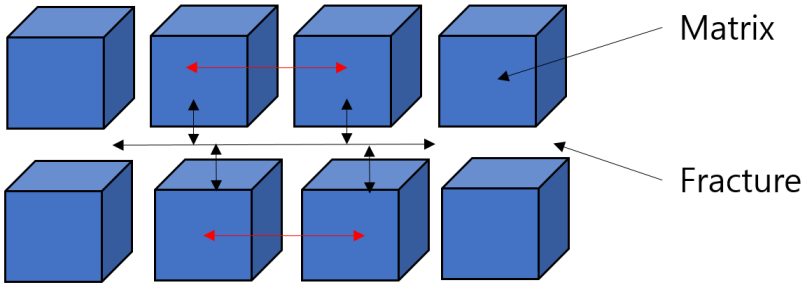

Dual Permeability Model

Figure-2.4 Comparison of dual porosity and dual permeability model

2.4 Artificial Neural Network

Artificial neural networks (ANN) are mathematically formed networks that act similarly like biological nerve systems for information, recognition, and learning processes. ANN consists of a pool of simple data processing units with enormous number of weights and biases transferring and receiving signals to each neuron. ANN is deemed to be a powerful tool for prediction, pattern recognition, abstraction, and interpretation of sporadic data. Since ANN doesn't require any order, structure of computing elements, it can be used to solve complicated problems just like human brains. Graupe (2007) claimed that ANN solves complex, mathematically ill-defined, non-linear or stochastic problems.

Warren Mcculloch and Walter Pitts (1943) introduced the first design of ANN. Hebb (1949, 1961) and Rosenblatt (1957) showcased Mark I perceptron, a successful neurocomputer, specialized in pattern recognition. That network was one layered. From that, in 1960s, multi-layered neural network was derived. Werbos (1974) introduced a back-propagation algorithm for three layered perceptron network. Until 1980's, the application of the multi-layer-perceptron network has not been widespread due to unstable network issues. Hopfield network in 1982 had one layer that all the neurons are linked to each other. Later on, a different Hopfield network was developed resulting in development of the Boltzmann machine. Since 1980, various kinds of network had bloomed. Broomhead and Lowe (1988) coined Radial Basis Function networks. Kohonen (1982) introduced the Self-Organizing Map (SOM).

Changes in external and internal environment increase adaptability of animals, and what makes that possible is their nerve system to react those changes. In the nerve systems, a number of elements are interconnected, formed working together. The information is transferred and processed through nano-sized units such as a body, axon and dendrites (Yegnanarayana, 1999). There have been many mathematical models for human brains developed. In reality, most are

different from one after another. Regardless of these facts, they have similar features in common, that is, a unit of a neural network is the processing unit (Braspenning, Thuijsman F, Weijters, A. J. M.M, 1995).

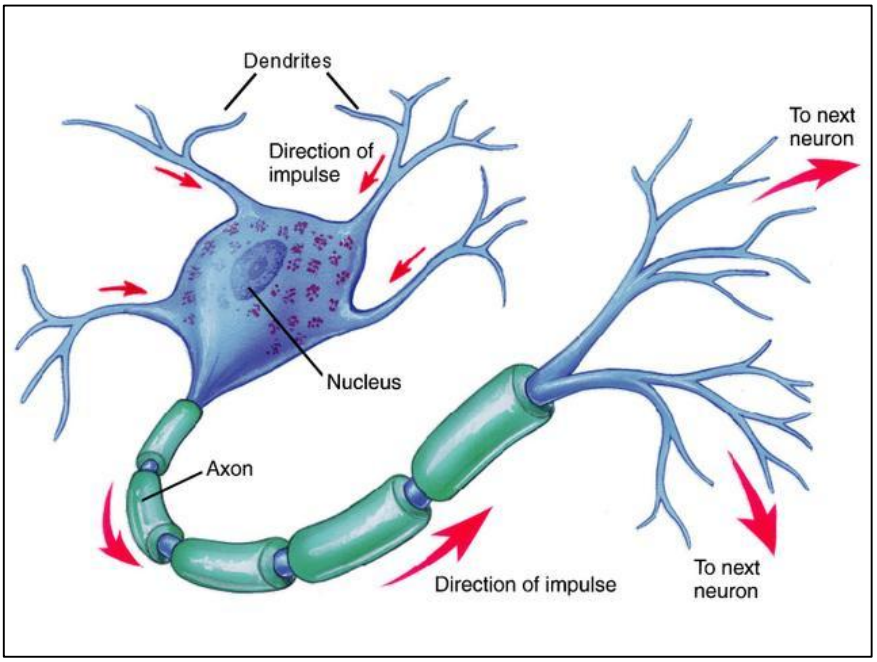

Figure-2.5 Anatomy of a Neuron (Learnfast For Schools , 2014)

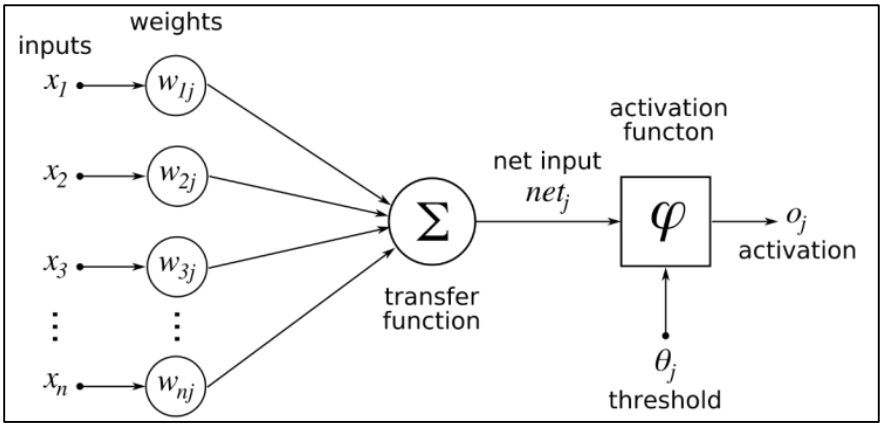

Figure-2.6 Artificial Neural Net (Creative Commons license, 2012)

Each neuron has a sets of summation (or integration) of an input weight, and bias represented as x, w, and b. Each also has an activation function (or transfer function) that controls the magnitude of outputs to make the neural network stable. Range of transfer functions is typically between -1 and 1 or 0 and 1. Different combinations of activation functions and structures may be able to enhance the efficiency of the neural network. Each inputs weighted, and biased are integrated before being fired out to the next layers, hidden layers or output layers such that the output becomes either another input or output. Typically, activation functions are all the same to all the neurons in hidden layers (Fausett, 1994).

Integration function are M-P neuron, quadratic, spherical, polynomial functions. Mostly, M-P neurons are used. Activation neurons are M-P neurons, hard limiter (threshold function), ramp function, unipolar sigmoid function, bipolar sigmoid function and etc. Activation functions is one of the most important features of ANN. Performance of ANN can be dependent on choosing suitable activation functions. Followings are activation functions described earlier.

Linear function: so called, identity function, the input units obviously uses linear function. Linear function changes input values into output values ranging from -1 and 1.

$$g(x) = x$$

Binary function: The output is limited to either o or 1. Binary function is also known as threshold or Heaviside function. Commonly binary function is used in single layer neural network.

$$g(x) = 0 \quad when\, x \geq \theta \quad or \quad 1 \quad when\, x \leq \theta$$

Log sigmoid function: in back-propagation neural network, log sigmoid function is also very useful since training process requires less computation load. As shown, it is applicable when output are between 0 and 1.

$$g(x) = \frac{1}{1 + e^{-x}}$$

Bipolar sigmoid function: Similar to log sigmoid function. This function is used for outputs that ranges between -1 and 1.

$$g(x) = \frac{1 - e^{-x}}{1 + e^{-x}}$$

The fastest training function is Levenberg-Marquardt (LM) algorithm. Bayesian Regularization algorithm is quasi-Newton training method, also known as fast. Although two algorithms are fast, they have a tendency to less efficient to deal with huge networks that consists of thousands of weights and biases. LM algorithm, however yields better performance for non-linear regression problems than for pattern recognition problems. When having large datasets and networks, Scaled Conjugate Gradient (SCG) algorithm performs well since it requires less memory than LM algorithm. There are several training algorithms in ANN. Those are followings.

Table-2.2 Training algorithms and their command in MATLAB

Function Algorithm	MATLAB training function
Levenberg-Marquardt	trainlm
Scaled Conjugate Gradient	trainscg
Bayesian Regularization	trainbr

Back-propagation is one of the most widely used training algorithm for training multiple-layered neural network. The term, back-propagation stems from evaluation of errors from the derivatives of weights and biases. The back propagation networks has following features: the network has more than one hidden layers, and all neurons within the layers interconnected to the next layers (maybe other hidden layers or the output layer); there are no-connections between non-successive layers (A.J. M.M. Weijters, G. A. J. Hoppenbrouwers, 1995).

However, there are some drawbacks on backpropagation networks. Convergence through backpropagation learning is very slow. Particularly, when networks have many hidden layers and neurons, learning rate is much slow. But this is not an issue the advances in modern computing technology that are available today. Backpropagation algorithm often gets stuck with local minima.

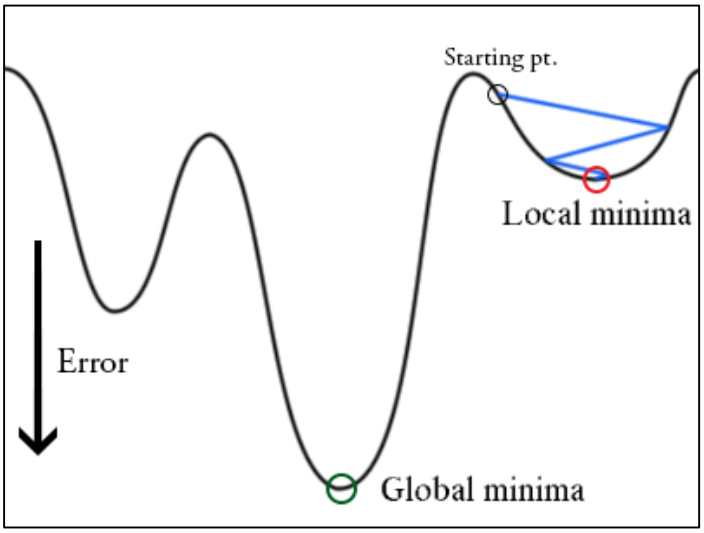

Figure-2.7 Gradient struck to Local minima (TengYifei, 2014)

There is no absolute rule of how to structure the network. One may wonder such things like how many hidden layers should be between input and output layer, how many neurons

should be in hidden layers, which of activation functions should be added, etc. The followings are generally accepted discussions to build robust result-yielding networks.

Practically, most problems rarely require more than two hidden layers networks. In a case that requires more than two hidden layers in the networks, a network applied with a single hidden layer practically performs better than that with two or more. To a large extent, there are two reasons that can explain the rationale behind number of hidden layers. First, in backpropagation training algorithms, most of them are based on calculation of gradients. Complex networks often result in large errors. In some cases, local minima make it difficult for the network to find global minima. Within a few iterations, the network finds the best performance, but with increasing number of iterations, the networks fall into the local minima thereby resulting in an over-fit. In some cases, however, the network with more than two hidden layers may perform well in terms of learning a non-linear relation in specific problems. In general, it is a good idea to start with one hidden layer. As indicated in prior works, when a single-hidden layered network does not work as desired, it may call for a more complicate network.

It is known that using large number of neurons result in over-fitting while fewer number of neurons may cause under-fitting. The appropriate numbers rely on several circumstances, numbers of inputs, outputs neurons, training algorithms, complexity of the network, etc. The following are few existing "rule of thumbs" to select the number of hidden nodes.

- $m \in [l, n]$ - between the input layer size and output layer size
- $m = \frac{2(l+n)}{3}$ - two third of the input layer size plus the output layer size
- $m < 2l$ - less than twice the input layer size
- $m = \sqrt{l \cdot n}$ - squared input layer size multiplied by output layer size

To find the best numbers of nodes, so-called “trial and error” are practically imposed, although that method requires lots of time. The recommended approach would be “smaller and bigger” selection of neurons. First, one starts with minimum numbers of neurons, then record performance, then increase the neurons. When comparing those records, one can figure out how many neurons can be the optimal one for specific problems. Although it is time-intensive, this process works.

Chapter 3

Literature Review

Muskat, M. and Wyckoff (1935) first coined the term “water coning” and presented related physics through an analytical development. Muskat, M. and Wyckoff analyzed the phenomenon by using a vertical well in a homogeneous sandstone reservoir. Later on, many researchers worked on extending the results of Muskat and Wyckoff on parameters on water coning and their correlations in vertical wells. Yang (1991) analyzed the water coning behavior for vertical and horizontal wells. The correlations are based on flow equations and validated through numerical simulations. These resulted in correlations of critical rate, breakthrough time and water-oil ratio with breakthrough. Van Golf-Racht, T. D. (1994) extended their investigation to the coning criteria in a fracture reservoir comprising of both oil and water production, not limited to prevention of water production.

Al-Alfaleg and Ershaghi (1993) found empirical correlation for calculating breakthrough time and critical rate for homogeneous single porosity reservoirs. This work is not applicable to naturally fractured systems. However, they found that it is applicable for homogeneously fractured reservoir systems to estimate breakthrough time, if bulk fracture properties are pre-attained via well-testing data. They observed two different paced cones form in a naturally fractured reservoir; a fast forming cone in the fractures and a slow one in the matrix.

Golf-Racht and Sonier (1994) concluded that it is not feasible to apply the critical rate defined by Muskat in a naturally fractured reservoir. They concluded that the vertical permeability originated from a high vertical fracture density is a key component that impacts the formation of water cones in a naturally fractured reservoir.

Bahrami et al. (2004) investigated correlations of naturally fractured reservoirs through simulations. They found that increase in porosity in both matrix and fracture slows down breakthrough, but results in high water cuts. Specifically, breakthrough is more sensitive to fracture porosity, and water cut is to matrix porosity. They also found that matrix block size in numerical simulation of fractured reservoirs does not influence breakthrough time and water cut.

Namani et al. (2007) found that various fractured reservoir properties, net pay thickness, perforation length, horizontal and vertical fracture permeability, mobility, storativity, conductivity, and production rate influence water coning. They claimed that fracture patterns are more crucial than fracture spacing, skin factor, and aquifer potential. Also they concluded breakthrough is delayed by high horizontal permeability that prevents water from forming a cone.

Several researchers have utilized Artificial Neural Networks to predict the water saturation from the well logs data. Shokir (2004) developed ANN for predicting water saturation in a shaly formation using core data and well log data. Using wire-line logs and core data in sandstone formations, prediction tool based on ANN was developed to predict water saturation.

Chapter 4

Problem Statement

Numerical simulations are based on physics and deterministic problem solving. It is necessary to find the right solutions to engineering problems, needless to say accurate in terms of physics, however they are time-consuming and cost intensive. Water coning is an undesirable production situation. A study for water coning in a naturally fractured reservoir can help engineer inform production issues involved. To help understand this phenomenon, the following questions need to be answered.

1. How long can a well produce oil without water coning?
2. When does water cone reach the wellbore?
3. Given the reservoir parameters, what would the production be?
4. Can water coning be predicted for a given set of reservoir parameters?

To answer those questions, this study is focused on development of an expert system that can predict water coning phenomenon in reservoirs. The artificial neural network based expert system is a proxy model that is trained by many reservoir scenarios. The model based on artificial intelligence could accurately capture the water coning phenomenon and production performance in single and dual porosity systems. The model can also reduce computational and manpower overheads as a screen tool for evaluating efficiency of various completion scenarios. The following figures explain the envisaged methodology.

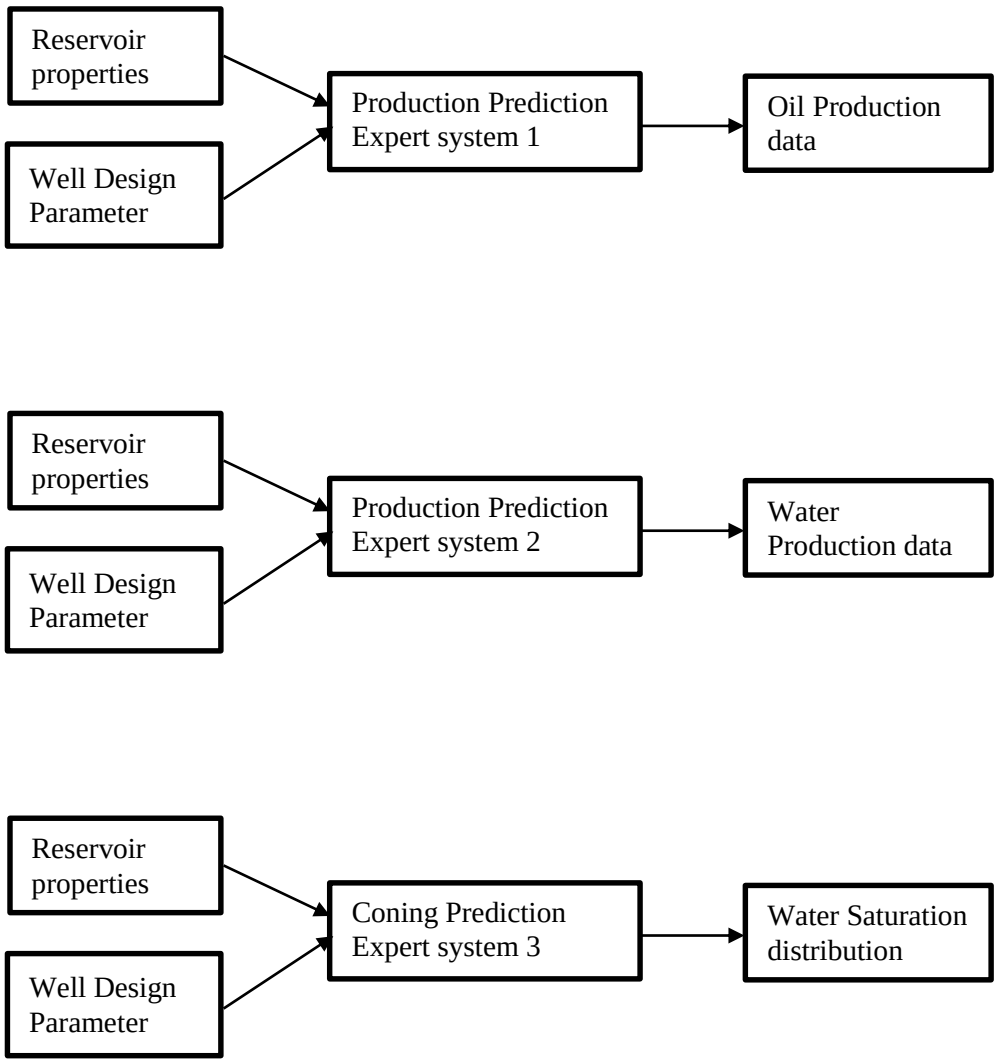
Reservoir properties
Well Design Parameter
Production Prediction Expert system 1
Oil Production data
Reservoir properties
Well Design Parameter
Production Prediction Expert system 2
Water Production data
Reservoir properties
Well Design Parameter
Coning Prediction Expert system 3
Water Saturation distribution

Chapter 5

Methodology

This chapter presents how datasets for training and testing are generated and used. Input datasets are created through programming scripts that result in input data. IMEX, CMG is used to yield water saturation values for each grid block and production data for the specified production duration.

5.1 Assumption for Reservoir Discretization

This study deals with water coning phenomenon both in a conventional single porosity reservoir and in a naturally fractured (dual porosity) reservoir. Certain assumptions need to be made in performing this analysis. Assumptions of single porosity model are provided in table A.1 in Appendix. Reservoir description of the dual porosity model considered is outlined as follows.

The reservoir is a two phase (oil and water), homogeneous, anisotropic, square shaped, with a strong bottom-water drive from an aquifer. Number of reservoir grid blocks are 25 in x and y direction and 15 in z direction. The aquifer is located at bottom of the reservoir, and is assumed to be infinitely large. Reservoir under consideration is two phase. Hence, there is no gas cap on the top of the reservoir. Depth of reservoir is 5000 ft. Reservoir pressure declines slowly because of constant pressure support from the aquifer. A constant value of bubble point pressure is assumed. Compressibility of matrix and fracture is assumed to be identical. Water formation volume factor remains constant through the production period. The reservoir is produced at isothermal conditions. Relative permeability curves are set to be constant in both the models. In dual porosity model, there are two different relative permeability curves for matrix and fracture

respectively. Capillary pressures are assumed to be prevalent forces in matrix, not so significant in fractures. Matrix permeability(k_m), and fracture spacing (d_{xf}) is assumed to be isotropic. Fracture permeability(k_f) in x and y direction are identical, but in z direction it is varied case by case. Permeability in horizontal direction (x, y) is set to be less than that in vertical direction. Other key reservoir properties and reservoir conditions are indicated in tables 5.1 through 5.4. Permeability assumptions are listed below.

$$k_{xf} = k_{yf} \neq k_{zf},\ k_{xm} = k_{ym} = k_{ym},\ d_{xf} = d_{yf} = d_{zf}$$, for a dual porosity model

$$k_x = k_y \neq k_z$$, for a single porosity model

The total production period is set for 1000 days. The focus is to determine how quickly water cones reach a horizontally drilled wellbore. The water coning behavior is observed by analyzing the saturation profiles are specified times of 0, 30, 60, 90, 120, 150, 180, 210, 240, 270, 300, 400, 500, 600, 700, 800, 900, and 1000 days. These time periods are selected based on several numerical experiments and optimized to save computation overheads. For the single porosity model, the production time needs to be extended up to 3000 days. In a single porosity model the transport of water is slower than a dual porosity model owing to the lack of fractures. The single porosity model requires longer production times for water encroachment to be observed toward the horizontal well.

In this study, 560 reservoir cases are simulated for production performance prediction, 680 cases for water saturation prediction. There are 16 variables provided to the numerical simulator.

Table-5.1 Matrix Relative Permeability

S_w	k_{rw}	k_{row}	P_{cow}
0.2	0	1	5.0
0.25	0.0004	0.6027	4.0
0.3	0.0024	0.449	3.0
0.35	0.0075	0.3242	2.5
0.4	0.0167	0.2253	2.0
0.45	0.031	0.1492	1.8
0.5	0.0515	0.0927	1.6
0.6	0.1146	0.0265	1.4
0.7	0.2133	0.0031	1.2
0.8	0.3542	0.001	1.0
0.9	0.5438	0.0005	0.5
1	0.7885	0	0

Table-5.2 Fracture Relative Permeability

S_w	k_{rw}	k_{row}
0.05	0	1
0.25	0.25	0.75
0.5	0.5	0.5
0.75	0.75	0.25
0.95	0.95	0.05
1	1	0

Table-5.3 Reservoir Properties

Reservoir Properties	Value	Unit
Matrix Compressibility*	3×10^{-6}	1/psi
Fracture Compressibility	3×10^{-6}	1/psi
Water Compressibility	3.5×10^{-6}	1/psi
Water Formation Volume Factor**	1.0	RB/STB
Reference Pressure**	14.6	psi
Reservoir Temperature**	170	F
Bubble Point Pressure**	100	psi

Note: *Rock compressibility in a single porosity reservoir is the same.

**These properties are the same in a single porosity reservoir.

Table-5.4 Range of reservoir parameters and design characteristics

Parameter	Minimum Value	Maximum Value	Unit
Matrix Porosity (Φ_m)	0.01	0.2	-
Fracture Porosity (Φ_f)*	0.001	0.01	-
Oil density (r_o)	48	58	lb/ft^3
Water Density (r_w)	59.8	62.4	lb/ft^3
Water Viscosity (μ_w)	0.5	1	cp
Fracture Spacing (d_f)*	30	100	ft
Matrix Permeability (k_m)**	0.01	30	md
Fracture horizontal Permeability (k_{hf})*	100	500	md
Fracture vertical Permeability (k_{vf})*	100	3000	md
Reservoir Thickness (h_t)	150	450	ft
Reservoir Drainage Area (acre)	140	570	acres
Initial Reservoir pressure (p_i)	2000	4000	psi
Length of Well perforation (l_{wp})	600	3560	Ft
Distance from well to OWC(d_{owc})	35	333	ft
Bottom Hole Pressure(p_{sf})	1000	4000	psi
Flow rate (q)***	500	5000	STB/d

Note: *These parameters are not applied in a single porosity reservoir.

**Horizontal and vertical permeability is given in a single porosity reservoir.

***Flow rate is used only in prediction of water saturation.

5.2 Development of ANN

Input and output datasets are prepared with the help of numerical simulator. These datasets are used for ANN based model development. With the help of Neural Network tool box built in MATLAB, various architectures are tested.

In literature, conjugate gradient algorithm in backpropagation networks is indicated to be the most successful. However, in the process of developing a model for predicting water saturation distribution and production profiles, Bayesian Regulation training algorithm yielded superior results. Mostly, either combination of log sigmoid (*logsig*) and tangent sigmoid (*tansig*) transfer function, or multiple *tansig* transfer functions are used in the hidden layers. In addition, linear transfer function is set to deliver values to the output layers. The detailed explanation of

ANN architecture for different prediction method is presented in section 5.4. And validation of the network is presented in section 6.1.

With forward looking ANN model, the production data comprising of oil rate, cumulative oil production, water rate, and cumulative water production is predicted. Percentage errors in the process of getting those profiles range from 0.1 % to more than 100%. ANN tends to be accurate in predicting oil production data compared to water production data. The reasons for these discrepancies are explained in the results section.

Since input datasets are randomly generated, ANN output data obtained from numerical simulations varies case by case. Training and testing datasets are approximately 95% and 5% of the whole datasets. The list of input datasets is presented in Appendix D. It is observed that complex architectures with higher number of hidden layers and neurons performs inferior compared to the simple architectures. As discussed in the Chapter 3, search for the optimum numbers of hidden layers and neurons begin with conservative approach of hidden layers and hidden neurons. When ANN model fails to achieve the desired performance, i.e. 20 average percentage error, by using “trial and error”, more hidden layers, and neurons are incorporated for improving the performance. Work flow chart is presented in figure 5.1 that summarizes the algorithm followed in obtaining the optimum architecture.

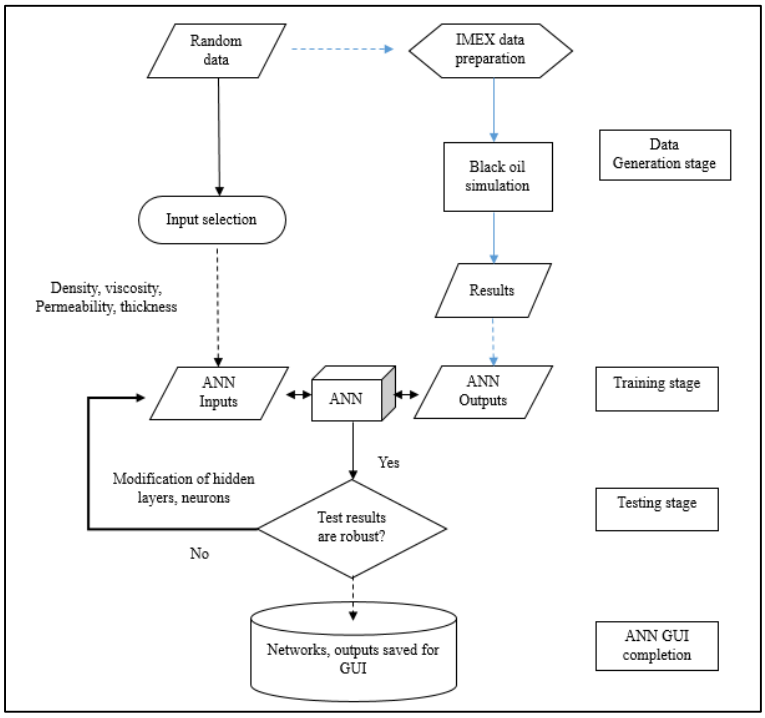

Figure-5.1 Overall work flow chart

5.3 Development Approach of Water Saturation Distribution

This part outlines the model development that will be used to predict water saturation maps. Multiple arrays of water saturation that are representative of various x-z planes from the numerical model are collected at specified times. Collecting all of water saturation values from all of 9375 grid blocks increase computational overheads. Utilizing the symmetry that exists in the reservoir, a set of 375 water saturation values in x-z plane that corresponds to the central plane of the reservoir cross section is collected for each production time. Then, those datasets are utilized to build the ANN based model. During numerical simulation runs, it has been observed that water cones are always symmetrical in nature. Therefore, only 195 out of 375 water saturation values need to be recorded. With the help of these observations, only 13 x-direction blocks of water saturation data are needed to build the model, hence the data from other 12 blocks is excluded.

Until now, developing model for water saturation distribution, there are 18 sets of 13 by 15 in x-direction and z-direction respectively. Each of the 18 sets belongs to the designated production times. This study chooses horizontally allocated water saturation values, 13 water saturation blocks. On obtaining an optimal architecture, the model is stored. 15 neural network architectures are generated, one for each production time. For each of the 18 layers, architectures are designed (z-direction), hence in total 270 neural network architectures are generated for predicting water saturation maps.

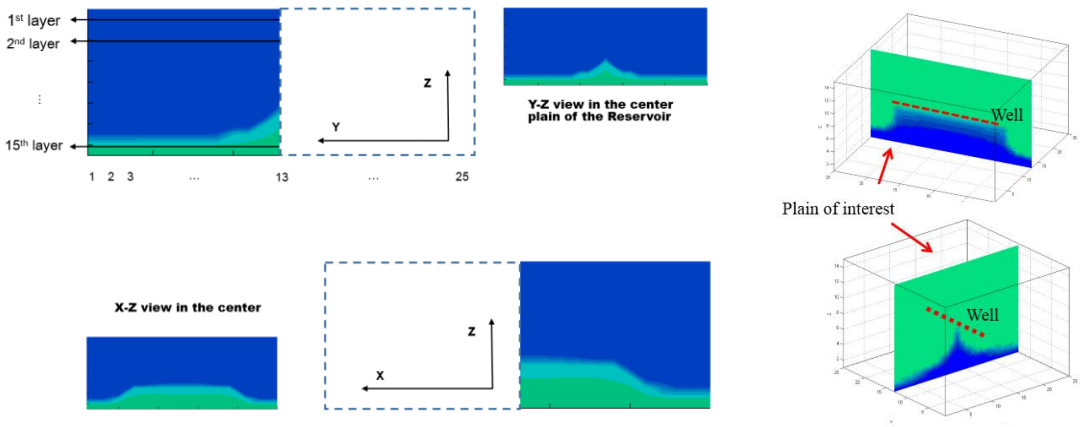

Figure-5.2 Visual representation of symmetry in the reservoir

5.4 Architecture of ANN

The structure of the architecture along with input and target are defined in the following sections. Solutions comprising of variety of water coning problems are presented. The work is primarily divided into two parts namely production prediction model, and water cone prediction model.

5.4.1 Prediction of Production Performance

Input datasets are categorized as reservoir properties and well design parameters. Reservoir properties comprise of fracture porosity, matrix porosity, fracture vertical/horizontal permeability, matrix permeability, fracture spacing, initial reservoir pressure, reservoir thickness, oil density, water density, water viscosity, and drainage area. In case of horizontal wells additionally design parameters, length of well perforations, distance from wellbore to oil-water contact, and bottom hole pressure form input data.

In addition to aforementioned input parameters, functional links are incorporated to obtain better correlations. Functional links are used to capture the physical relationship that exists between inputs and outputs. Backpropagation networks with Bayesian Regulation training algorithm performs better than those with either Levenberg-Marquardt algorithm or Scaled Conjugated Gradient training algorithms. A combination of transfer functions, *tansig* and *logsig*, are used in building the ANN architecture. List of input and output parameters are outlined in Table 5.5.

Table-5.5 Input and output groups for predicting production profile

Input (20)	Reservoir Properties	Matrix, Fracture, Fluid	Φ_m , Φ_f, k_m, kv_f, ,kh_f, , d_f , p_i h_{res}, μ_w r_o r_w
		Drainage	Acres
	Well Design parameters		P_{sf} , L_{wp}, d_{owc}
	Functional Link		λ_1 λ_2 λ_3 λ_4
Output (18)	**Production profile** 1. cumulative oil production 2. oil production rate 3. cumulative water production 4. water production rate		[q_1 q_{30} q_{60} q_{90} q_{120} q_{150} q_{180} q_{210} q_{240} q_{270} q_{300} q_{400} q_{500} q_{600} q_{700} q_{800} q_{900} q_{1000}]
	Functional Link		Not used

Functional link λ_1 is equivalent to storativity ratio of a dual porosity system as outlined in the Chapter 3. Storativity ratio describes relative storage capacity of matrix pores in the system compared to fracture pores. Functional link λ_2 describes the permeability anisotropy and λ_3 the mobility ratio. Function link, λ_4 is aspect ratio. Aspect ratio is defined as reservoir thickness divided by reservoir length, which is important in the process of water cone formation. Formulas used to generate the functional links are as follows:

$$\text{Quasi-Storativity: } \lambda_1 = \frac{(\Phi_m+\Phi_f)*0.1}{\Phi_f}$$

$$\text{Permeability anisotropy: } \lambda_2 = \frac{k_{hf}}{k_{vf}}$$

$$\text{Water Mobility: } \lambda_3 = \frac{r_o}{\mu_o}$$

$$\text{Aspect Ratio: } \lambda_4 = \frac{h_t}{reservoir\ length}$$

Initially a single hidden layer with 16 neurons comprised of preliminary inputs without functional links is used to generate a model for Production Profile Prediction. This network was

unable to capture the correlation between the inputs and outputs. Hence, functional links and additional hidden layers are introduced using trial and error. It is indicated that by numerous trial and error process, the current problem needs more than 1 hidden layer to achieve desired precision. The final architecture of the Production Profile Prediction model comprises of two hidden layers with 30 and 18 neurons for cumulative production profiles and three hidden layers with 30, 40, and 18 neurons for production rate profiles respectively along with tangent sigmoid transfer functions. Proposed ANN architecture is presented in figure 5.3.

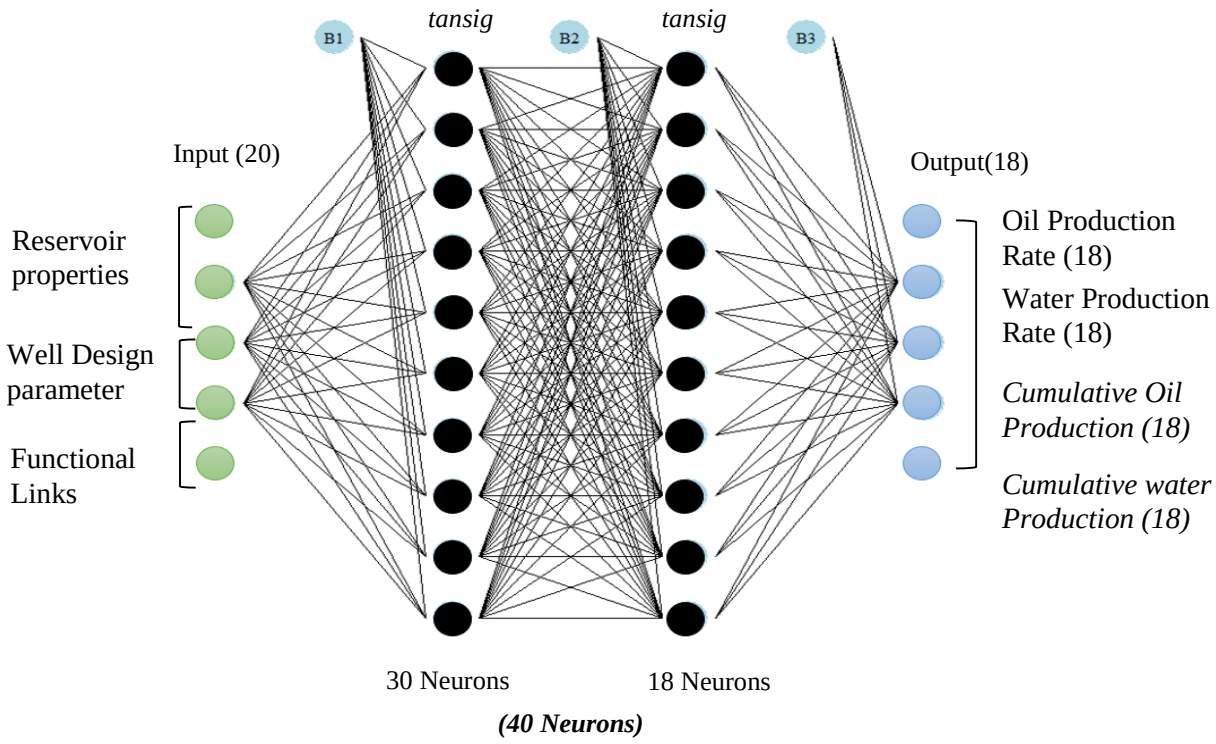

Figure-5.3 Neural network architecture of production profile prediction model

5.4.2 Prediction of Water Saturation

In order to generate water saturation maps at the specific production times, arrays of water saturation values are configured as described in section 5.3. Reservoir properties comprise

of fracture porosity, matrix porosity, fracture vertical/horizontal permeability, matrix permeability, fracture spacing, initial reservoir pressure, reservoir thickness, oil density, water density, water viscosity, and drainage area. In the case of horizontal wells, design parameters, length of well perforations, distance from wellbore to oil-water contact, and total fluid rate are provided along with other input parameters. Input and output parameters are listed in Table 5.6.

Table-5.6 Input and output groups for predicting water cone

Input (16)	Reservoir Properties	Matrix, Fracture, Fluid	Φ_m , Φ_f, k_m, kv_f, ,kh_f, , d_f , p_i h_{res}, μ_w r_o r_w
		Drainage	acres
	Well Design parameters		Q_{total} , Lwp, d_{owc}
	Functional Link		Not used
Output (13)	Water saturation profile		Sw_1 Sw_2 Sw_3 Sw_4 Sw_5 Sw_6 Sw_7 Sw_8 Sw_9 Sw_{10} Sw_{11} Sw_{12} Sw_{13}
	Functional Link		Not used

Initial training was carried out using Levenberg-Marquardt (LM) training algorithm. This process could not achieve the desired accuracy. For instance, the worst average percentage errors of the network with LM algorithm is more than 300%. This has prompted for additional trials using alternate training algorithms.

In the second trial, Scaled Conjugated Gradient (SCG) algorithm was used to train the ANN model. The lowest Mean Square Error obtained through this training is 0.01, which means that the some results are still not as satisfactory as 20 average percentage error.

Bayesian Regulation training algorithm is used in the third trial. Bayesian Regulation algorithm is the slowest training algorithm when compared to LM and SCG, however it provided a prediction that satisfied the accuracy criteria. On further trial and error, the optimal ANN architecture is established. The architecture comprised of two hidden layers with 30 and 13

neurons with a combination of *tansig* and *tansig* transfer functions. In this model, functional links weren't necessary compared with prediction of production performance. Overall summary of the ANN architecture is tabulated as table 5.7.

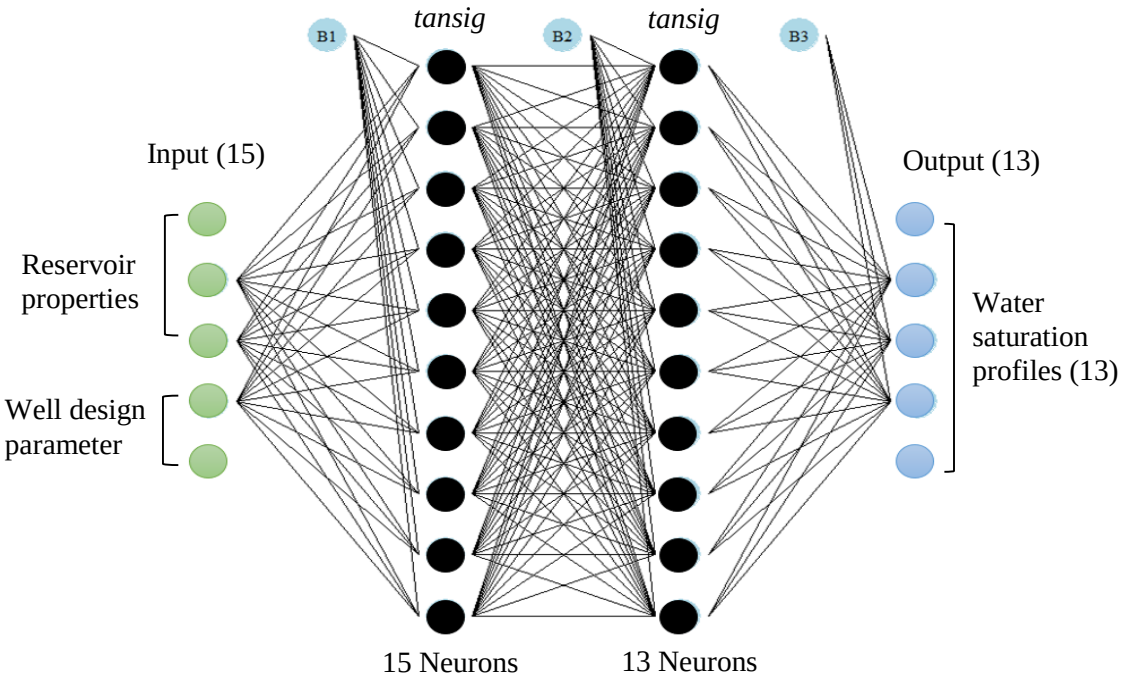

Figure-5.4 Neural network architecture of water cone predictor

Table-5.7 Summary of ANN architecture

Prediction type		Total case	Training	Testing	# of hidden layer	# of hidden neurons	Transfer function	Training algorithm
Production Performance	cumulative oil production	560	530 (94.6%)	30 (5.4%)	3	30, 40, 18	*tansig, tansig, tansig*	*Bayesian Regulation*
	oil production rate	560	530	30	2	30, 18	*tansig, tansig*	
	cumulative water production	560	530	30	3	30, 40, 18	*tansig, tansig, tansig*	
	water production rate	560	530	30	2	30, 18	*tansig, tansig*	
Water Saturation	Sw prediction (XZ view)	680	650 (95.5%)	30 (4.5%)	2	30, 13	*tansig, tansig*	
	Sw prediction (YZ view)	680	650	30	2	30, 14	*tansig, tansig*	

Chapter 6

Results and Discussions

This chapter discusses the results of current study. In the first part, Production Profile Prediction model predicting the cumulative oil production, oil rate, and water oil ratio is presented. Later Water Cone Prediction model predicting the water saturation profile for the specified production times is discussed. Two reservoir models are considered in this study, single porosity model and dual porosity model.

6.1 Performance Analysis

Performance evaluation is necessary to establish the robust nature of the models. There are several ways in which the models could be tested for their accuracy and robustness. In the current work, the following parameters are utilized to establish performance of the ANN based model.

$$Absolute\ Error = \left|Value_{prediction} - Value_{numerical}\right|$$

$$Percentage\ Error = \frac{\left|Value_{prediction} - Value_{numerical}\right|}{Value_{numerical}} \times 100$$

$$Averaged\ Percentage\ Error = \frac{\sum Percentage\ Error}{N}$$

$$Mean\ Square\ Error = \frac{1}{N}\sum_{i=1}^{n}(Value_{prediction} - Value_{numerical})^2$$

$$Averaged\ Mean\ Square\ Error = \frac{\sum Mean\ Square\ Error}{N}$$

First, the absolute error is equivalent to the difference between ANN model outputs and numerical simulation data. Absolute error contours are presented as indicated in Figure 6.1 to highlight the difference between ANN model predictions and data from numerical simulator. The dashed line indicates the water cone. There are some absolute errors around the outside of the water cone ranging from 0 to 0.05.

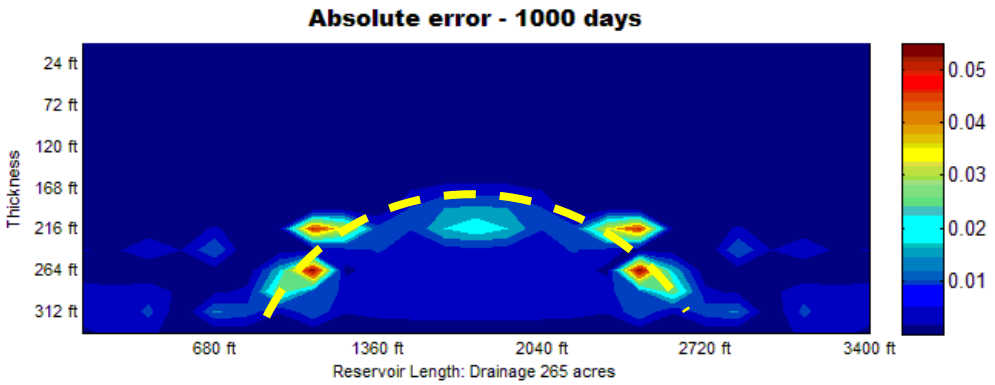

Figure-6.1 Example of absolute error in reservoir water saturation

Percentage errors are measured to analyze the relative errors. Testing results with less than 10% error are deemed as good results in this study. In addition, average percentage errors are used for evaluation of each test case.

Third, Mean Square Error (MSE) measures the average of the squares of absolute error. The MSE is mostly used for training and testing ANN architecture.

6.2 Results and discussions

To show the overall performance of the neural network model developed in this study, 3 test cases, the best, normal, the worst test results are presented. Single porosity and dual porosity systems are presented separately.

6.2.1 Single Porosity Model

Prediction of oil production data

Bayesian Regulation algorithm is used for training the ANN architecture to obtain an optimal structure to predict oil production data. Up to 30 iterations, MSE of the training data reaches about 10^{-4}. Regression of the outputs of the ANN shows promise with correlation of 0.99. Inputs for test cases are tabulated below table 6.1. Among those input, three test cases are selected for evaluating of performance of ANN model; test case 28(the best), 12(normal), and 8(the worst). Specifically, test case 8 yields big difference between numerical data and ANN prediction data. Since the production profile of the test case 8 is linear and other cases show non-linear, it can be inferred that the performance of ANN prediction is good when the production profile is non-linear.

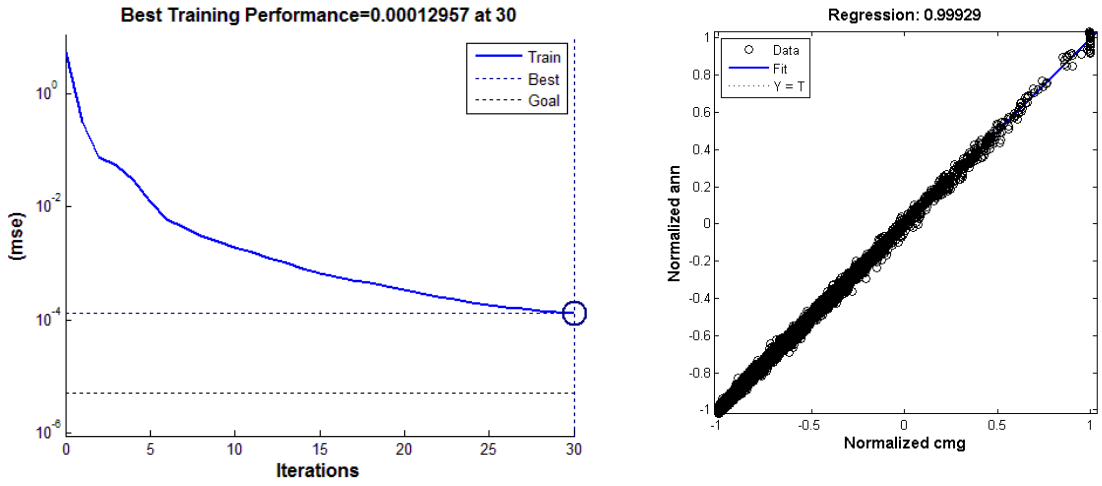

Figure-6.2 Training performance and Regression for cumulative oil production

Table-6.1 input data of sample test cases

	Φ	k_h	k_v,	r_o	r_w	μ_w	h_{res}	p_{sf}	d_{owc}	L_{wp}	p_i	Acre
test #8	0.187	1	418.6	51.3	61.9	0.963	390	1293	273.0	2184	3183	475.3
test #12	0.058	87	215.3	51.5	61.0	0.550	375	3497	237.5	1408	3728	444.4
test #28	0.120	96	16.4	48.8	59.9	0.853	225	1405	112.5	3402	2916	512.5

Cumulative oil production predictions of 30 test cases exhibit agreeable results. Percentage errors range from 2 % to 35%. The worst result, test cast #8, shows disparities between model predictions and numerical simulation data. In test case #8 there is no water produced out of the reservoir. In cases of no water production models tend to yield high error while predicting water flow rates. In spite of that, the model captured the cumulative oil production profiles satisfactorily. The table of average percentage error depicts that performance of the model is fairly accurate since most of average errors are less than 10%, 23 test cases out of 30.

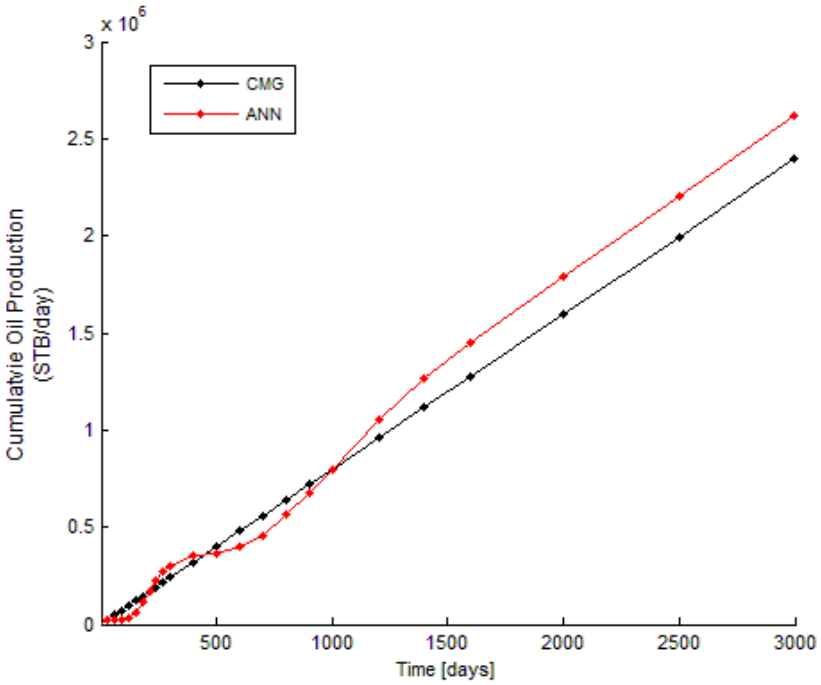

Figure-6.3 Test case #8 for prediction of cumulative oil production

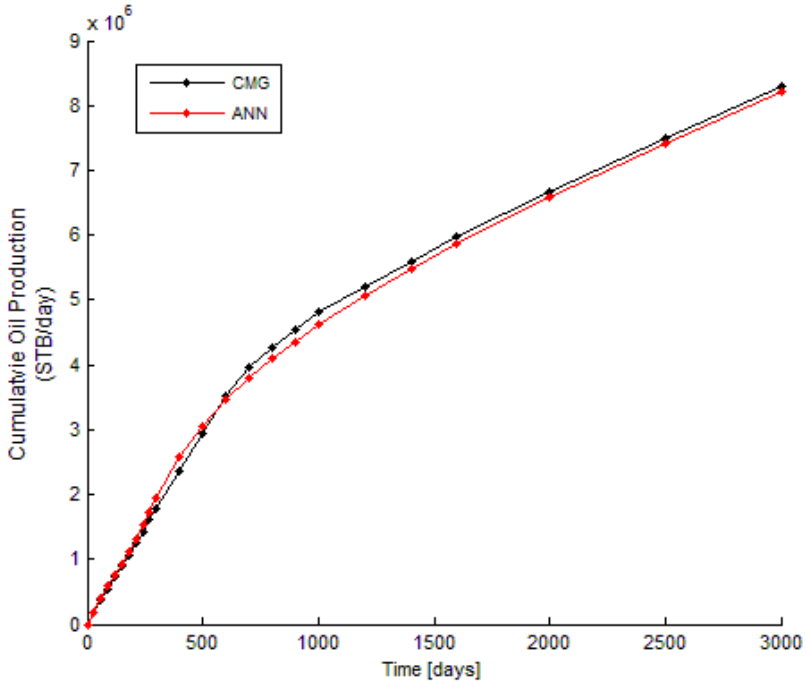

Figure-6.4 Test case #12 for prediction of cumulative oil production

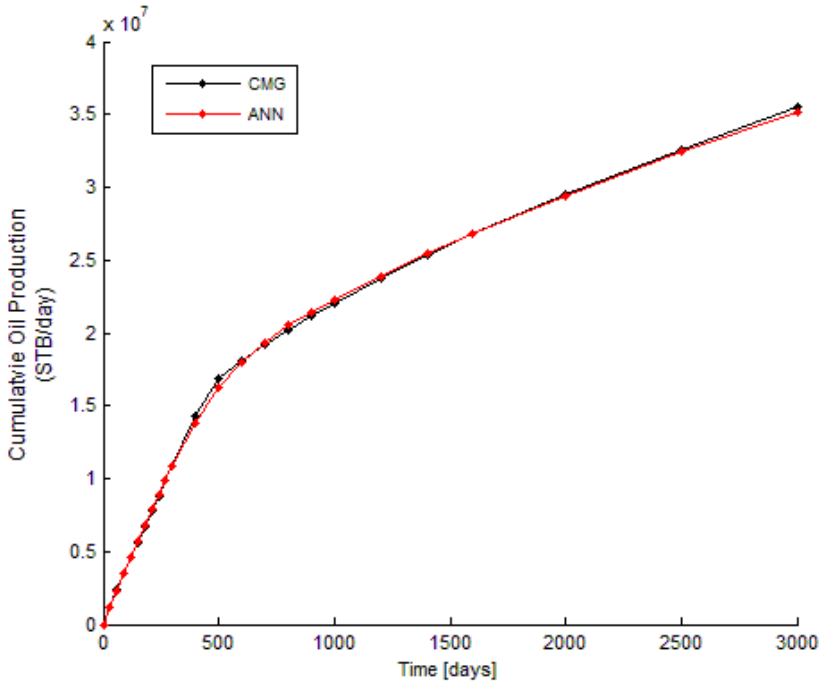

Figure-6.5 Test case #28 for prediction of Cumulative Oil Production

Simulation data indicates that reservoir test case #8 produced oil alone for 3000 days. This case had low vertical permeability and very wide drainage area. Whereas test cases #28, #12 produced water within 500 days and thereby resulted in decline of cumulative oil production curve. This is due to high vertical permeability and low horizontal permeability.

To sum up, cumulative oil production results in single porosity models are relatively good indicating that the model understands behavior of oil production in the entire production period. However, some test cases that barely produce water. Due to this, the model finds it difficult to understand the production profile. Cumulative oil production nearly becomes linearly constant as time goes on.

Oil production rate is predicted by using the same network structure as that of cumulative oil production prediction. Unlike cumulative oil production prediction, MSE and regression shows unsatisfactory results: MSE is about 0.00113 and regression is 0.9929. Most of results are between 10% and 30% average percentage errors. It is observed that a reservoir test case that has no water production has resulted in high errors.

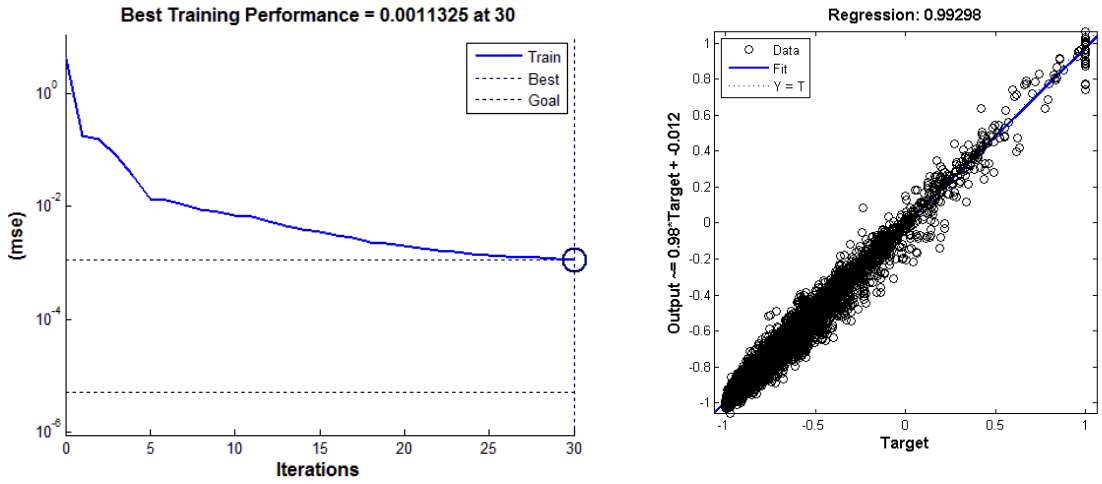

Figure-6.6 Training performance and Regression for oil production rate

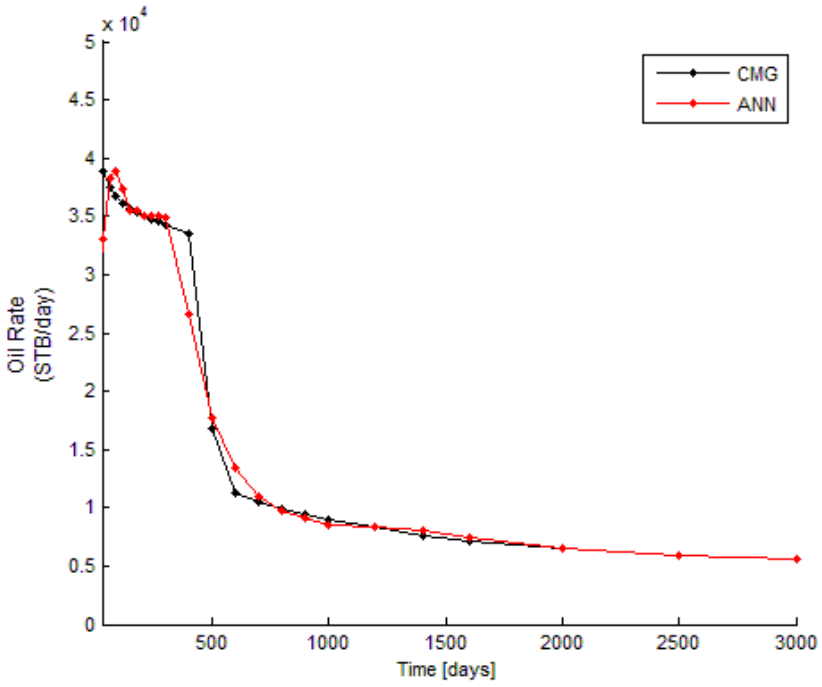

Figure-6.7 Test case #28 for prediction of oil production rate

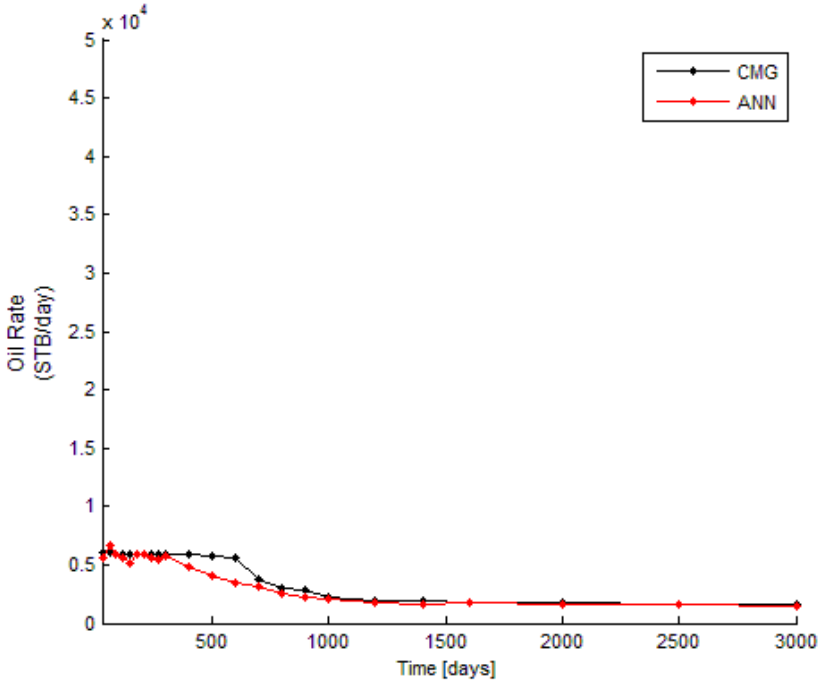

Figure-6.8 Test case #11 for prediction of oil production rate

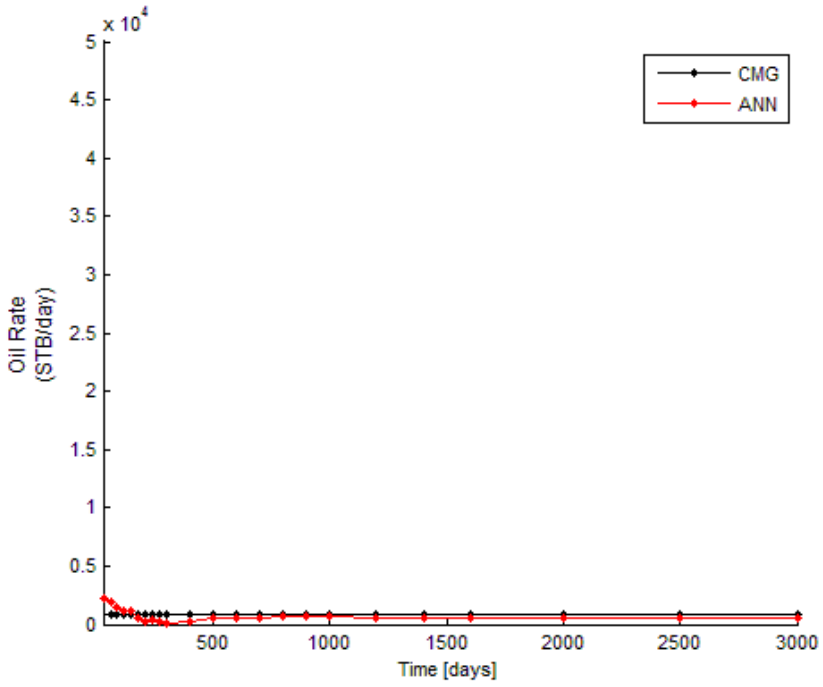

Figure-6.9 Test case #18 for prediction of oil production rate

Unlike prediction of cumulative oil production, results of oil rate show poor to satisfactory accuracy. In particular, test case #8, oil production rate is constant. Due to lack of water production, test case #8 had resulted in large errors.

Table-6.2 Average percentage error for prediction of oil production data

# of test case	Average percentage error (%)	
	Cumulative Oil Production	Oil Production Rate
1	2.55	8.60
2	6.22	8.15
3	6.67	31.22
4	2.36	6.57
5	3.40	10.09
6	1.78	11.94
7	5.45	13.35
8	34.94	59.36
9	23.24	87.52
10	2.53	14.38
11	5.12	11.64
12	6.39	15.55
13	12.36	32.83
14	3.41	16.08
15	17.84	29.41
16	9.79	12.43
17	2.93	8.84
18	3.57	15.27
19	11.85	34.13
20	27.06	25.53
21	4.44	16.88
22	4.10	23.99
23	4.45	14.76
24	2.37	8.82
25	8.59	25.21
26	4.27	11.12
27	19.84	56.00
28	1.73	6.81
29	5.69	11.20
30	3.14	10.94

Prediction of Water Saturation

Among 24 production time steps used for modeling purposes, three production times (500, 2000, 3000 days) are selected for comparison purposes. Water saturation maps predicted by the model versus the target water saturation data is presented in the following figures. In the appendix, all the other time step water saturation distributions are presented. Average mean square errors are used since a number of some prediction data are non-numeric values. The model takes longer to predict water saturation results when compared to production prediction model. Bayesian Regulation training algorithm is employed in building the optimal architecture to predict water saturation data.

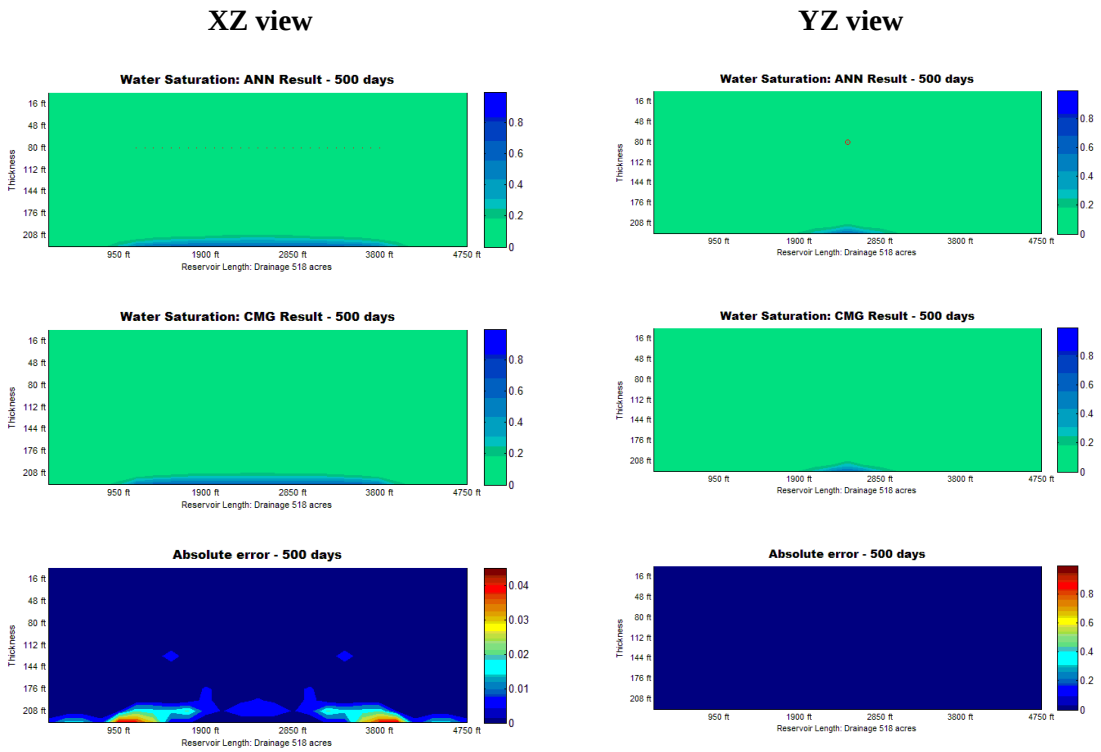

Figure-6.10 Prediction of water saturation for test case #7 at 500 day

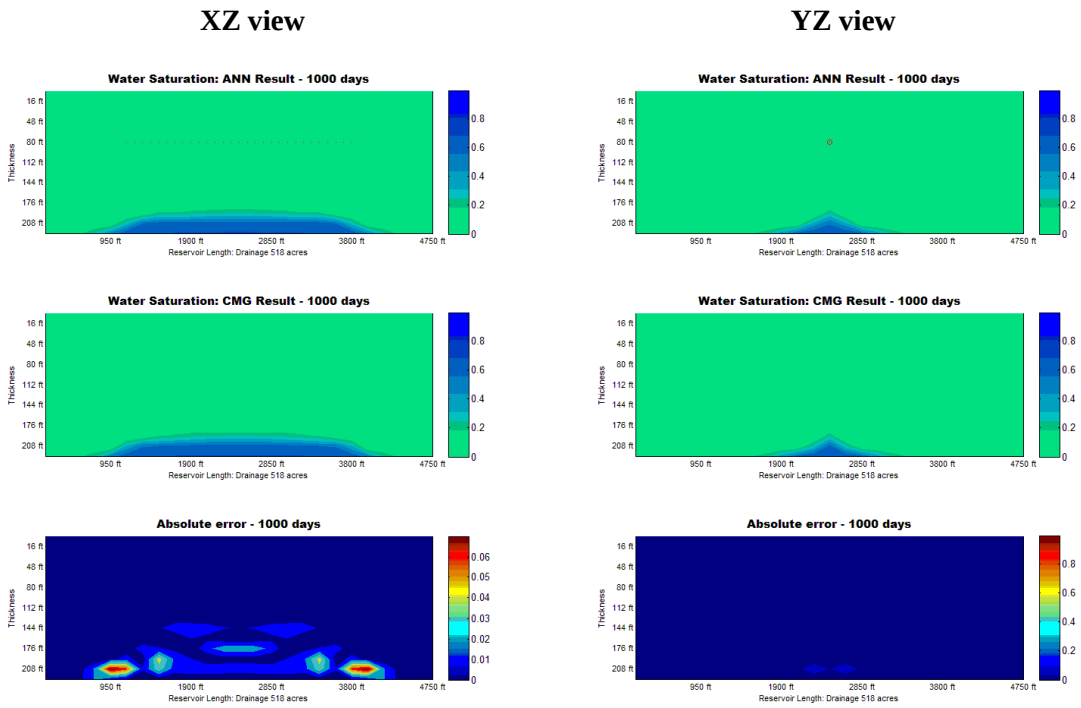

Figure-6.11 Prediction of water saturation for test case #7 at 1000 day

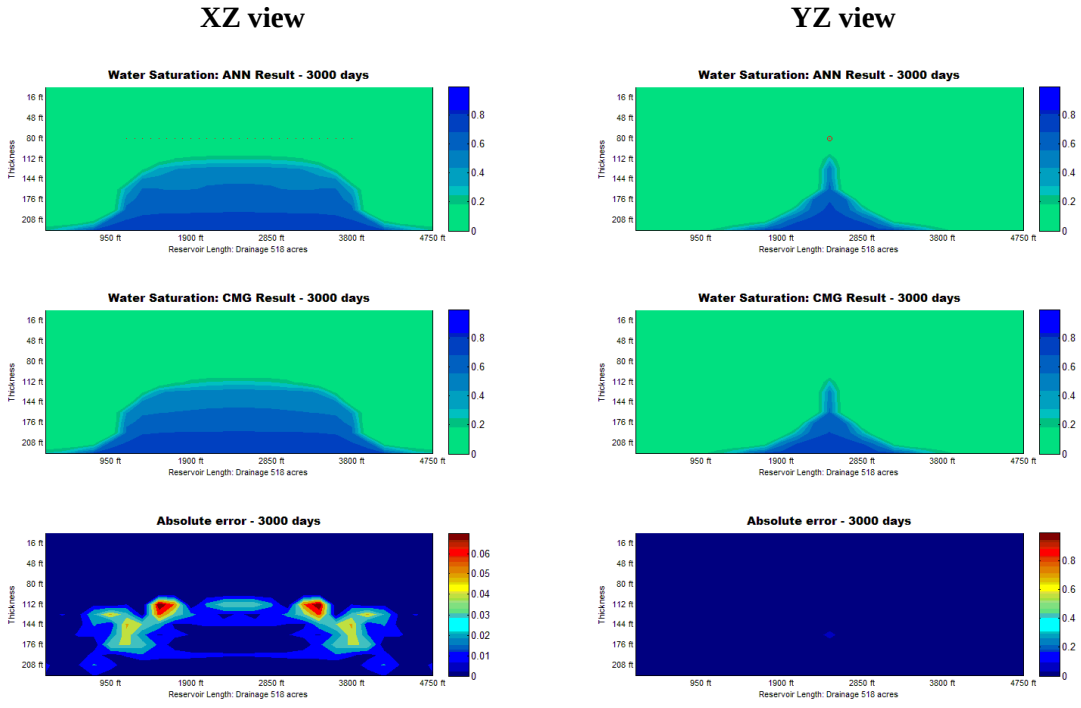

Figure-6.12 Prediction of water saturation for test case #7 at 3000 day

Water saturation values are always between 0 and 1, hence absolute error and mean square errors are presented to indicate the difference between numerical simulation data and model predicted water saturation data. In absolute error contour maps, differences are only observed at boundary of water cones at 3000th day. Maximum absolute errors are less than 0.1 and all of average mean square errors are less than 0.0005.The model is able to accurately capture the shape of water cone. Water saturation prediction on Y-Z view of the reservoir indicates better results than X-Z view for water saturation. Average mean square errors for water saturation map for each production time is tabulated in Table 6.3.

Table-6.3 Average mean square error for water saturation map for test cases

Production days	Average mean square error (%)	
	X-Z view	Y-Z view
30	7.01E-06	1.24E-06
60	1.35E-05	3.16E-06
90	1.52E-05	5.46E-06
120	1.91E-05	6.07E-06
150	2.48E-05	5.49E-06
180	3.52E-05	6.01E-06
210	5.12E-05	1.11E-05
240	9.04E-05	7.97E-06
270	7.43E-05	1.06E-05
300	1.01E-04	1.31E-05
400	7.72E-05	2.35E-05
500	1.66E-04	3.04E-05
600	2.40E-04	3.14E-05
700	2.39E-04	3.67E-05
800	2.61E-04	4.76E-05
900	2.99E-04	7.13E-05
1000	2.49E-04	5.26E-05
1200	4.19E-04	1.04E-04
1400	4.75E-04	9.40E-05
1600	4.53E-04	9.20E-05
1800	6.75E-04	1.27E-04
2000	6.73E-04	1.45E-04
2500	7.59E-04	2.06E-04
3000	7.01E-06	1.24E-06

6.2.2 Dual Porosity Model

Prediction of oil production data

In a dual porosity model, oil and water production data are predicted via different neural networks. Production data comprise of cumulative oil production data, oil rate data, cumulative water production data, and water rate data.

530 reservoir cases are used for training the ANN model and Bayesian Regulation algorithm (BR) is used to generating the optimal architecture to predict oil production data. Mean square error of the training data almost reaches 10^{-4} at 44 iterations. Also, regression of the outputs of the ANN model indicated correlation coefficient of 0.99. There are 30 reservoir test cases selected for evaluation of performance of ANN model. Input parameters of three sample cases are indicated in Table 6.4. Test case #5(the best), 13(normal), and 20(the worst).

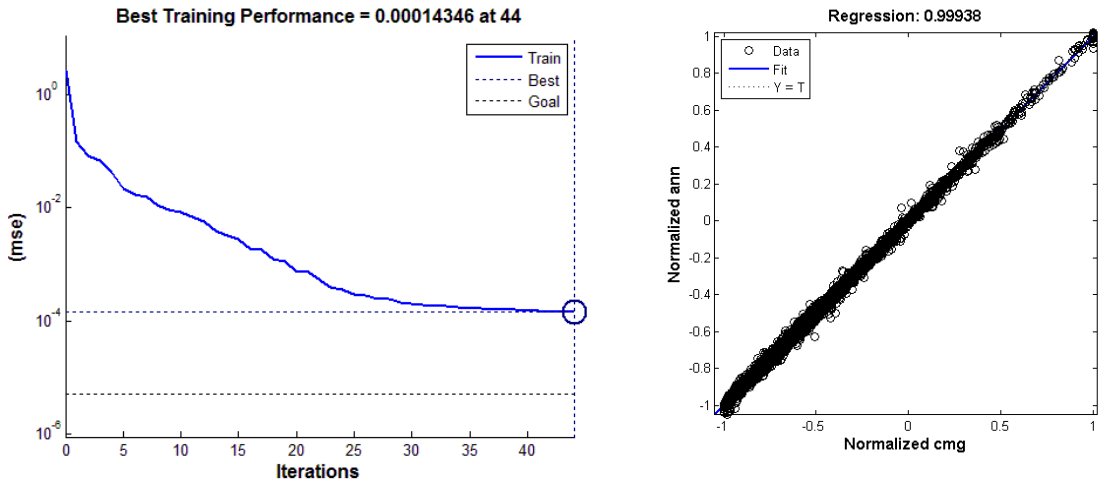

Figure-6.13 Training performance and regression for cumulative oil production

Table-6.4 Input data of sample test cases

	Φ_m	Φ_f	k_m	kv_f,	kh_f	d_f	r_o	r_w	μ_w	h_{res}	p_{sf}	d_{owc}	L_{wp}	p_i	Acre
test #5	0.128	0.0018	6.01	2601	410	27	51.6	61.9	0.593	210	1881	147	2632	3122	507.1
test #13	0.130	0.0051	16.37	1881	157	10	57.3	62.3	0.676	165	1348	93.5	1224	2160	149.3
test #20	0.018	0.0028	19.49	2316	165	15	53.2	62.1	0.830	180	1397	78	2556	2267	289.3

Most cumulative oil production predictions of 30 test cases indicate good agreements. Average percentage errors range from 0.1 % to 15%. Test case #20 is the worst case scenario with huge disparities between model results and numerical data. In fact, the delay in water breakthrough causes disparities in the results between outputs from model and numerical simulator. Nevertheless, the model tries to capture the pattern of cumulative oil production profiles satisfactorily. The table of average percentage error for cumulative oil production depicts that performance of the model is fairly accurate since most of average errors are less than 5%, 27 test cases. At the end of production of test case # 20, the amounts of oil producing is significantly decreased. It can be seen that soon after water breakthrough, water oil ratio rapidly increases as oil rate decreases.

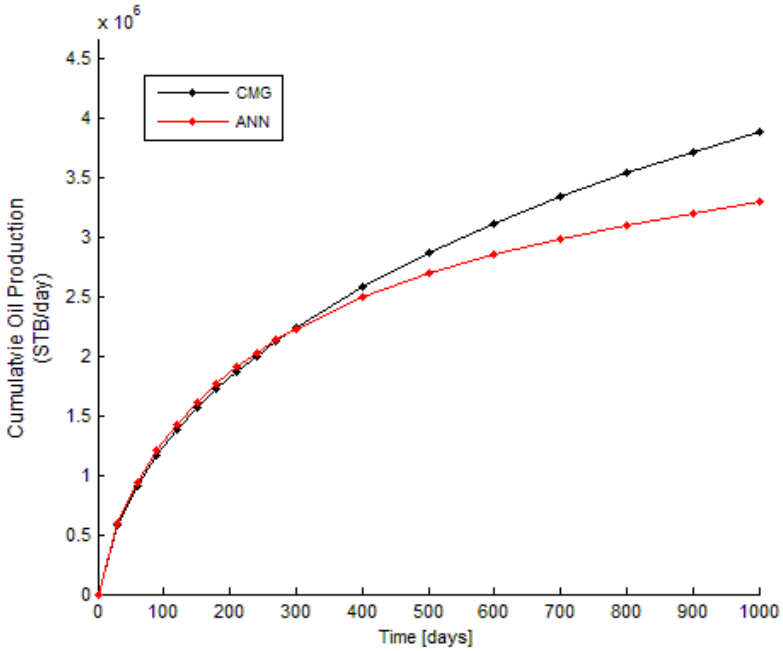

Figure-6.14 Test case #20 for prediction of cumulative oil production

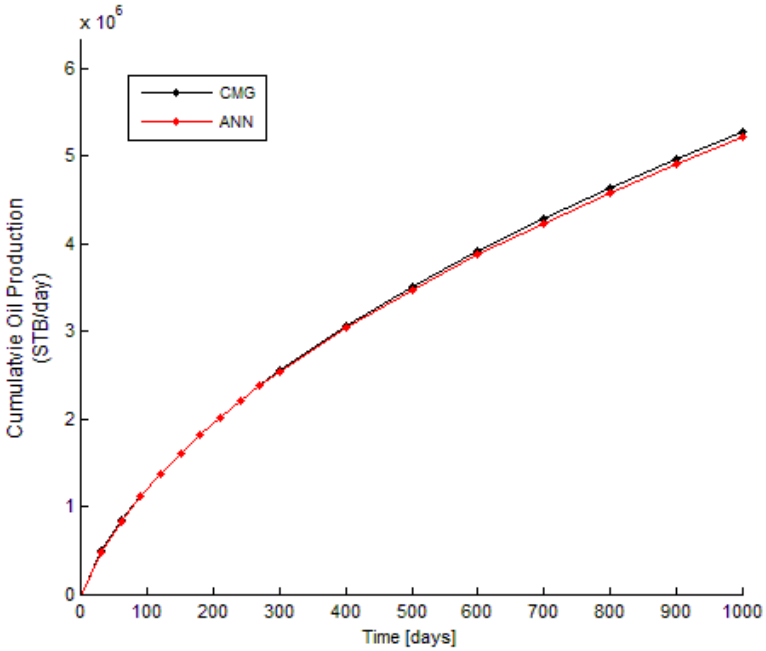

Figure-6.15 Test case #13 for prediction of cumulative oil production

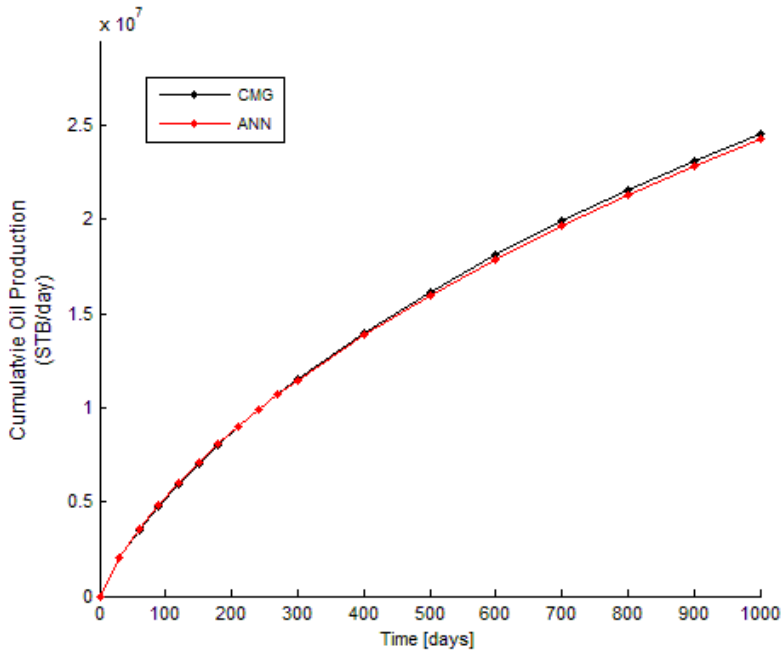

Figure-6.16 Test case #5 for prediction of Cumulative Oil Production

Reservoir test case #20 produces more water than oil after 400 days due to huge pressure difference between initial reservoir pressure and bottom hole pressure. This difference creates large fluid flow rates. It is evident that pressure drawdown is one of the significant factors that results in formation of water cones and thereby large water production rates.

To sum up, cumulative oil production results of test case #5, #13 show that the model is able to capture behavior of production in the entire production period. However, in test case #20, after 300 days production, the model finds it difficult to understand the production profile since oil production is significantly reduced. The model prediction indicates a decline after 700 days, which does not agree with increasing trend of cumulative oil production curve.

Oil production rate is predicted by using the same network structure as that of cumulative oil production prediction. MSE and regression shows good results: MSE is about 0.0001 and correlation coefficient of regression is 0.99. Although most of results are less than 5% average percentage error, test case #20 has large errors between numerical simulation data and model data. In spite of discrepancies for the entire production, the model prediction matches the trend from the numerical simulation data. In 30 tests case results, average percentage errors of 25 test cases are less than 5%. Other 5 test cases have less than 15% average percentage errors.

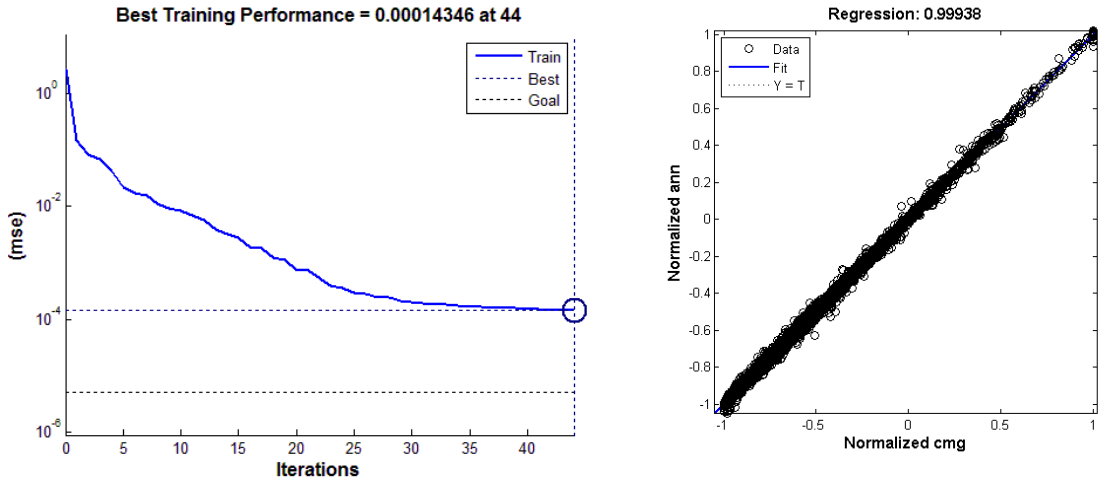

Figure-6.17 Training performance and regression for oil production rate

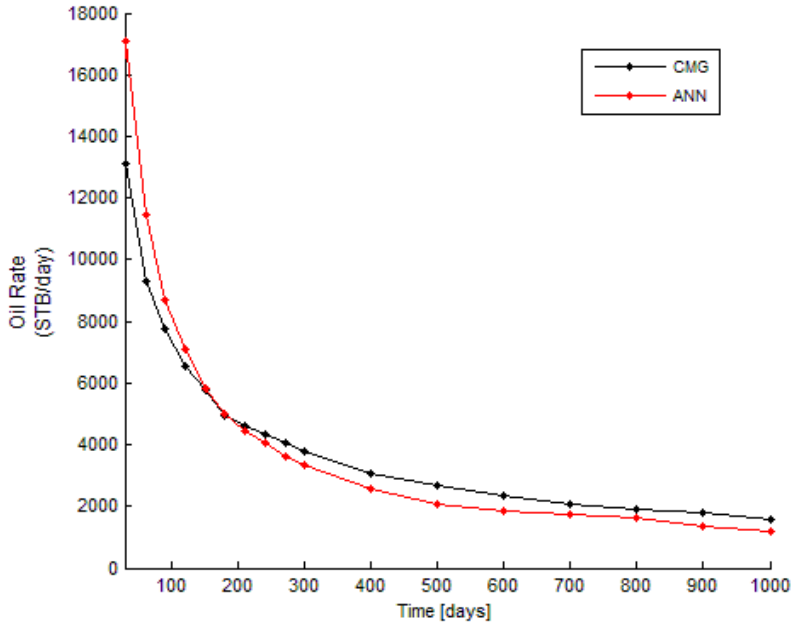

Figure-6.18 Test case #5 for prediction of oil production rate

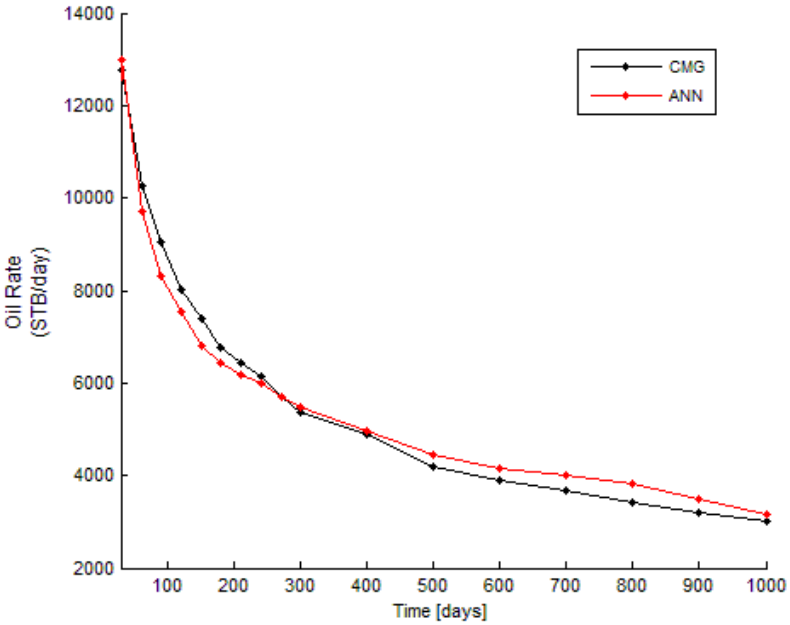

Figure-6.19 Test case #20 for prediction of oil production rate

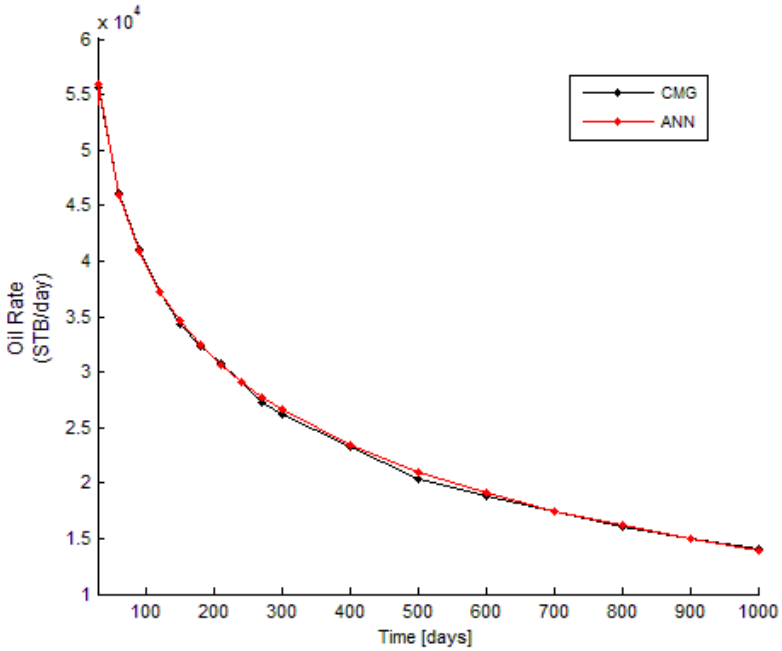

Figure-6.20 Test case #5 for prediction of oil production rate

Results of test case #5 showcase a good agreement. But those of test case #15, 20 have discrepancies. Test case #15, 20 have low initial reservoir pressure and bottom hole pressure that cause low oil rate. The ANN yields good results when predicting high production rate, but tend to yield large errors for reservoir cases with low production rates. Thus, given a wide range of input variables, prediction is accurate when high oil production is observed in the reservoir.

Table-6.5 Average percentage error for prediction of oil production data

# of test case	Average percentage error (%)	
	Cumulative Oil Production	Oil Production Rate
1	3.44	2.40
2	7.27	7.07
3	0.60	4.54
4	3.37	3.66
5	1.53	0.88
6	1.94	1.14
7	0.64	1.53
8	0.87	1.35
9	1.60	2.38
10	0.56	2.33
11	2.69	3.22
12	0.72	1.22
13	5.75	5.49
14	1.51	2.28
15	7.05	10.15
16	0.55	3.75
17	0.44	1.29
18	1.66	0.94
19	0.84	1.64
20	4.51	14.68
21	1.63	3.27
22	0.92	2.87
23	1.22	2.80
24	3.45	1.17
25	1.52	2.30
26	0.69	1.14
27	1.10	2.21
28	0.82	1.87
29	3.09	1.87
30	4.95	5.26

Note: Yellow-highlighted results are examples discussed.

Prediction of water production

With the same architecture as oil production prediction, MSE of the training data of cumulative water production is 0.000005 and regression of the outputs of the ANN indicate a correlation coefficient of 0.99. For predicting water production rate data, MSE is less than 10^{-4} and regression is 0.99. The similar procedure is applied to water production rate. Mean square error and regression shows good results: MSE is about 0.00001 and regression is 0.99. Among 20 test cases, sample test cases are presented; 16(the best), 7(good), and 1(the worst). Input data are tabulated in the Table 6.6. In terms of percentage error, water production rate prediction model is less accurate than that of oil production data.

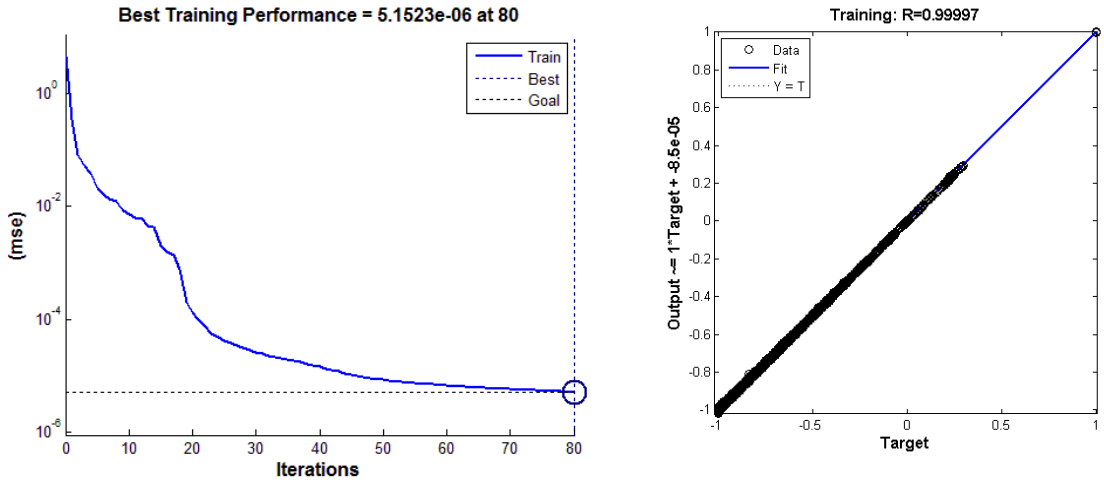

Figure-6.21 Training performance and regression for cumulative water production

Most percentage errors range from 0.4 % to 25%. The worst result, test case #1 exhibit large errors in relatively later production time periods. Test reservoir case #1 water production begins after 210 days. Rather, in test case #7 and 16, water is produced soon after production initiated.

The model tries to find the water production pattern. As production goes on, despite of some discrepancy, the production pattern between numerical simulator data and the ANN shows good agreement. The table of average percentage errors showcases that overall results are fairly good since average errors are less than 10% in 20 out of 30 test cases, 25% in 8 test cases

Table-6.6 Input data of sample test cases

	Φ_m	Φ_f	k_m	kv_f,	kh_f	d_f	r_o	r_w	μ_w	h_{res}	p_{sf}	d_{owc}	L_{wp}	p_i	Acre
test #1	0.18	0.0023	22.8	1297	222	28	50.1	61.4	0.59	420	2469	294	1872	2621	196.4
test #7	0.07	0.0044	12.2	462	348	17	55.5	62.1	0.53	315	2001	241.5	1860	3454	496.4
test #16	0.12	0.0067	28.0	659	397	7	54.0	60.9	0.73	225	1170	112.5	1428	3889	203.2

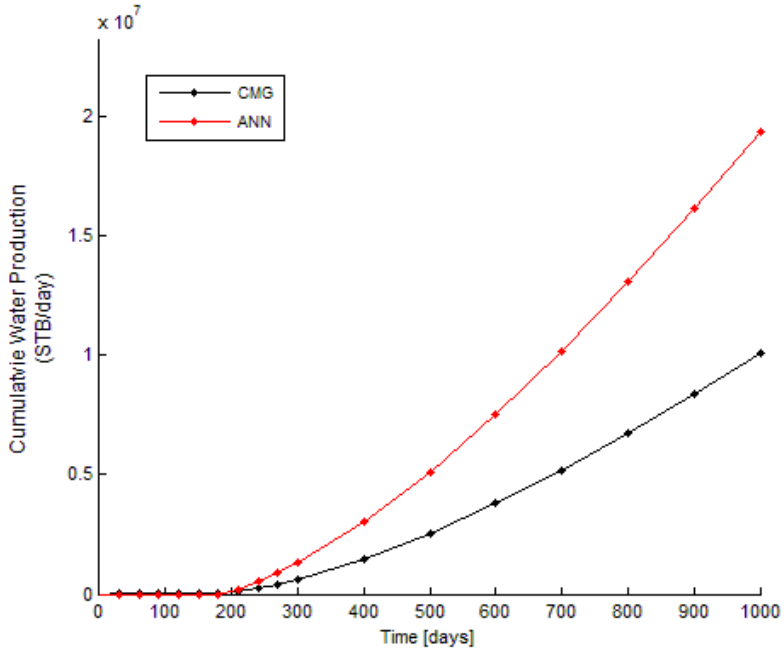

Figure-6.22 Test case #1 for prediction of cumulative water production

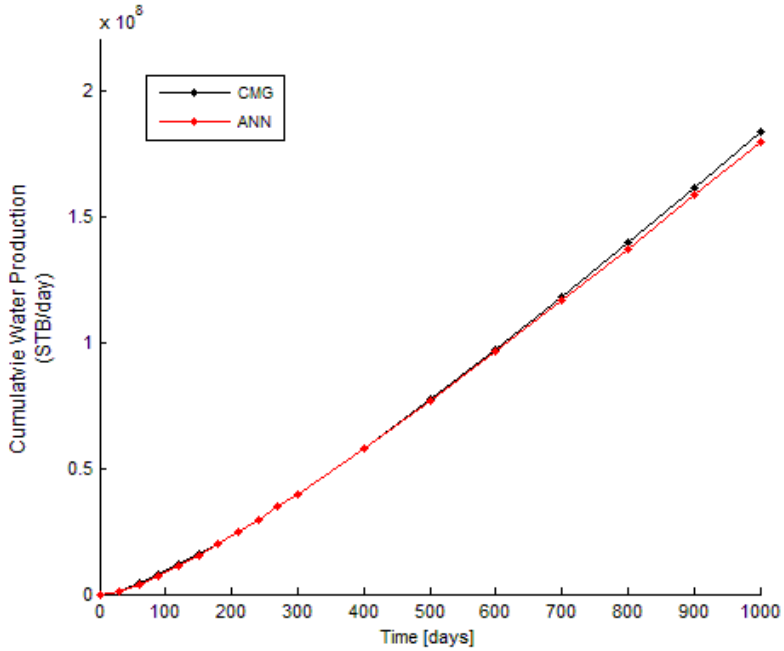

Figure-6.23 Test case #7 for prediction of cumulative water production

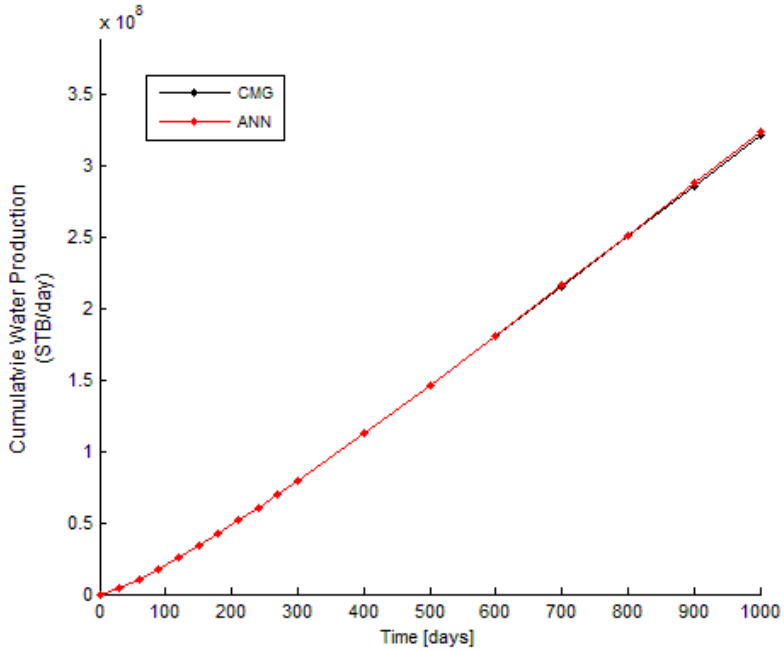

Figure-6.24 Test case #16 for prediction of cumulative water production

By using the same network as that of cumulative water production prediction, water production rate is predicted. Similarly, MSE and regression shows good results: MSE is about 0.0001 and correlation coefficient of regression is 0.99. Most of results are less than 5% average percentage error. Again, test case #1 has large errors between numerical simulation data and ANN data. In spite of discrepancies for the entire production, the ANN matches the trend of the numerical data. In 30 tests case results, average percentage errors of 26 test cases are less than 10%. Other test cases have average percentage errors ranging from 13% to 45%.

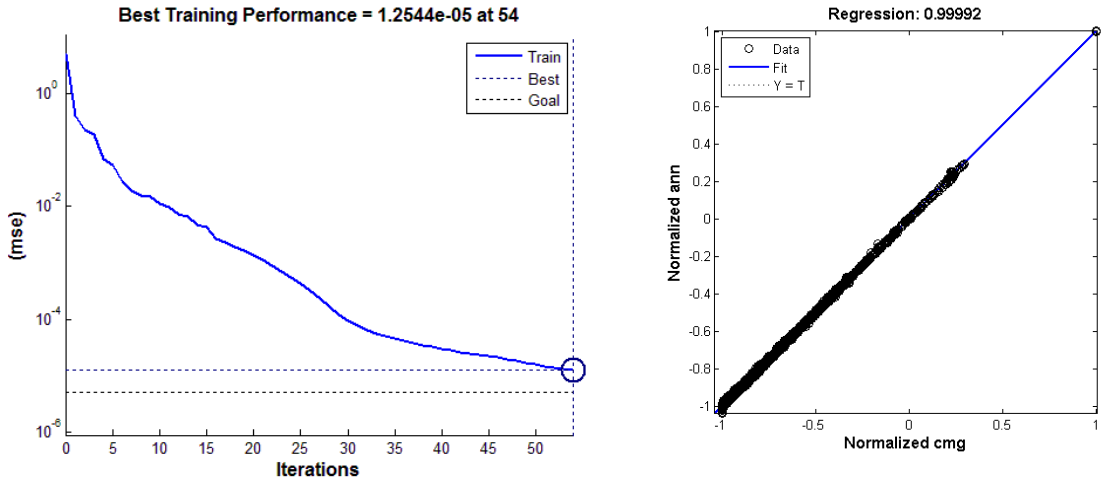

Figure-6.25 Training performance and regression for water production rate

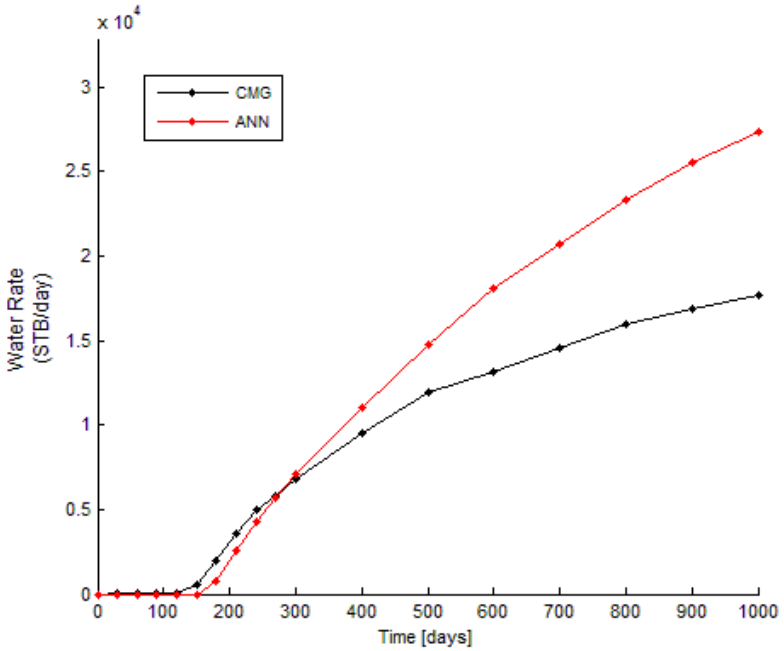

Figure-6.26 Test case #1 for prediction of water production rate

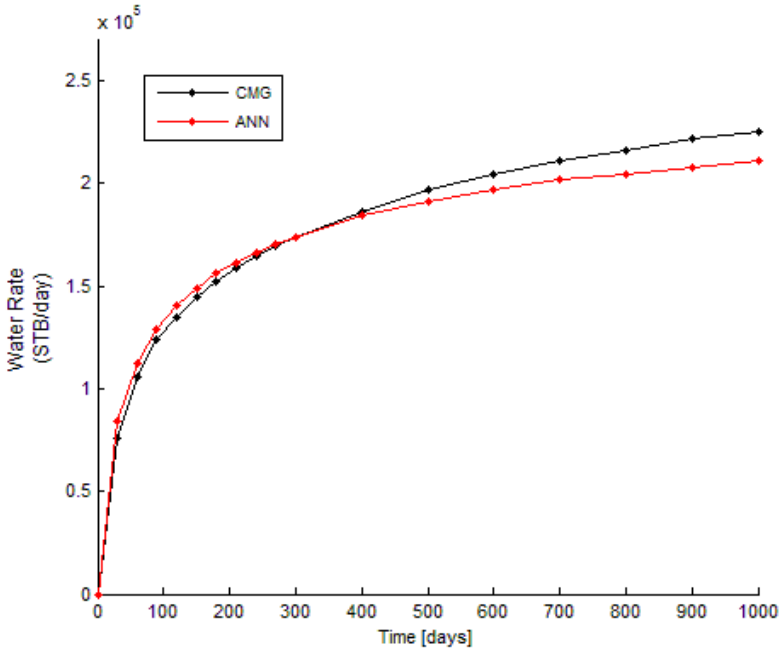

Figure-6.27 Test case #7 for prediction of water production rate

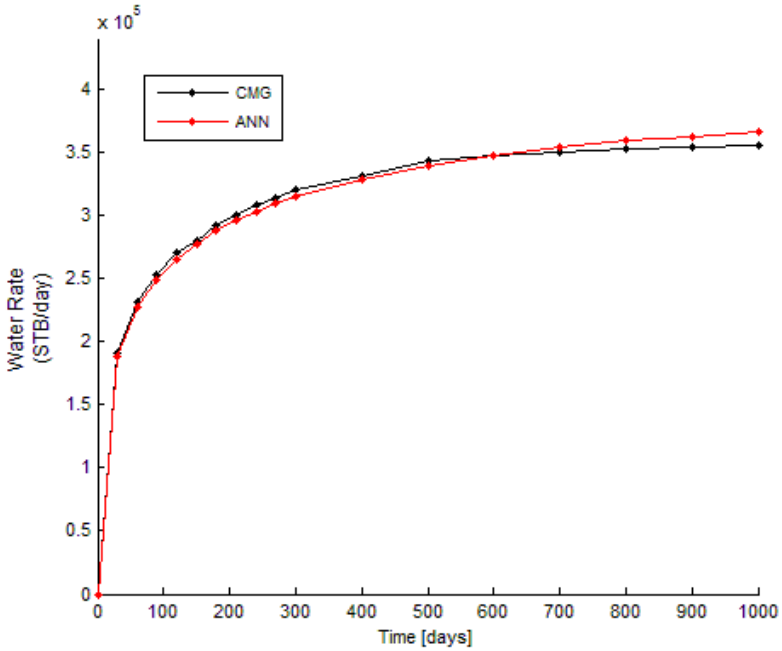

Figure-6.28 Test case #16 for prediction of water production rate

To sum up, most results of test cases show promise, although test case #1, 9, and 30 have large prediction errors. Most test cases produce water at early time, but combination of test cases #1, 9, and 30 produce amounts of water at relatively late time, so that the model could not accurately capture water prediction data. The probable cause could be that the ANN model is generalized with early water production pattern.

Table-6.7 Average percentage error for prediction of water production data

# of test case	Average percentage error (%)	
	Cumulative Water Production	Water Production Rate
1	97.6	31.9
2	10.4	7.0
3	1.4	5.1
4	22.3	1.1
5	3.3	2.8
6	1.0	3.5
7	1.2	3.0
8	1.3	1.5
9	**50.0**	**44.1**
10	1.5	2.6
11	16.1	10.0
12	3.8	1.9
13	13.5	5.7
14	13.4	12.4
15	22.8	5.2
16	0.3	1.5
17	1.2	0.5
18	1.7	3.3
19	1.2	0.8
20	4.2	4.9
21	1.0	1.4
22	3.1	1.9
23	1.5	1.7
24	8.8	1.5
25	2.8	3.9
26	3.7	5.9
27	19.8	4.9
28	25.0	6.5
29	3.7	4.0
30	2.4	**20.1**

Note: Yellow-highlighted results are examples discussed.

Prediction of Water Saturation distribution

To view the prediction results, three production time (240, 700, 1000 days) are selected to compare the model prediction of the water saturation profiles with the actual water saturation data. In the Appendix, water saturation profiles at the other time periods are included. Also, to measure overall performance of the model, unlike single porosity model, average percentage errors are presented for each production time and reservoir depth.

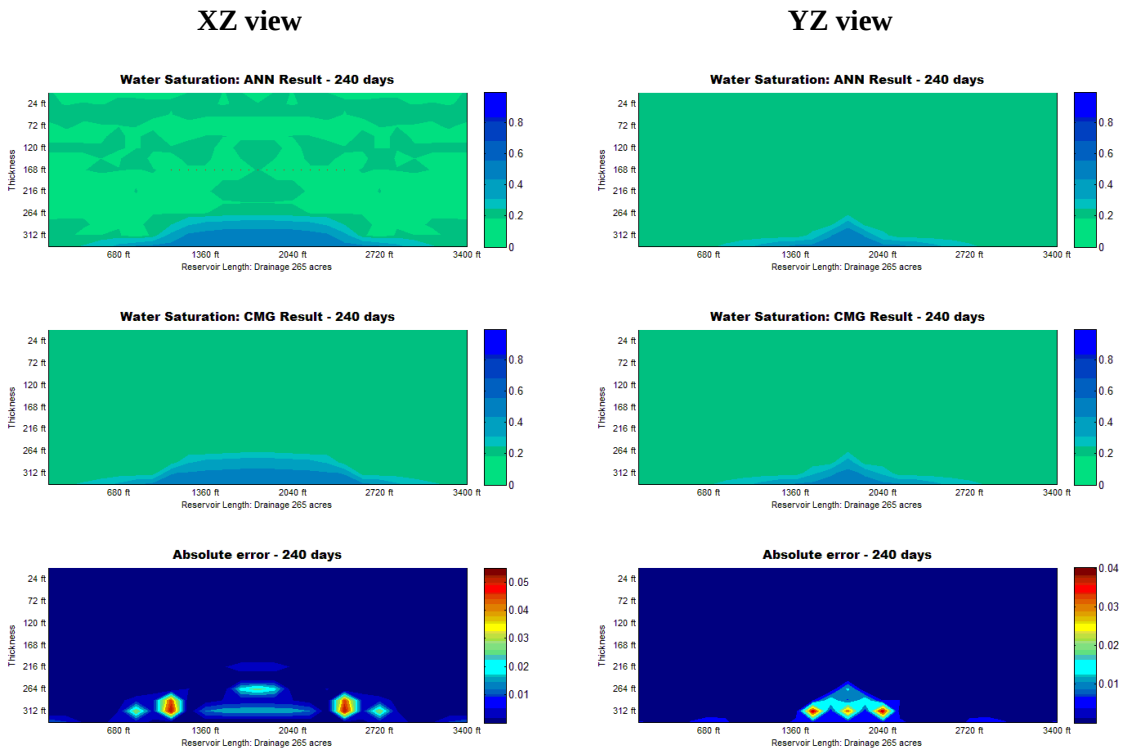

Figure-6.29 Prediction of water saturation for test case #3 at 240 day

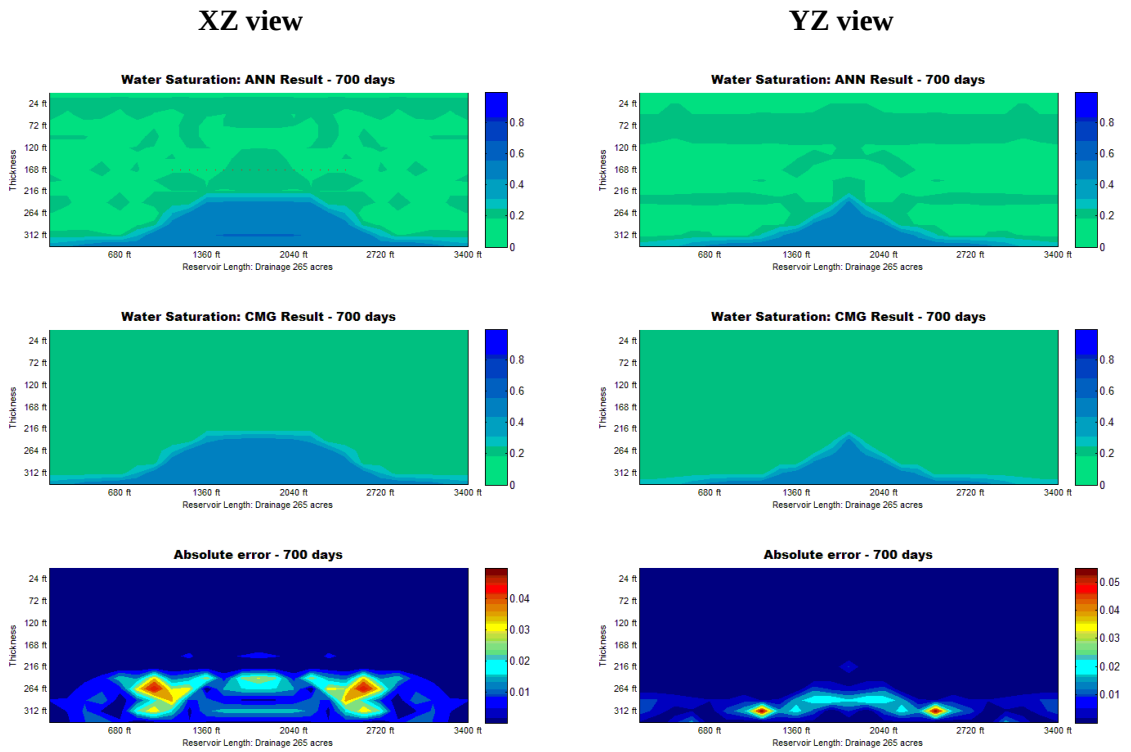

Figure-6.30 Prediction of water saturation for test case #3 at 700 day

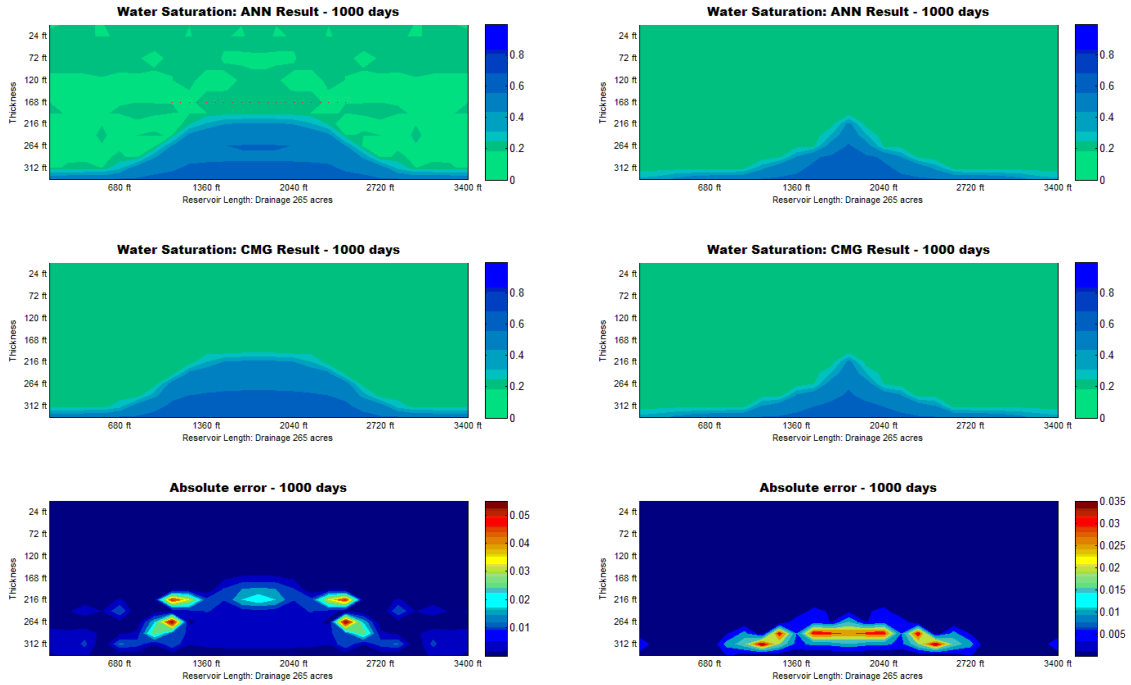

Figure-6.31 Prediction of water saturation for test case #3 at 1000 day

On observing absolute error contour maps, it can be concluded that the water saturation prediction model seems to be doing extremely well in predicting the water saturation values. Maximum absolute errors are less than 0.2. Thus, the results predicted by the ANN is accurate and can be used as a proxy tool for water coning problem provided that reservoir properties is within input ranges. It is also proven that contour map of numerical simulation data has symmetrical aspect in the middle of reservoir plane. Also, inside a water cone, there is minor disparity between numerical simulation data and ANN model results. Nevertheless, the model is able to predict the shape of water cone accurately. Average percentage error for water saturation map for each production time is tabulated followed by average percentage error for 30 test cases for 18 production times.

Table-6.8 Average percentage error for water saturation map of 3 test cases

Production days	Average percentage error (%)	
	X-Z view	Y-Z view
30	0.320	0.341
60	0.354	0.265
90	0.353	0.313
120	0.465	0.289
150	0.575	0.358
180	0.583	0.349
210	0.693	0.394
240	0.747	0.430
270	0.792	0.445
300	0.937	0.462
400	0.893	0.478
500	1.004	0.581
600	1.101	0.604
700	1.228	0.678
800	1.190	0.672
900	1.194	0.783
1000	1.306	0.921

Table-6.9 Average percentage error of water saturation data for 30 test cases

# of test case	Average percentage error (%)	
	Cumulative Water Production	Water Production Rate
1	0.91	0.66
2	0.73	0.38
3	0.53	0.41
4	0.90	0.46
5	1.01	0.54
6	0.49	0.36
7	0.41	0.30
8	1.10	0.72
9	0.52	0.32
10	1.12	0.67
11	0.88	0.56
12	0.98	0.44
13	0.49	0.33
14	1.06	0.60
15	0.83	0.55
16	0.84	0.46
17	1.04	0.56
18	0.72	0.47
19	0.73	0.43
20	1.00	0.55
21	0.99	0.51
22	0.64	0.33
23	0.81	0.45
24	0.86	0.55
25	0.90	0.62
26	0.75	0.44
27	0.62	0.49
28	0.88	0.53
29	1.16	0.71
30	1.44	0.64

6.3 Summary

This study is primarily focused on prediction of production profiles and water saturation distribution for reservoirs with strong water drive. There are two reservoir types used for this study: a single porosity model and a dual porosity model. For each reservoir type, production data, water saturation distribution at a certain production time is predicted by using the artificial neural network. Model developed in this study based on neural networks yield robust outputs compared to data from numerical simulators.

Water cone forms depending on various reservoir conditions and production conditions. And once a water cone reaches the wellbore, high water production begins. Water oil ratio rapidly increases and oil production decreases at a fast rate. There is a critical rate, after which water coning happens near the wellbore. In other words, when specified bottom hole pressure is low, or big differential exists between reservoir pressure and bottom hole pressure, water cones develop at early production times. High vertical permeability tends to cause water vertically to reach the wellbore while high horizontal permeability causes water to spread horizontally. Additionally in a naturally fractured reservoir (dual porosity model), fracture permeability accelerates water encroachment. It is seen that fracture acts as a conduit for water flow resulting in high water production. Thus, a well in dual porosity reservoir produces more water and also at a much earlier production period than a well in single porosity reservoir. Drainage area is a factor while analyzing water encroachment. For small drainage areas, level of high water saturation area spreading horizontally increases faster than for large drainage areas. In addition, location of the well perforation is another factor that influences water production. When well perforation is close to oil water contact, it is highly likely that water production happens earlier than in cases where the perforations are far away from the oil water contact.

Bayesian Regulation algorithm is predominantly used in this study owing to its accuracy in capturing both production profiles and water coning behavior. Even though Bayesian Regulation algorithm requires longer training times to converge, results obtained are in good agreement with data from numerical simulations. In particular, results of water saturation prediction show robustness.

Testing errors between the ANN outputs and numerical model is less than 5% in case of a dual porosity model. There are reservoir cases for the single porosity models that prediction of production data resulted in high percentage errors. Some prediction errors originated from input variables of reservoir cases that barely produce water during the production period. On occasions when the water coning phenomenon is delayed, the model tends to under predict the water evolution which in turn results in large errors. Rather, the ANN can be useful to generalize the frequently occurring pattern within the range of reservoir cases considered.

To summarize, the model developed in this work is able to capture the water coning phenomenon and can be used to forecast production. Through the extensive results, it is evident that ANN based model can act as a powerful proxy tool for rapid analysis to predict production profile and water saturation distribution. This tool would be extremely helpful for an engineer to perform rapid evaluation and screen out efficiency of various completion scenarios that result in water coning. A comprehensive analysis could be performed via various sensitivity studies.

Appendix A

Graphic User Interface (GUI)

Graphic User Interface (GUI) makes it easy for a user to understand water coning behavior with respect to various input parameters. In the main GUI, users can choose the type of the reservoir and prediction. The GUI consists of two model groups that have two prediction type subgroups. Model based ANN prediction can be visualized using this tool.

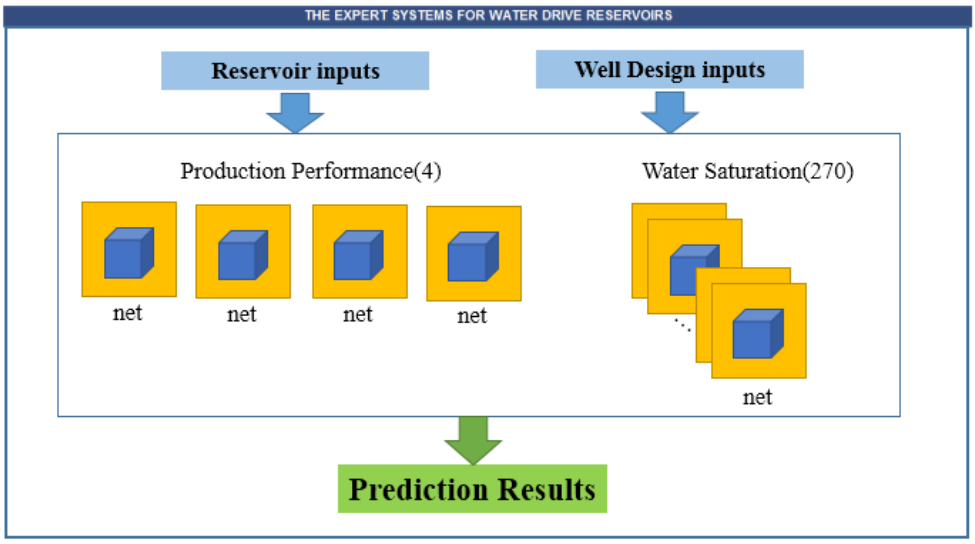

Figure-A.1 Schematic of the GUI

Input variables for reservoir parameters are oil density, water density, water viscosity, horizontal & vertical permeability, reservoir thickness, initial pressure and drainage area. In addition, users need to provide horizontal well design configuration such as well starting point in x-direction, location of horizontal well, and total flow rate (or bottom hole pressure). By setting those parameters, followed by clicking “Horizontal well design” button, the horizontal well in the reservoir is shown on the additional GUI panel, total reservoir thickness, and well length are automatically calculated in the shaded textbox.

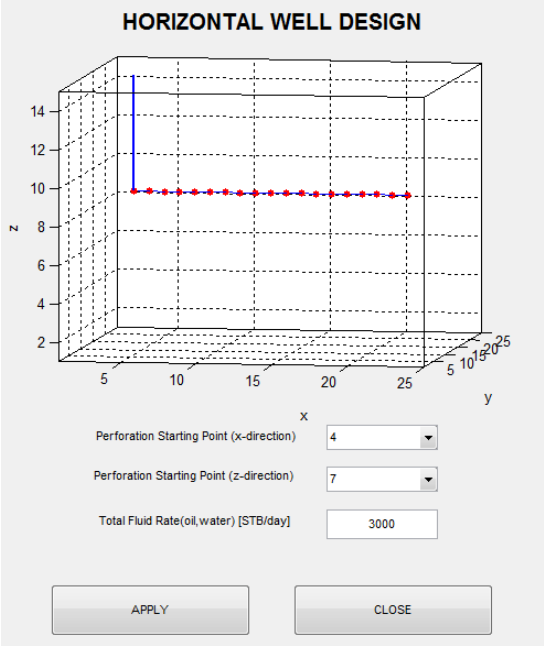

Figure-A.2 GUI for horizontal well design

Once input variables are entered appropriately or simply pushing "EXAMPLE" pushbutton, and then click on "UPDATE" pushbutton for updating the input variables. Then by clicking "SIMULATE" pushbutton after providing the input variables, prediction starts and after few seconds, the completion window pops up on the screen as indicated in Figure A.3. The results are oil production data and water production data for dual porosity model and oil production data for single porosity model. To view production data, change the radio button to either "oil" or "water", then push "PLOT' button. "TABLE" button instantly display the numerical values of the predicted data.

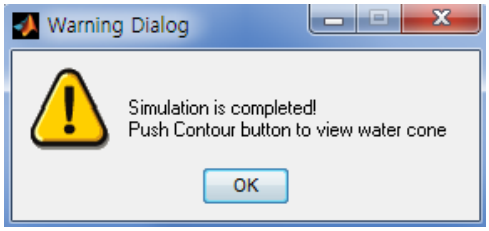

Figure-A.3 Popup window for prediction completion

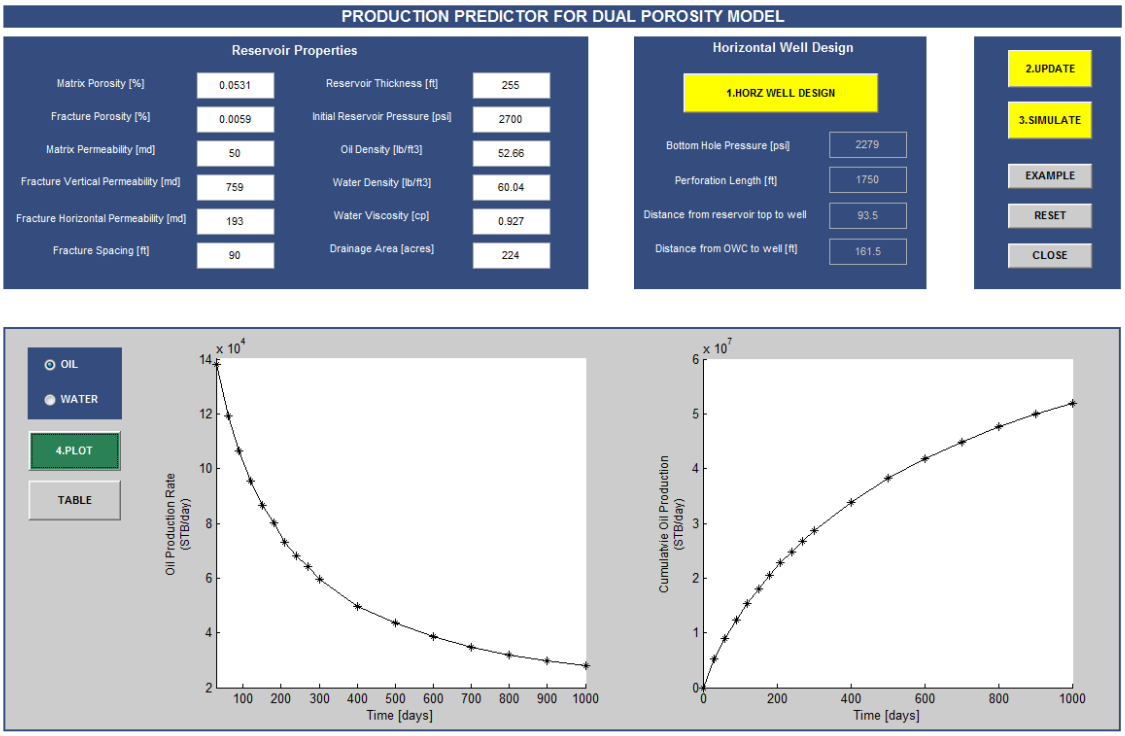

Figure-A.4 GUI for production prediction of a dual porosity model

To predict water saturation for a given reservoir and specified production time, the input variables are to be supplied and on updating the input variables, push the "SIMULATE" pushbutton. Normally, prediction might take a few minutes for each production time based on hardware specifications of the machine. Once the completion window pops up, users can view the specific water saturation distribution at certain production time. First, choose the production time, then push either " 2D CONTOUR" or "3D CONTOUR" button to view the water saturation in two and three dimensional view respectively. Additionally "Data-Cursor" and "Insert Colorbar" icon in the top of the GUI is provided for a user to identify water saturation values at any desired location. In the upper menu bar, the range of input variables are inserted as a reference for input selections.

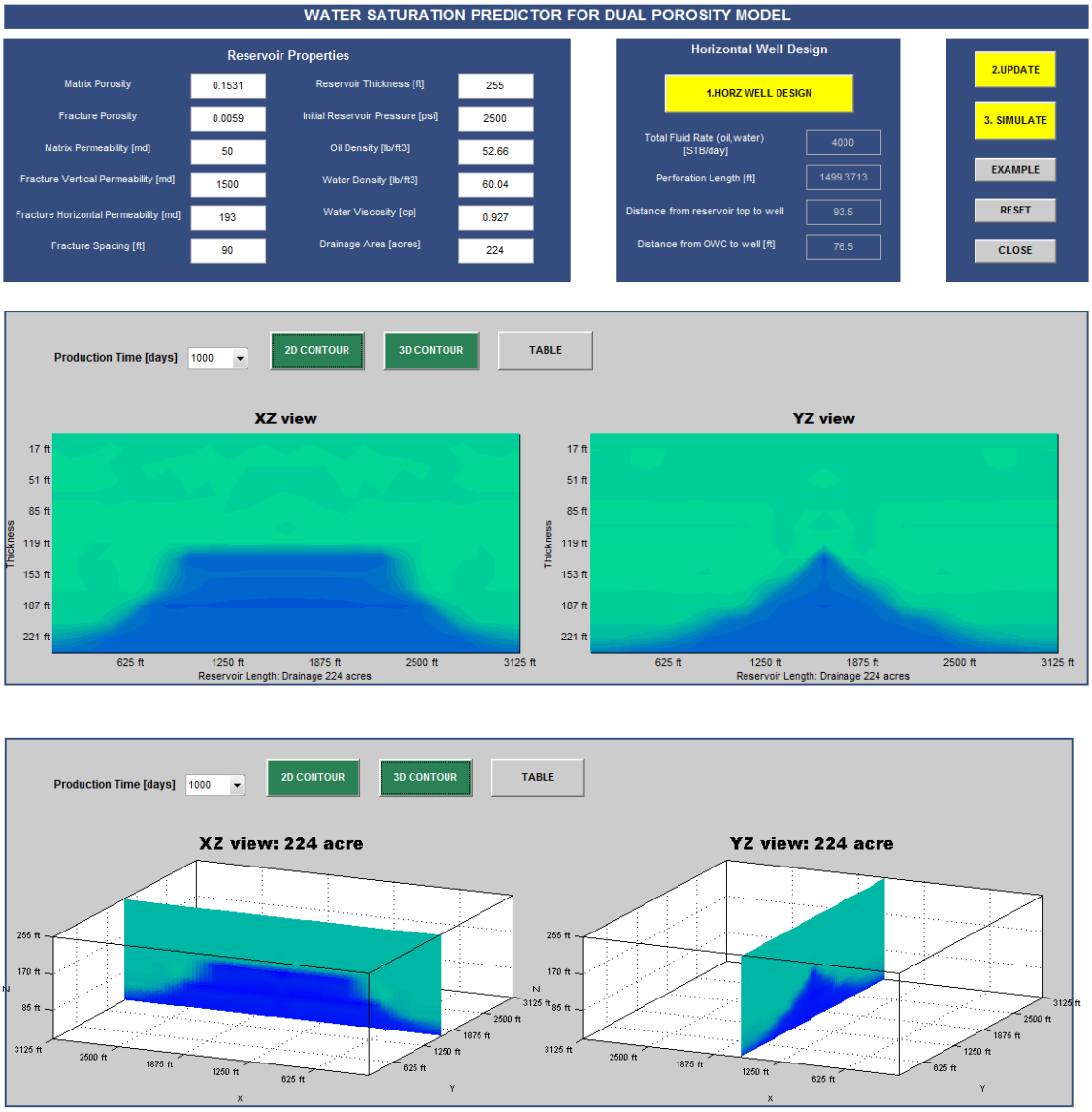

Figure-A.5 GUI for water saturation prediction of a dual porosity model

Table-A.1 Relative Permeability for single porosity reservoir

S_w	k_{rw}	k_{row}
0.2	0	1
0.25	0.0004	0.6027
0.3	0.0024	0.449
0.35	0.0075	0.3242
0.4	0.0167	0.2253
0.45	0.031	0.1492
0.5	0.0515	0.0927
0.6	0.1146	0.0265
0.7	0.2133	0.0031
0.8	0.3542	0.001
0.9	0.5438	0.0005
1	0.7885	0

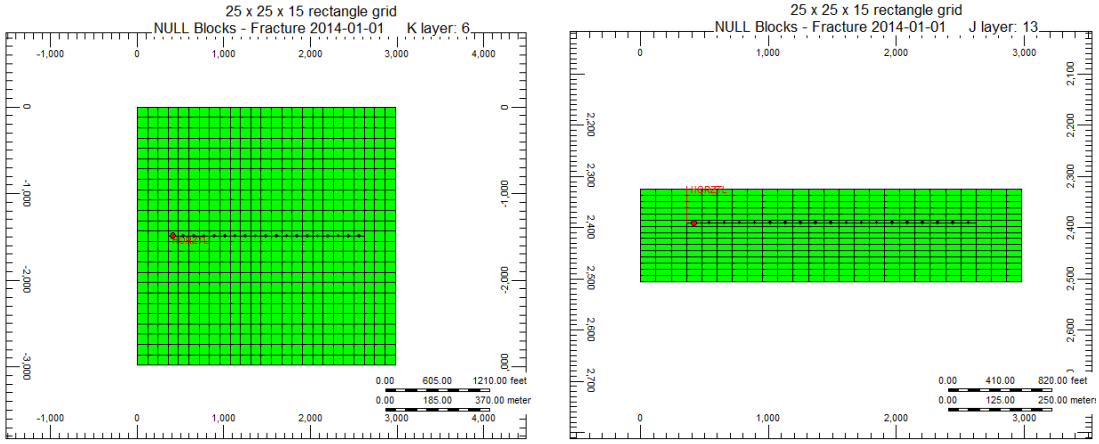

Figure-A.6 Overview of reservoir and horizontal well

Appendix B

Water saturation data (single porosity model)

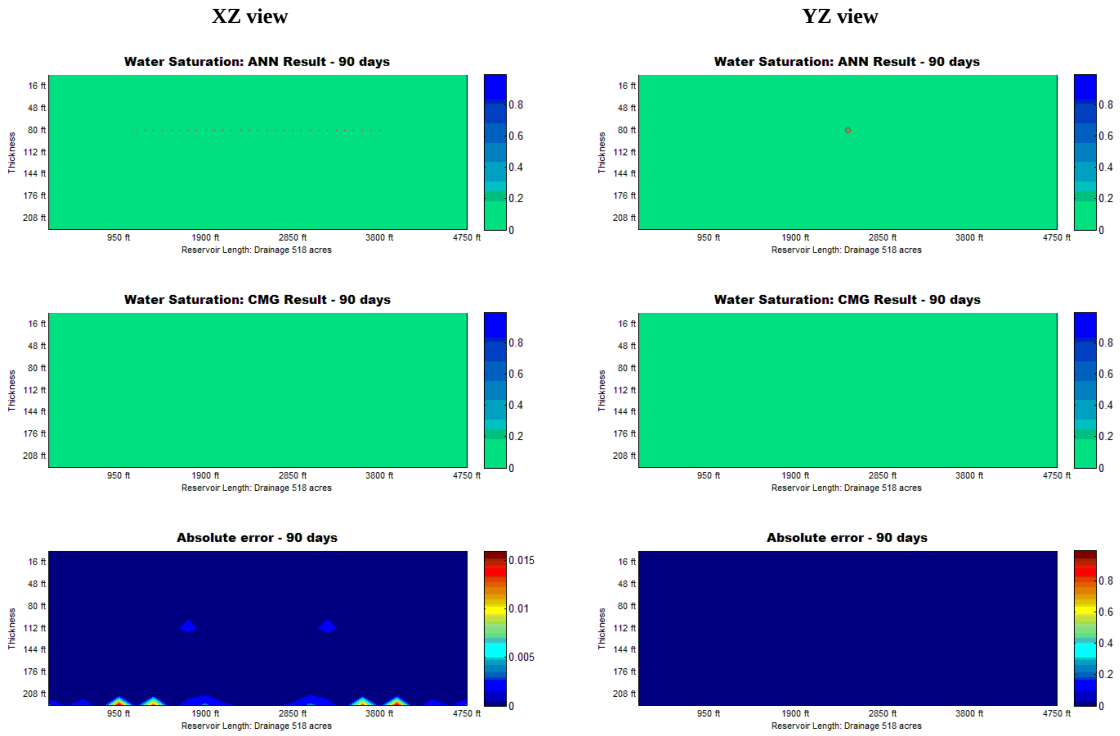

Figure-A.7 Prediction of water saturation for test case #3 at 90 day

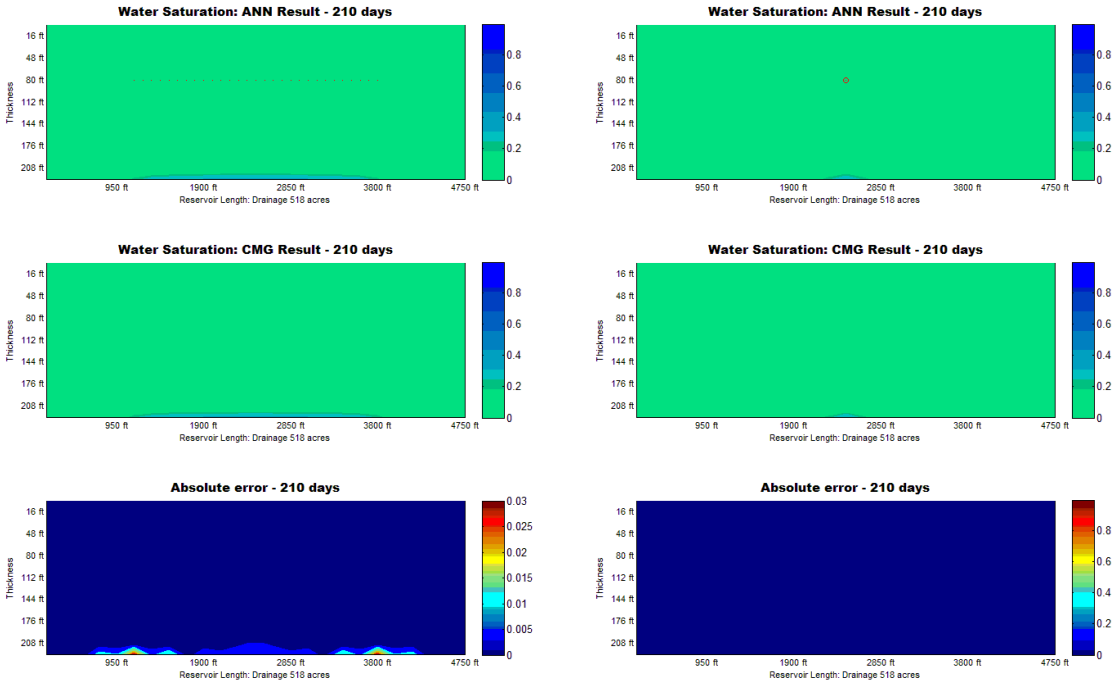

Figure-A.8 Prediction of water saturation for test case #3 at 210 day

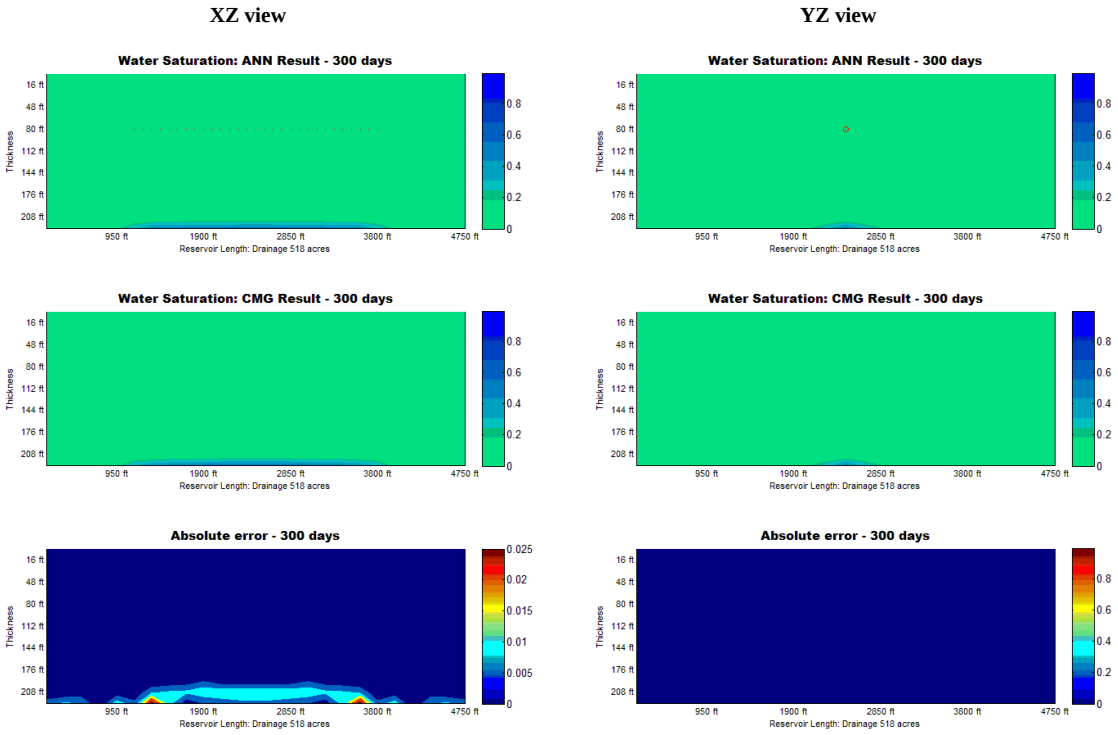

Figure- A.9 Prediction of water saturation for test case #3 at 300 day

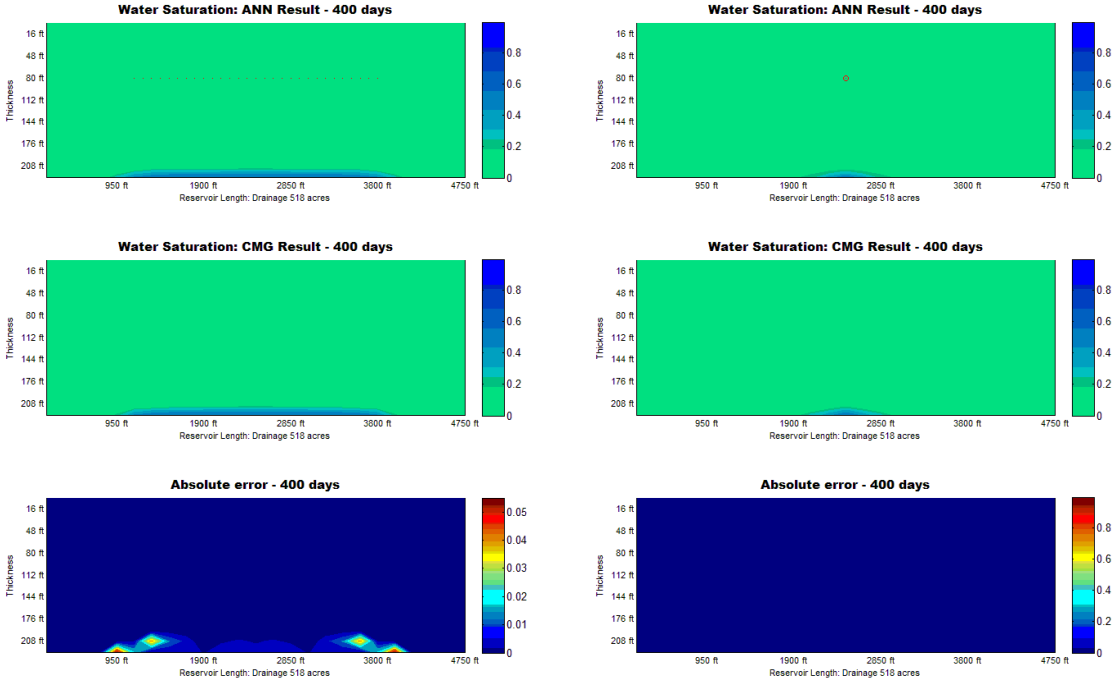

Figure- A.10 Prediction of water saturation for test case #3 at 400 day

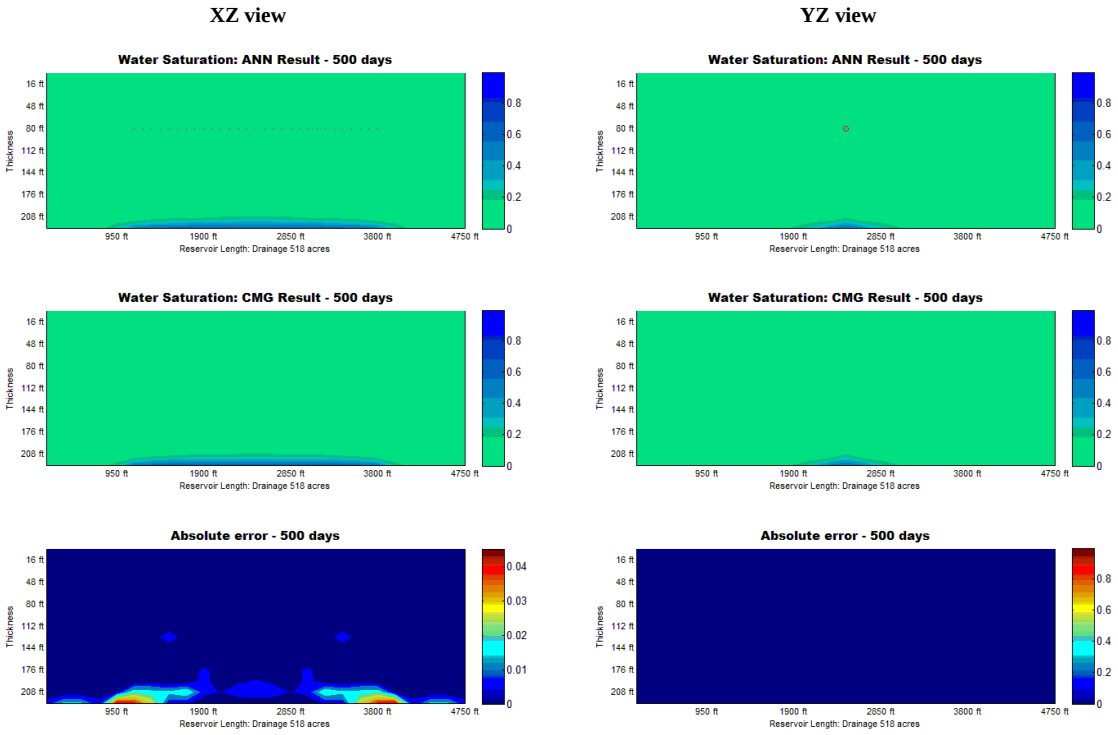

Figure-A.11 Prediction of water saturation for test case #3 at 500 day

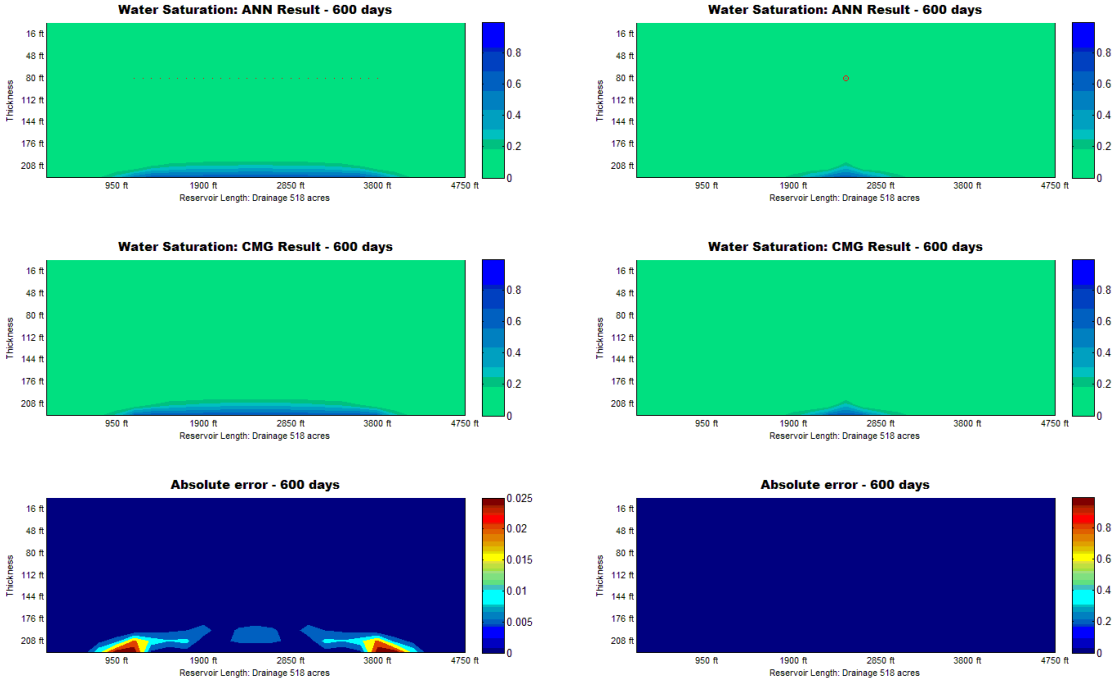

Figure-A.12 Prediction of water saturation for test case #3 at 600 day

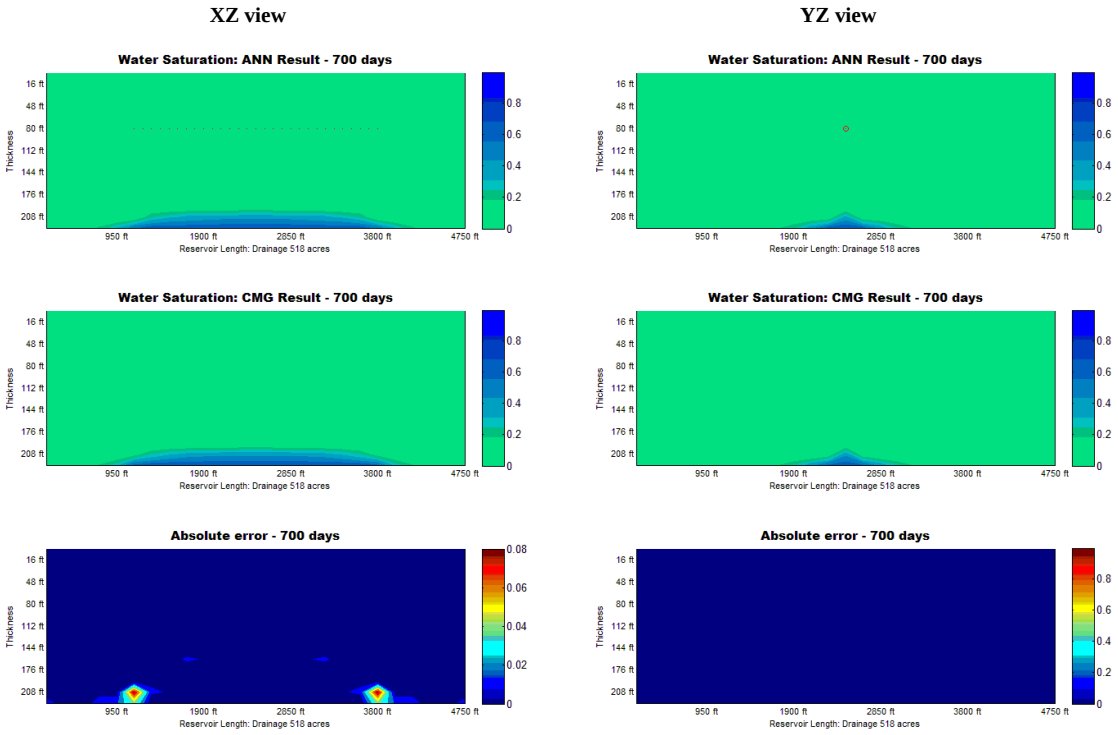

Figure- A.13 Prediction of water saturation for test case #3 at 700 day

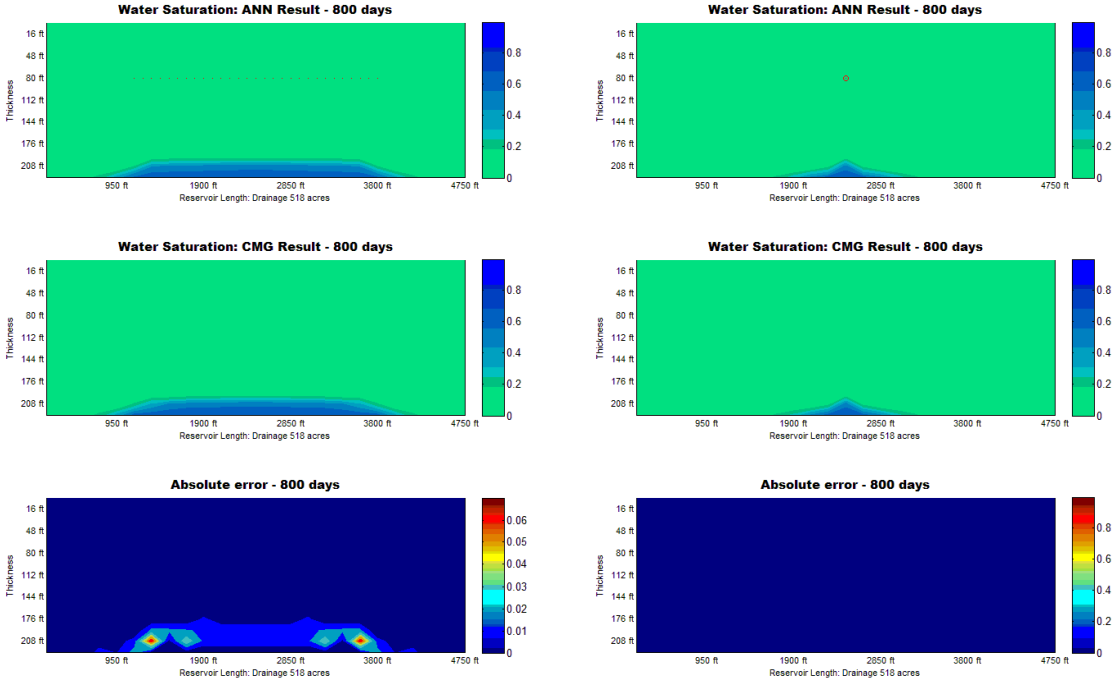

Figure- A.14 Prediction of water saturation for test case #3 at 800 day

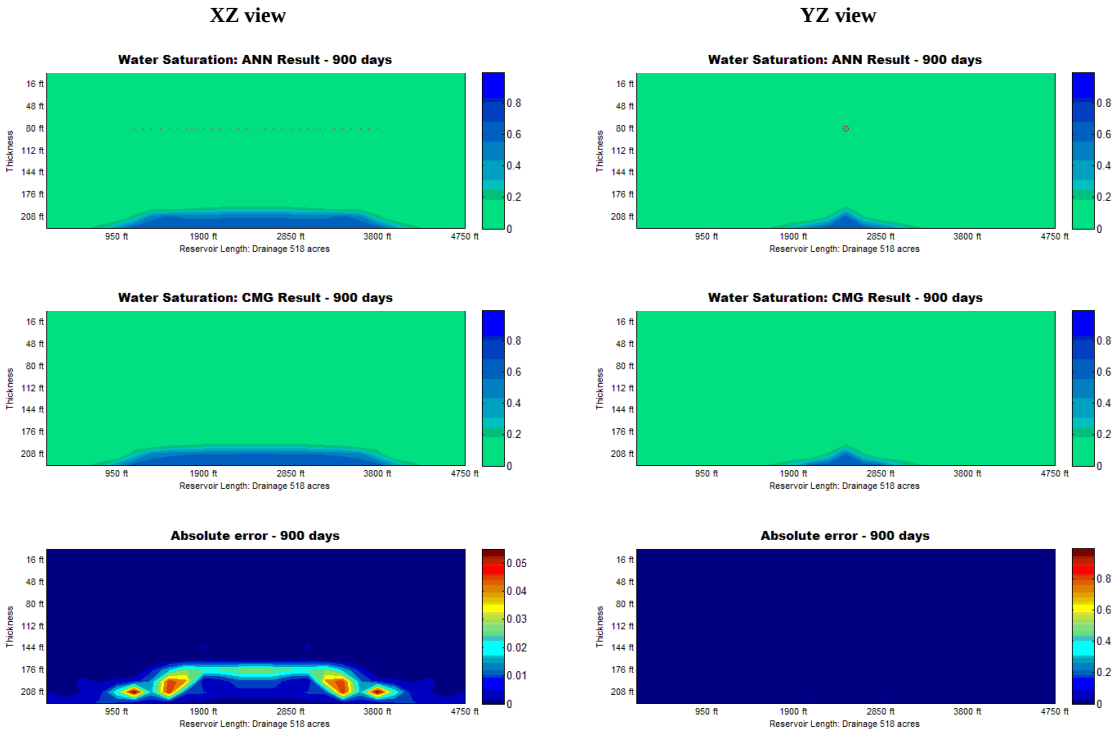

Figure- A.15 Prediction of water saturation for test case #3 at 900 day

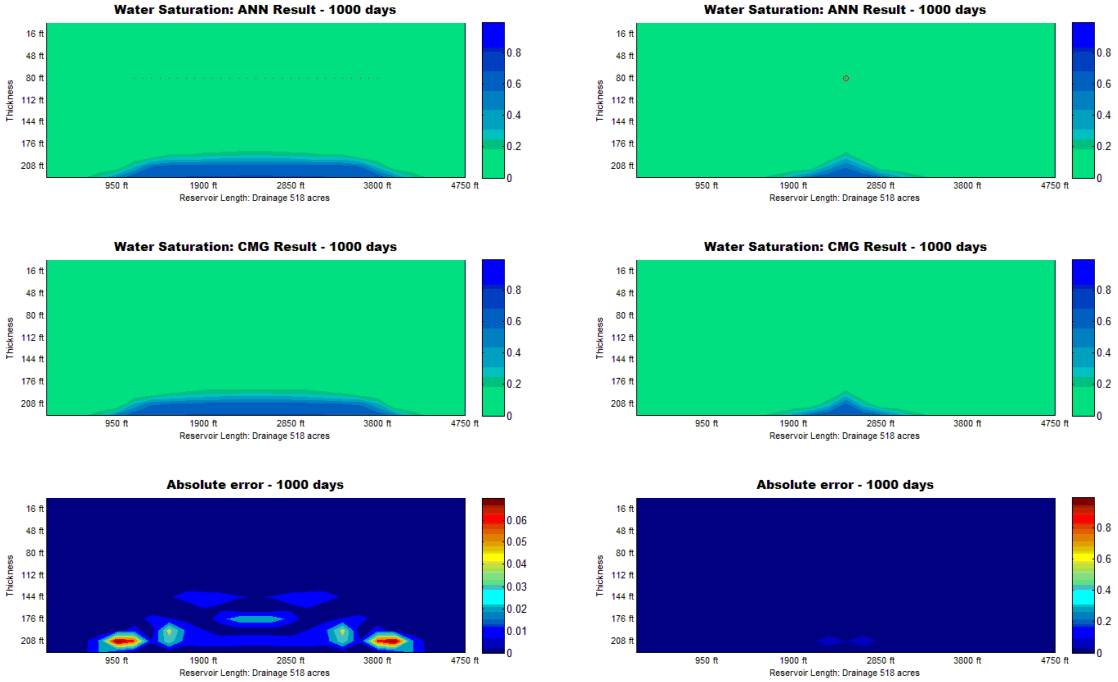

Figure- A.16 Prediction of water saturation for test case #3 at 1000 day

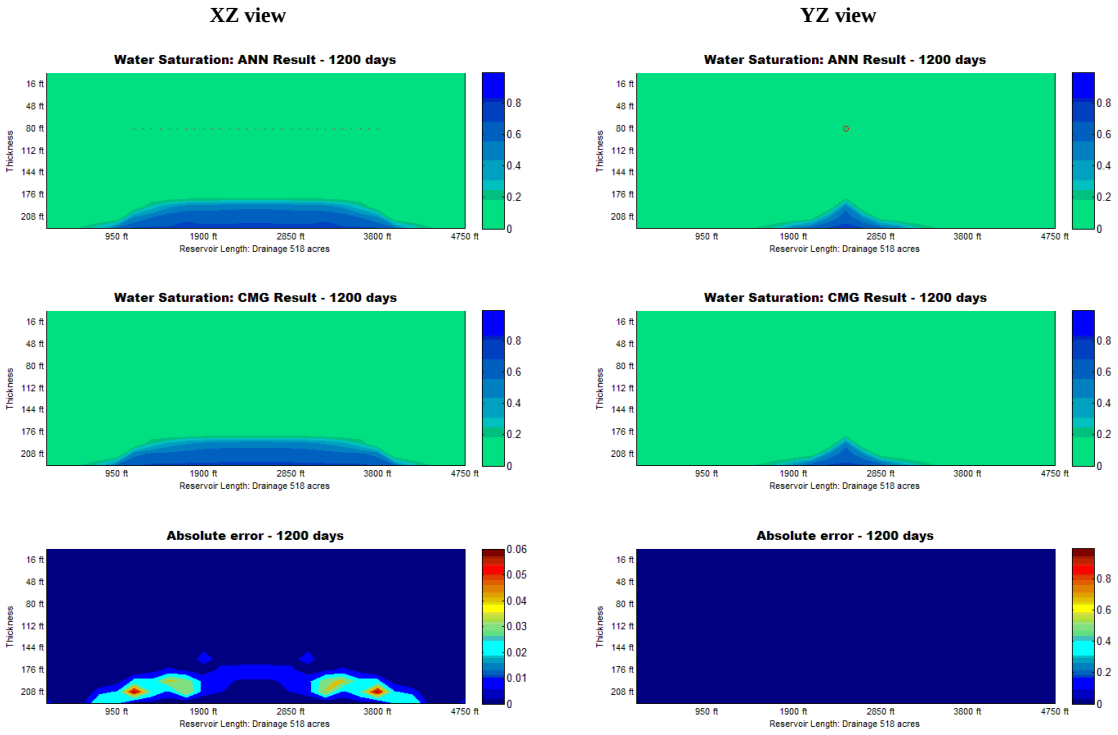

Figure- A.17 Prediction of water saturation for test case #3 at 1200 day

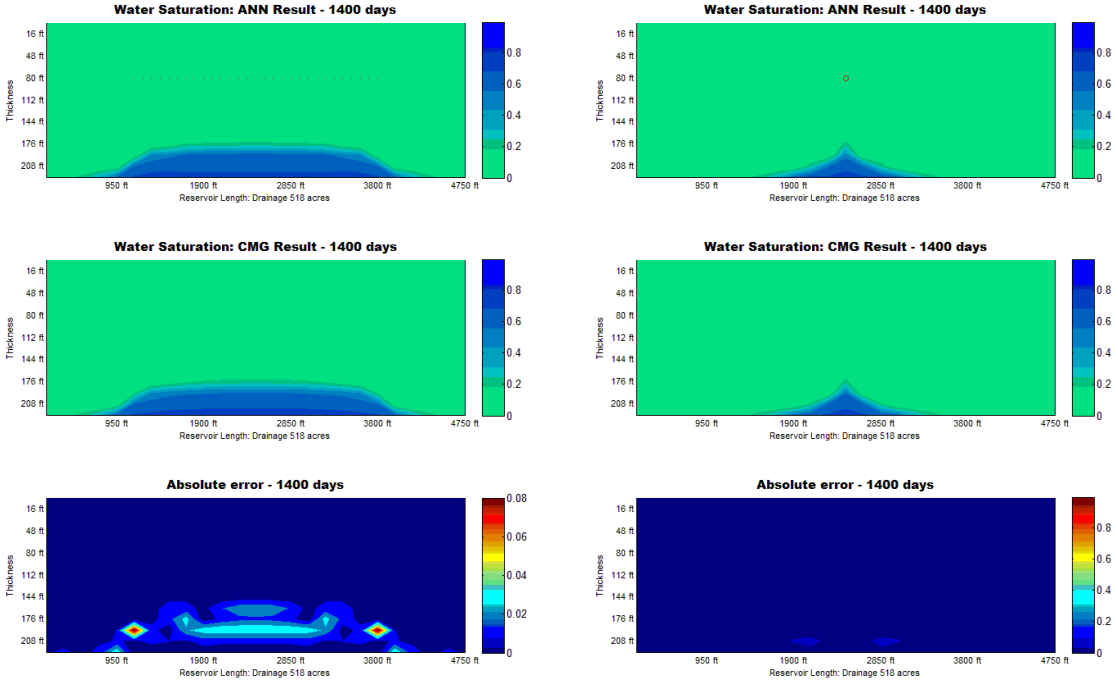

Figure- A.18 Prediction of water saturation for test case #3 at 1400 day

XZ view **YZ view**

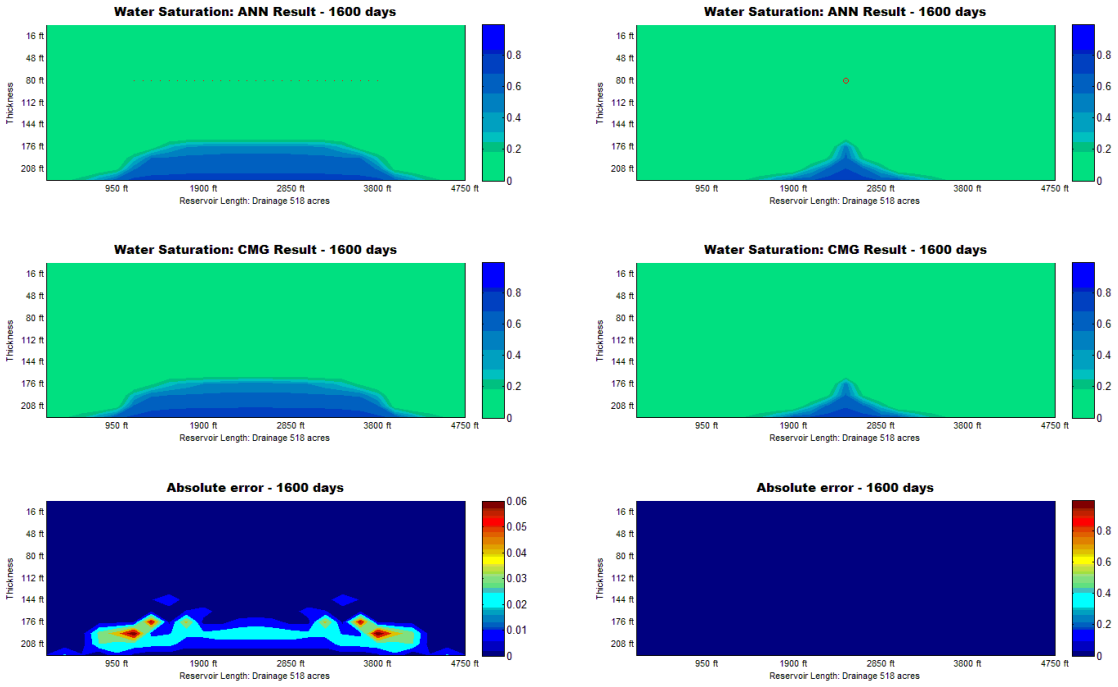

Figure- A.19 Prediction of water saturation for test case #3 at 1600 day

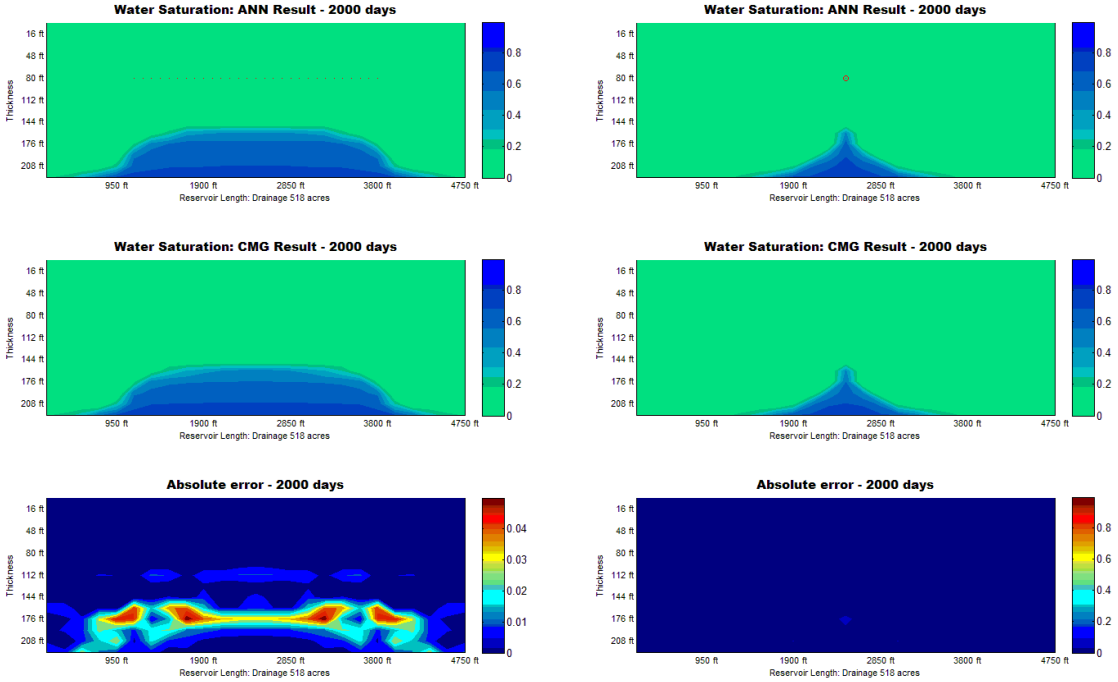

Figure- A.20 Prediction of water saturation for test case #3 at 2000 day

XZ view **YZ view**

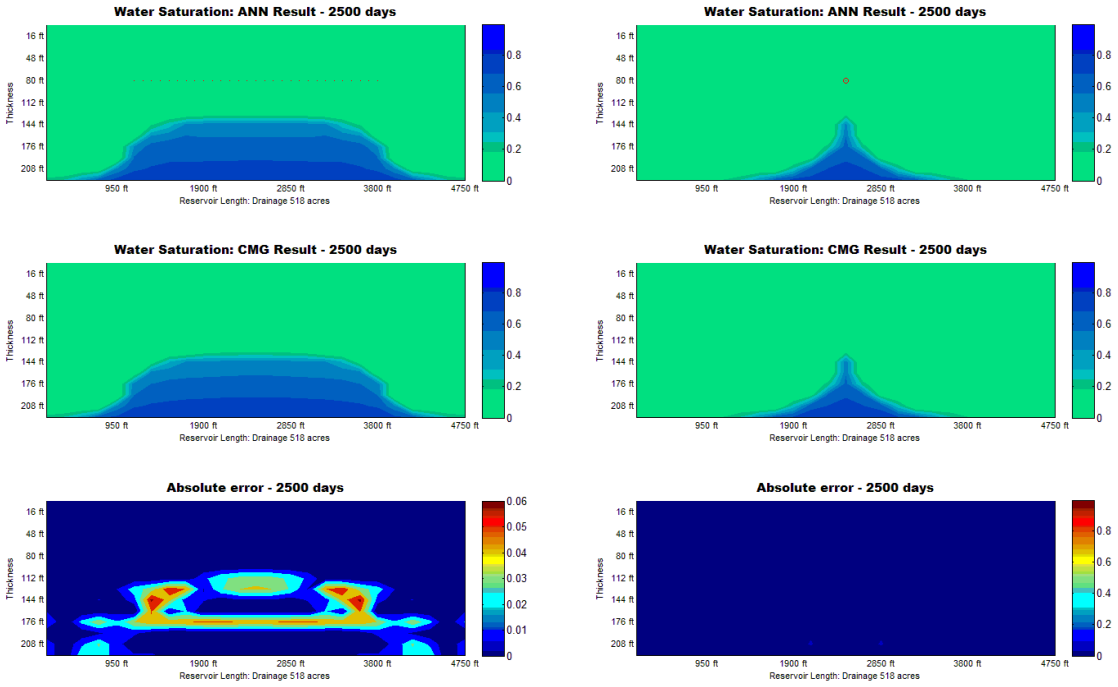

Figure- A.21 Prediction of water saturation for test case #3 at 2500 day

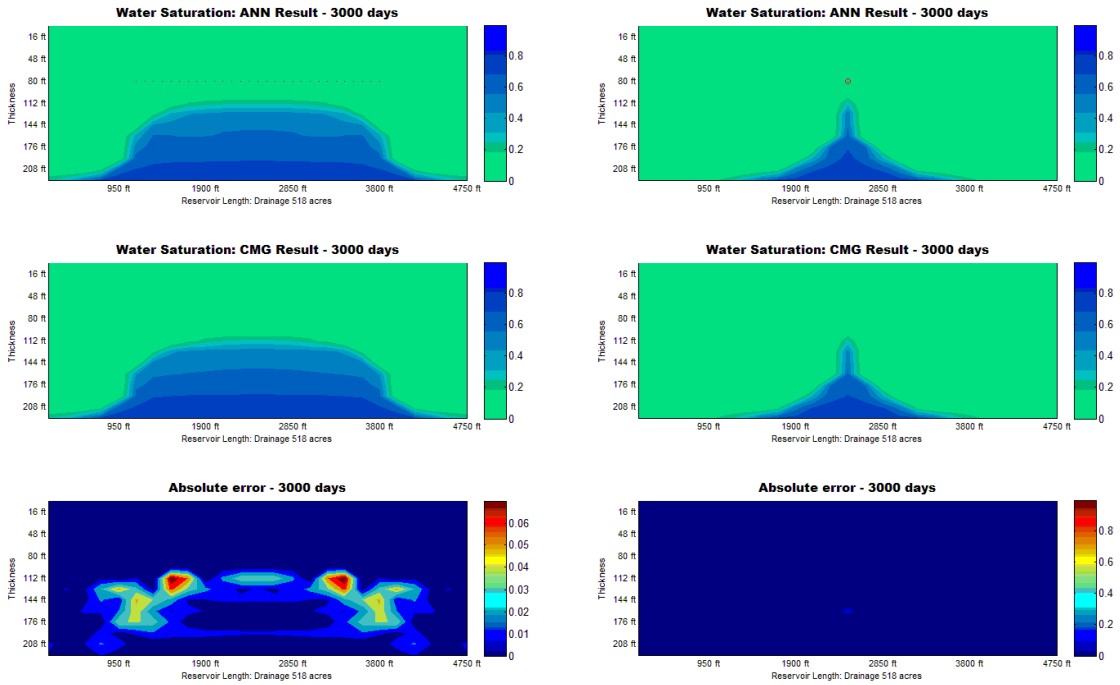

Figure- A.22 Prediction of water saturation for test case #3 at 3000 day

Appendix C

Water saturation data (dual porosity model)

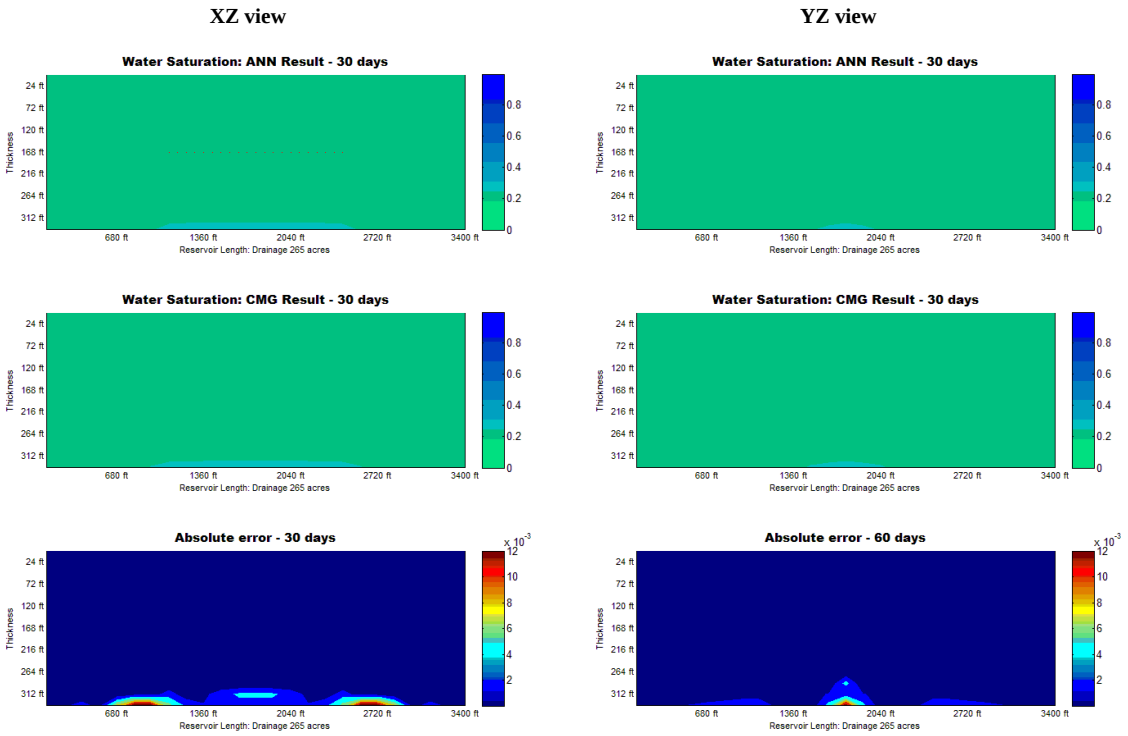

Figure-A.23 Prediction of water saturation for test case #3 at 30 day

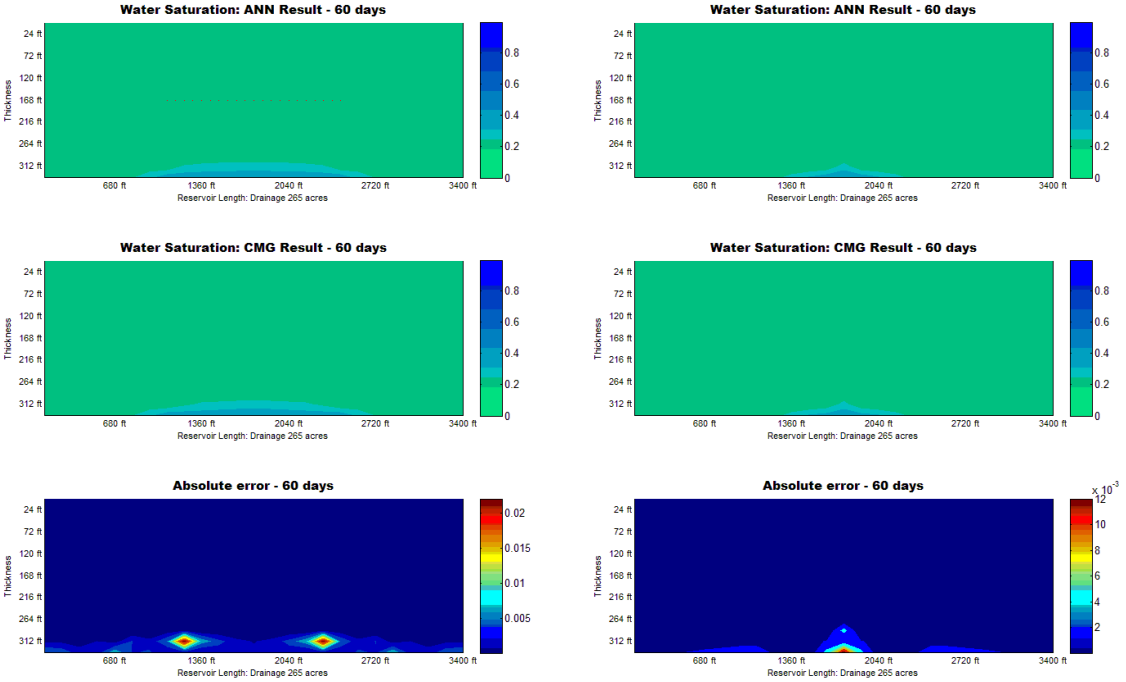

Figure-A.24 Prediction of water saturation for test case #3 at 60 day

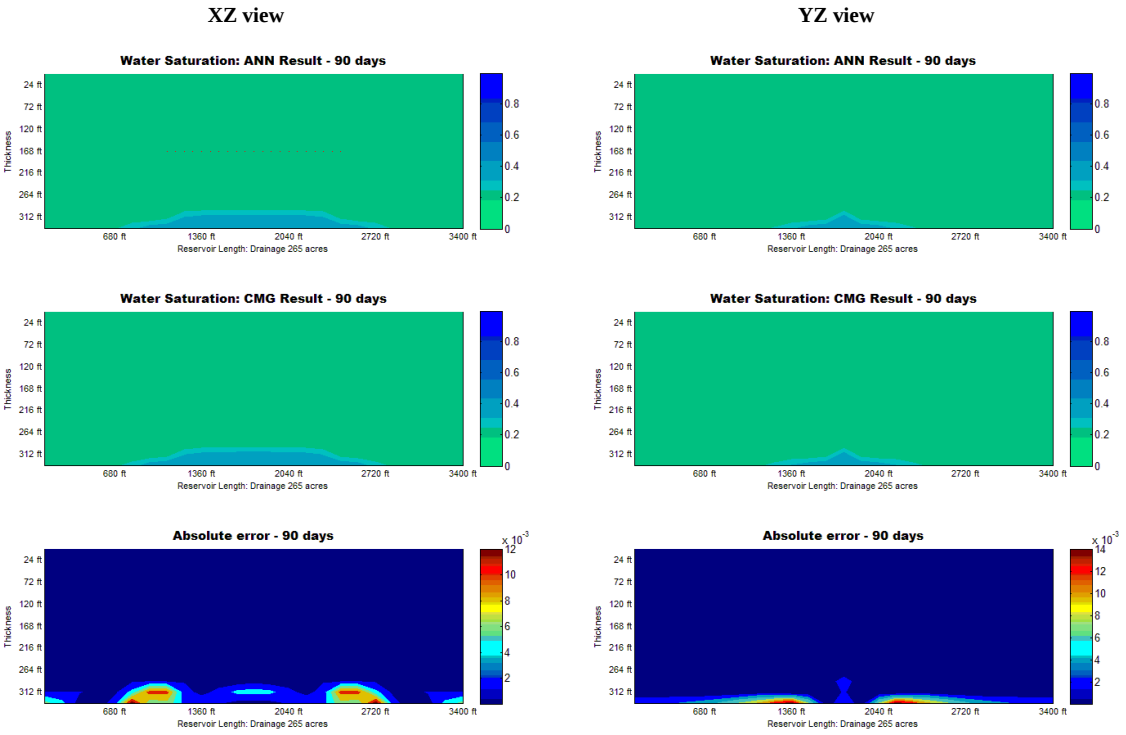

Figure- A.25 Prediction of water saturation for test case #3 at 90 day

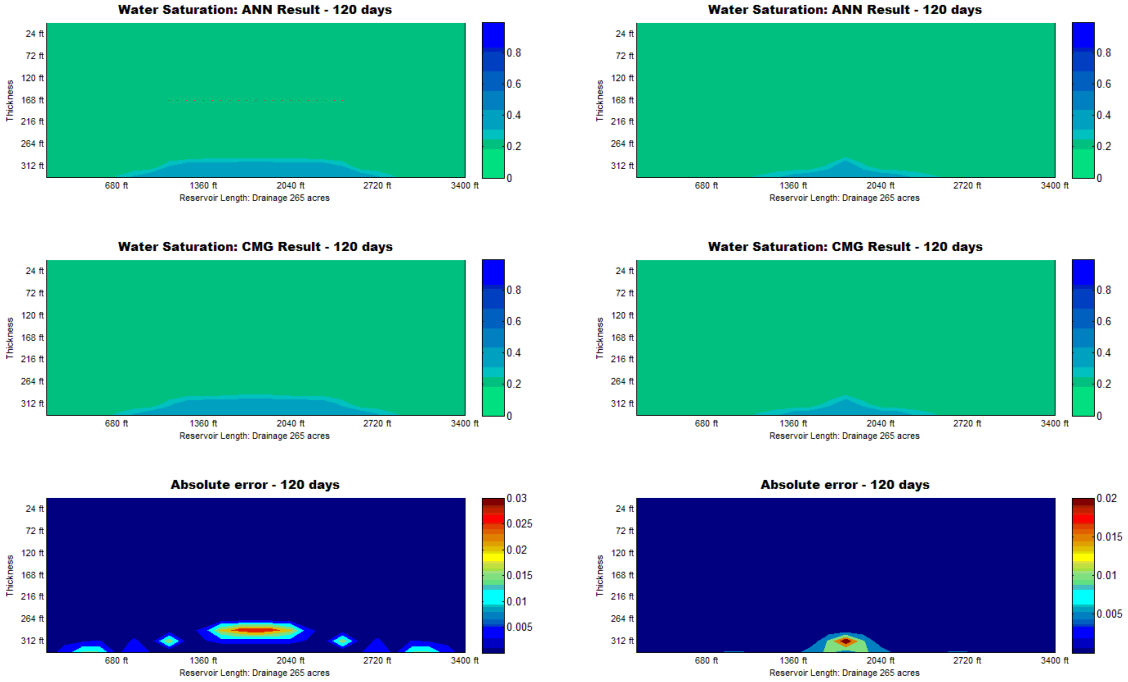

Figure- A.26 Prediction of water saturation for test case #3 at 120 day

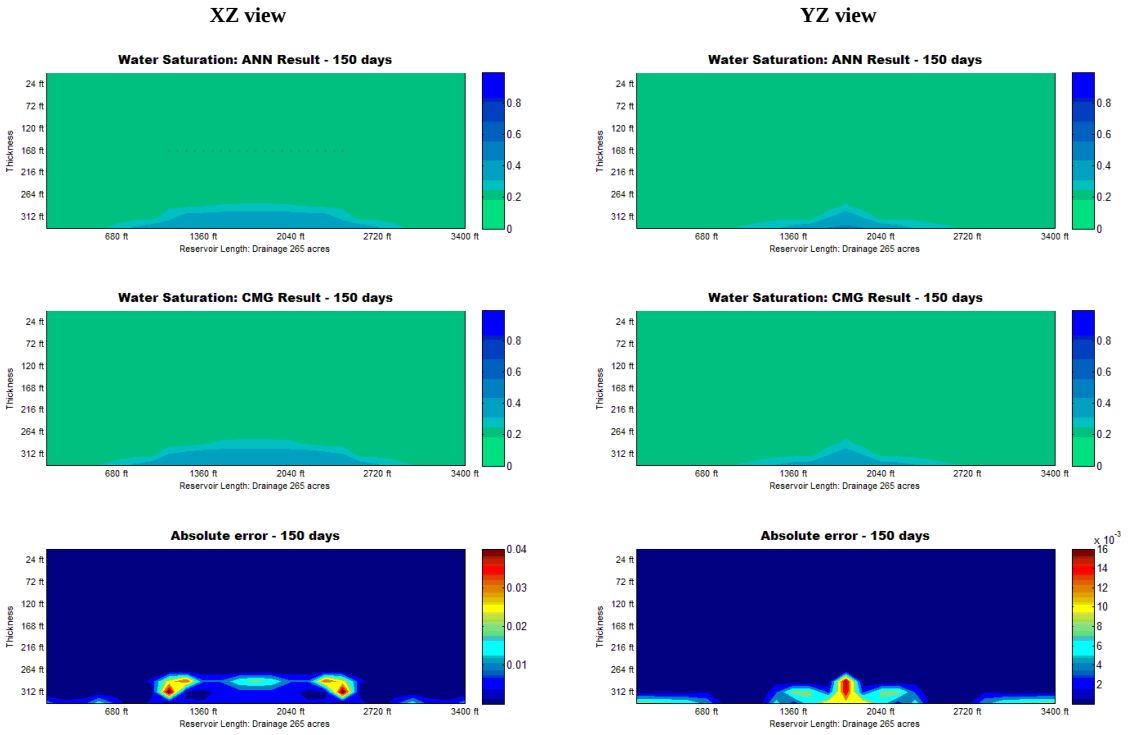

Figure-A.27 Prediction of water saturation for test case #3 at 150 day

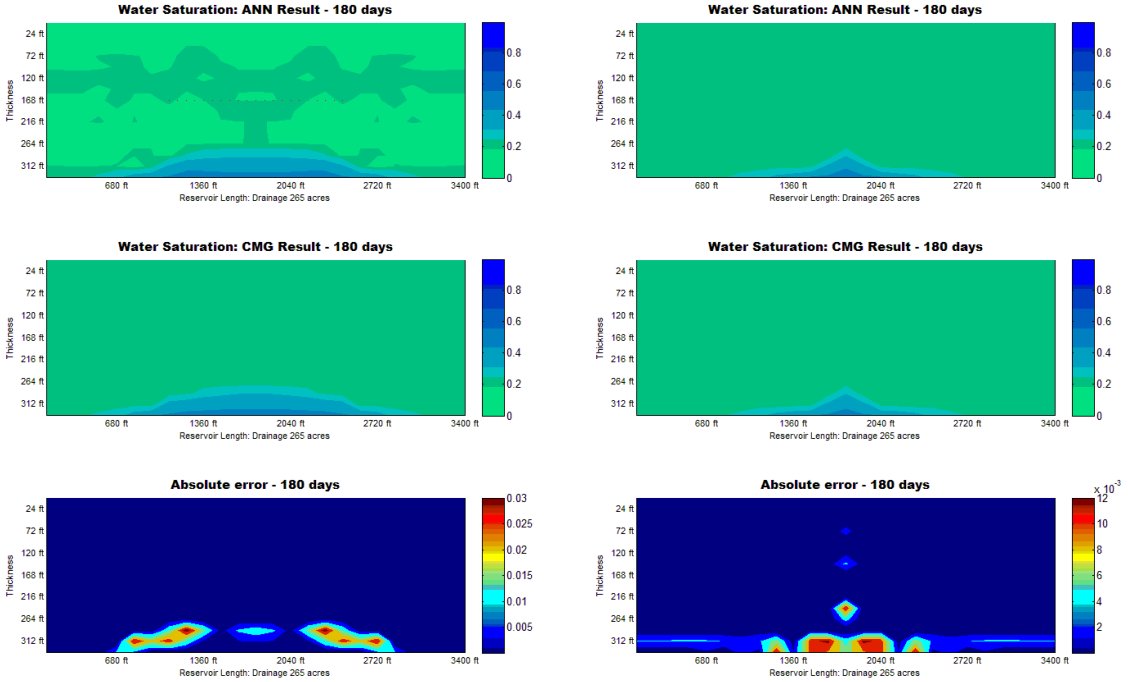

Figure-A.28 Prediction of water saturation for test case #3 at 180 day

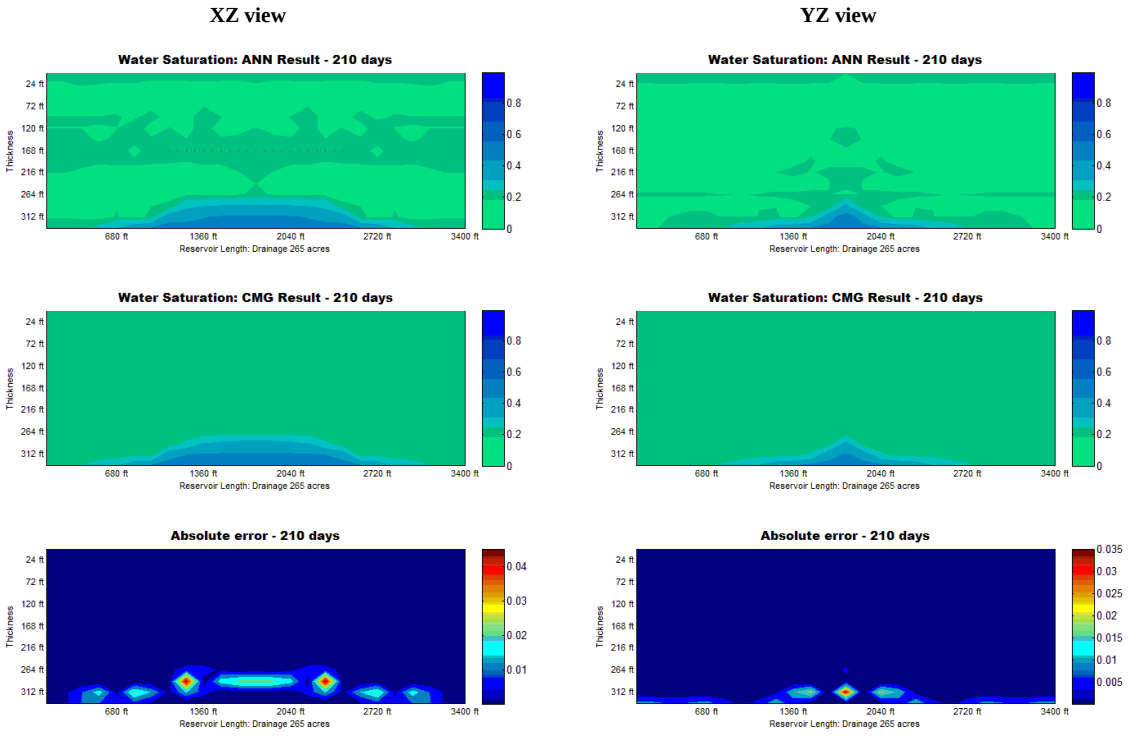

Figure- A.29 Prediction of water saturation for test case #3 at 210 day

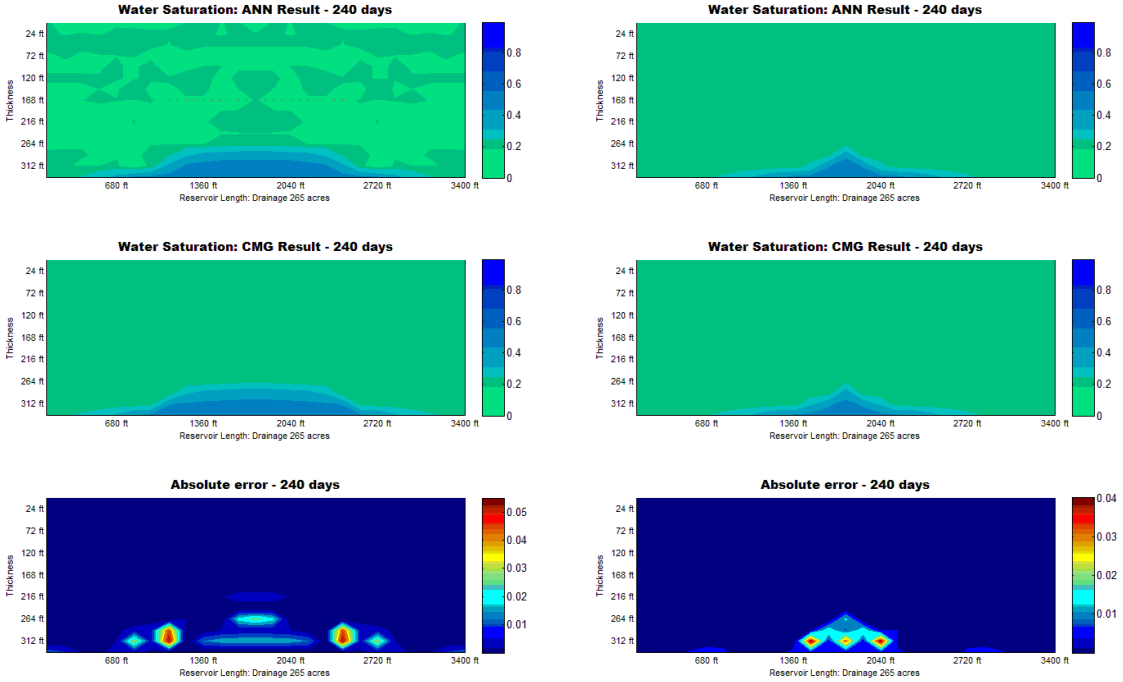

Figure- A.30 Prediction of water saturation for test case #3 at 240 day

XZ view **YZ view**

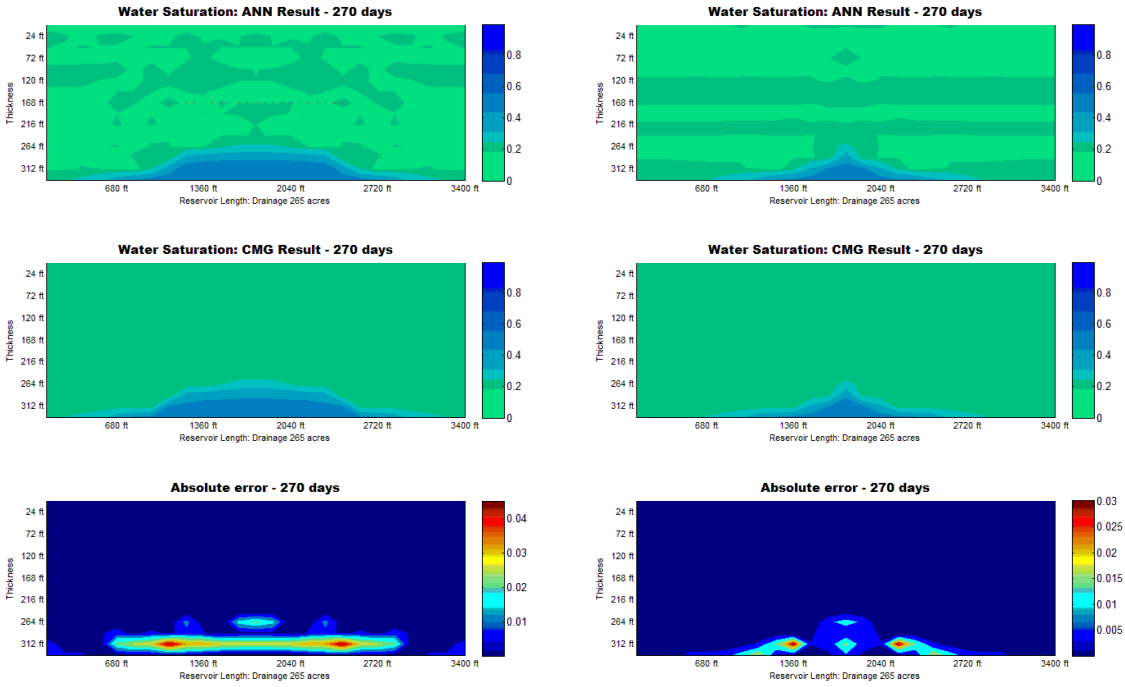

Figure- A.31 Prediction of water saturation for test case #3 at 270 day

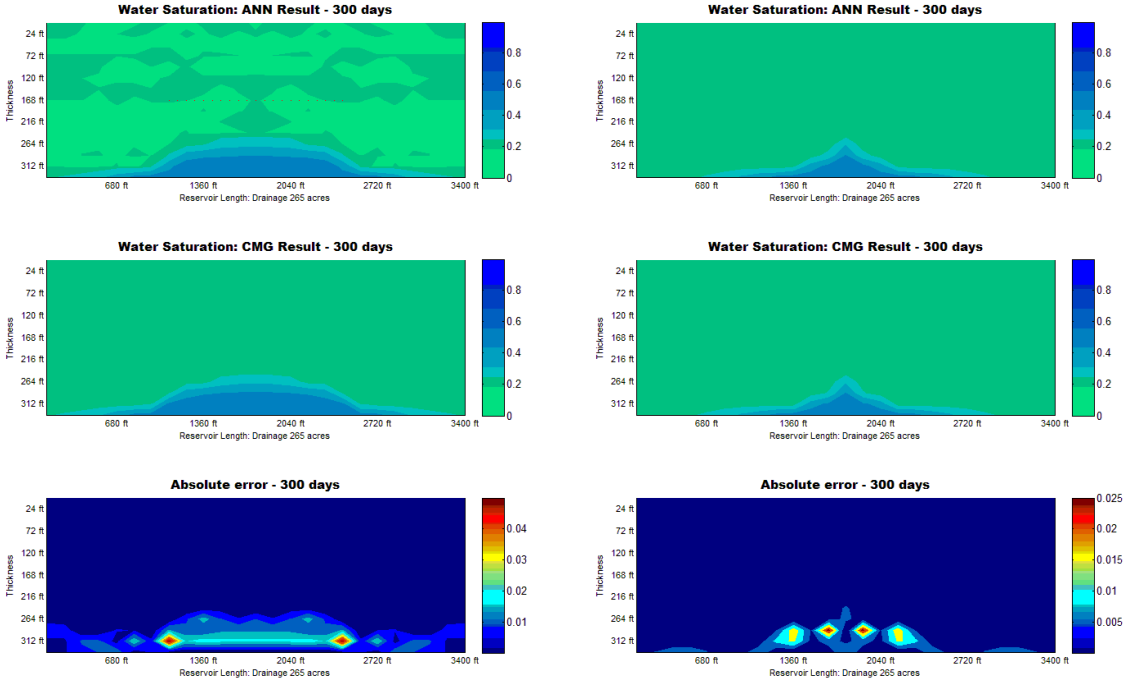

Figure- A.32 Prediction of water saturation for test case #3 at 300 day

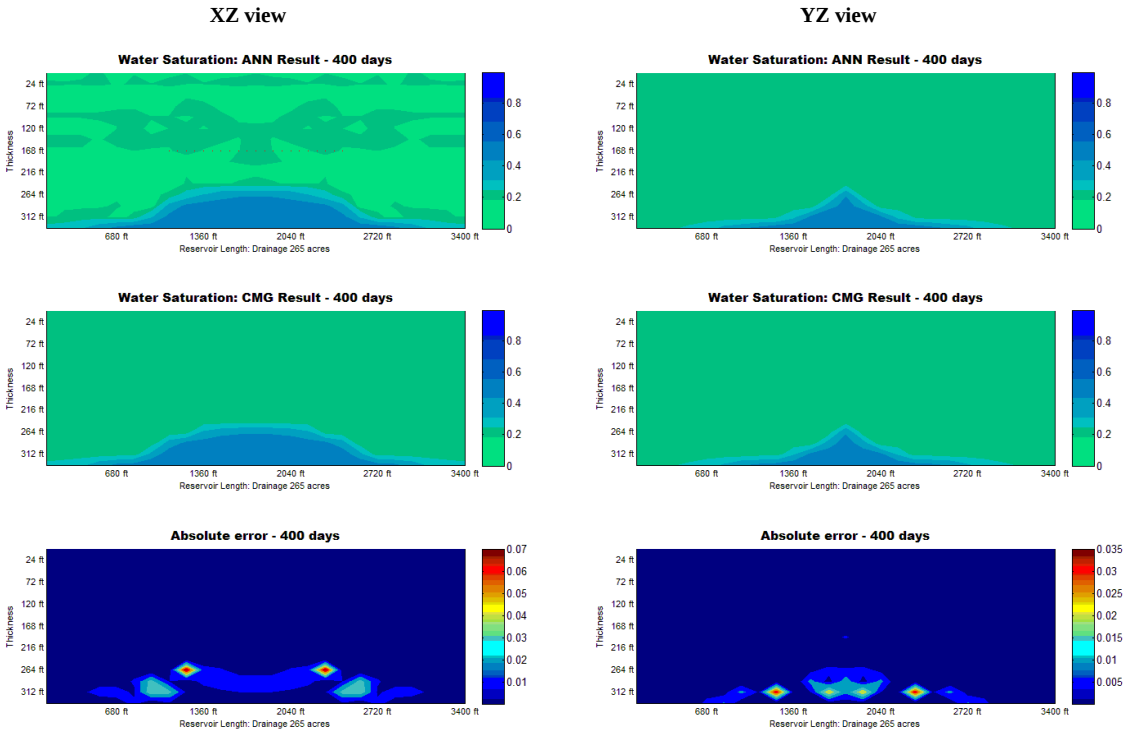

Figure- A.33 Prediction of water saturation for test case #3 at 400 day

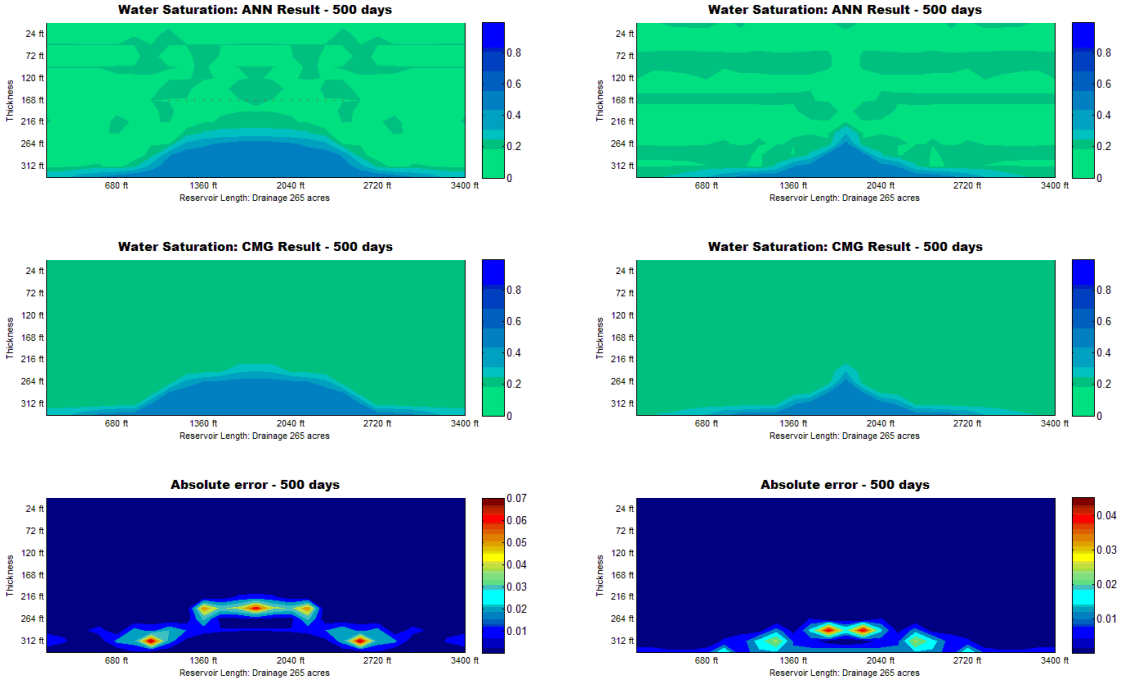

Figure- A.34 Prediction of water saturation for test case #3 at 500 day

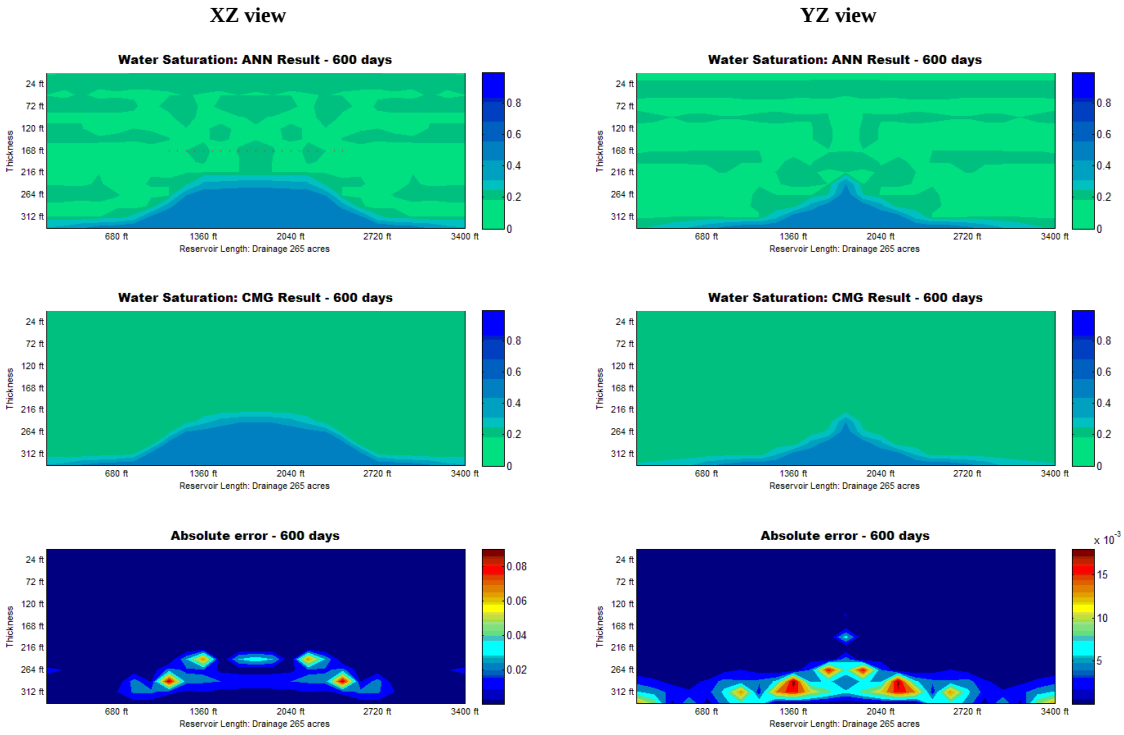

Figure- A.35 Prediction of water saturation for test case #3 at 600 day

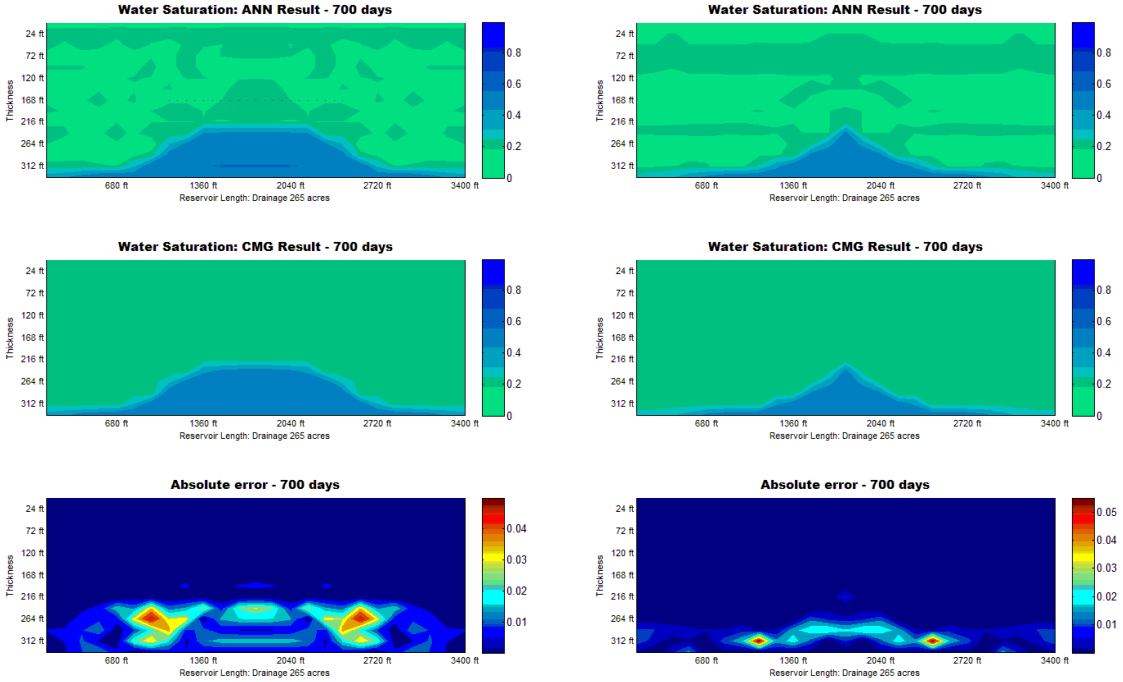

Figure- A.36 Prediction of water saturation for test case #3 at 700 day

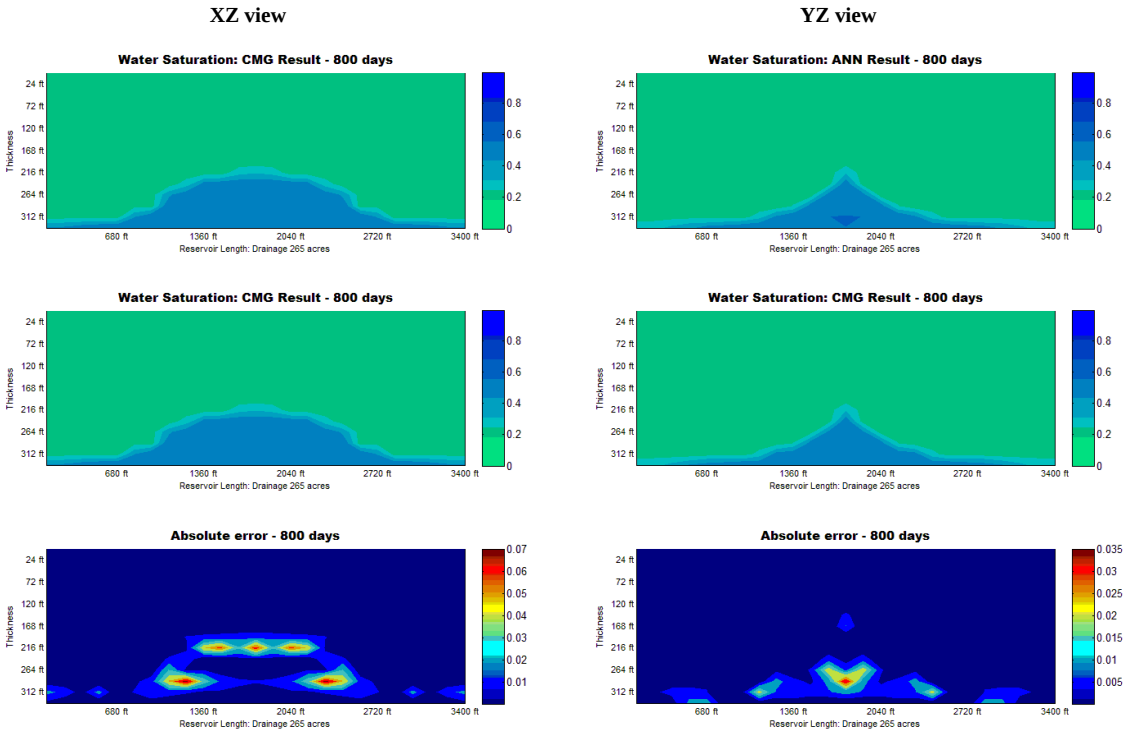

Figure- A.37 Prediction of water saturation for test case #3 at 800 day

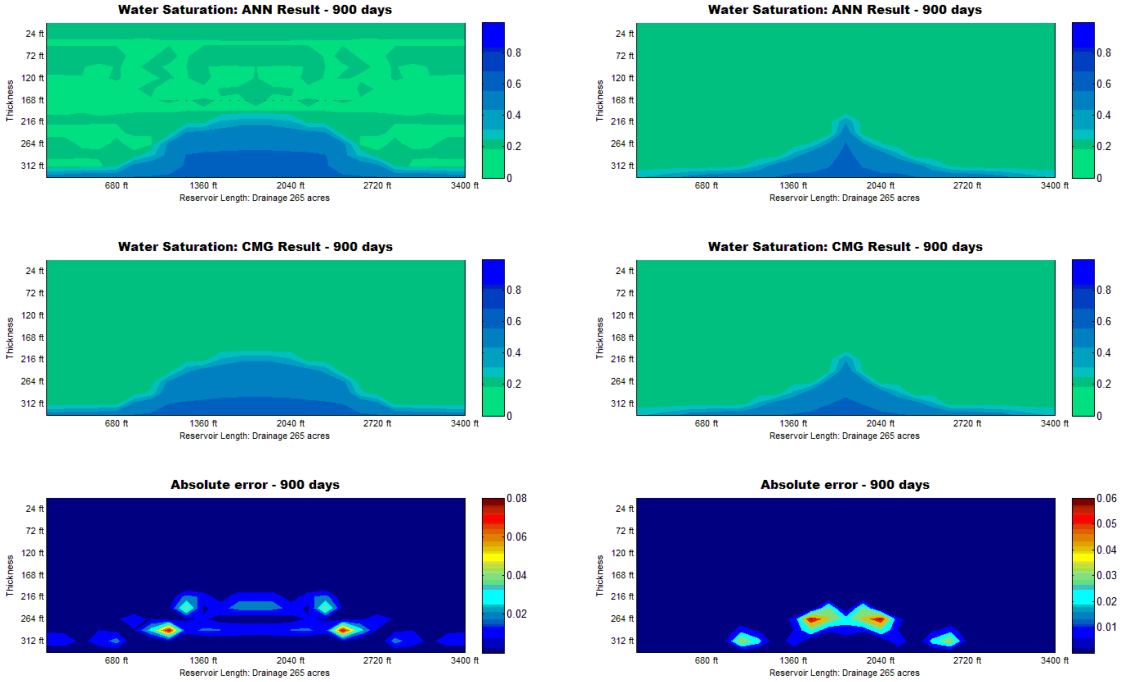

Figure- A.38 Prediction of water saturation for test case #3 at 900 day

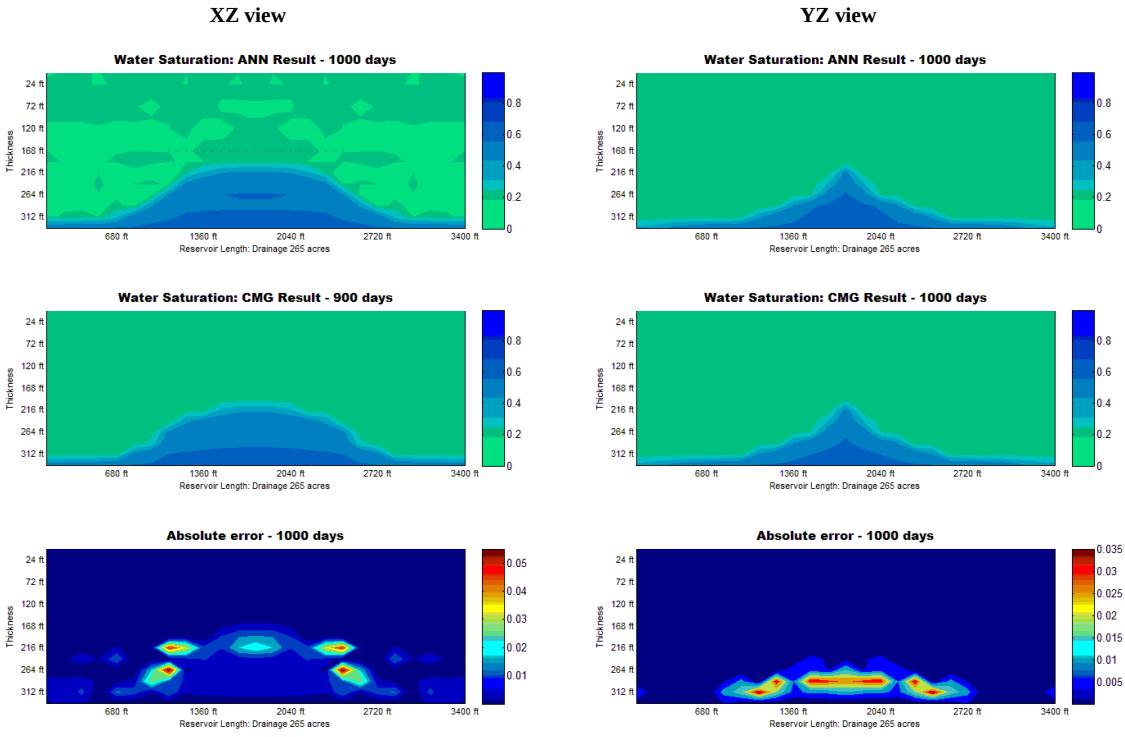

Figure- A.39 Prediction of water saturation for test case #3 at 1000 day

Appendix D

1. Input variables for training in dual porosity system

	Φ_m	Φ_f	k_m	k_{hf}	k_{hf}	d_f	r_o	r_w	μ_w	h	h_t	p_{sf}	d_{top}	d_{owc}	l_{wp}	p_i	wd	$acre$
1	0.165	0.0031	15.5	298	435	19	57.52	61.22	0.869	24	360	2215	252	108	1730	2305	173	429.4
2	0.182	0.0042	19.7	1365	333	19	57.20	61.48	0.532	19	285	3592	161.5	123.5	1040	3634	104	155.2
3	0.034	0.0084	28.5	604	479	10	48.53	61.21	0.930	12	180	3035	138	42	1428	3313	102	149.3
4	0.184	0.0011	21.7	175	124	24	55.38	61.67	0.967	23	345	1228	80.5	264.5	1136	3997	142	289.3
5	0.130	0.0014	12.0	2868	333	29	50.69	61.16	0.992	21	315	1887	178.5	136.5	1062	3073	177	449.5
6	0.029	0.0025	25.0	1348	214	29	52.23	62.38	0.929	19	285	1000	104.5	180.5	858	3055	143	293.4
7	0.063	0.0068	4.0	2888	431	4	53.48	60.37	0.893	17	255	2136	178.5	76.5	2088	3665	116	193.1
8	0.130	0.0053	4.2	1532	389	13	53.89	61.82	0.562	20	300	1200	90	210	2256	2096	141	285.3
9	0.192	0.0068	2.5	121	277	1	52.18	60.09	0.589	30	450	1065	195	255	2052	2266	114	186.5
10	0.067	0.0087	29.5	288	177	23	49.75	61.54	0.874	16	240	1677	104	136	1150	3989	115	189.8
11	0.146	0.0094	15.6	2843	295	3	56.80	61.03	0.655	18	270	2095	189	81	2322	2938	129	238.8
12	0.194	0.0037	9.1	1970	370	12	55.01	60.97	0.515	17	255	1760	161.5	93.5	1428	2962	102	149.3
13	0.192	0.0077	0.4	1701	183	26	54.66	60.75	0.970	13	195	1369	58.5	136.5	1002	2267	167	400.2
14	0.102	0.0027	16.2	732	227	16	53.39	61.79	0.651	19	285	1377	104.5	180.5	1644	3520	137	269.3
15	0.162	0.0072	2.9	2339	153	11	54.98	61.43	0.648	13	195	1158	58.5	136.5	2576	2268	184	485.8
16	0.037	0.0027	4.4	761	368	7	54.67	61.81	0.666	12	180	3162	114	66	2656	3302	166	395.4

	Φ_m	Φ_f	k_m	k_{hf}	k_{hf}	d_f	r_o	r_w	μ_w	h	h_t	p_{sf}	d_{top}	d_{owc}	l_{wp}	p_i	wd	$acre$
17	0.090	0.0043	18.9	1175	328	13	49.78	62.23	0.734	28	420	2025	238	182	1416	2335	118	199.8
18	0.184	0.0066	25.8	2683	167	28	49.28	62.33	0.824	10	150	3150	45	105	1014	3854	169	409.8
19	0.192	0.0017	17.1	1267	290	14	49.71	60.16	0.921	29	435	1380	217.5	217.5	1956	2377	163	381.2
20	0.135	0.0094	29.9	1022	463	25	48.33	61.61	0.780	22	330	1635	253	77	1512	2193	189	512.5
21	0.017	0.0080	16.6	1865	320	2	53.61	60.04	0.927	12	180	2044	90	90	2304	2801	128	235.1
22	0.171	0.0054	15.5	2739	113	21	56.82	61.17	0.674	24	360	1528	84	276	1760	3628	176	444.4
23	0.187	0.0049	9.9	2736	121	29	54.69	61.18	0.723	17	255	1659	59.5	195.5	1056	2047	176	444.4
24	0.139	0.0050	12.9	1815	422	9	49.90	62.04	0.527	12	180	1380	126	54	1600	2808	100	143.5
25	0.154	0.0038	14.8	1064	280	4	51.69	61.06	0.589	23	345	3047	172.5	172.5	3492	3146	194	540.0
26	0.151	0.0056	2.1	2573	253	20	52.61	60.82	0.831	29	435	1250	188.5	246.5	1310	3465	131	246.2
27	0.135	0.0084	1.9	2722	245	18	49.56	61.73	0.949	13	195	1017	84.5	110.5	1320	3040	132	250.0
28	0.144	0.0068	24.8	1644	384	6	54.45	60.70	0.994	30	450	3444	285	165	2256	3603	141	285.3
29	0.016	0.0044	11.8	2177	448	22	51.76	60.19	0.770	26	390	1008	273	117	1264	2117	158	358.2
30	0.063	0.0083	18.4	619	231	11	49.91	61.32	0.853	11	165	2310	60.5	104.5	2450	3170	175	439.4
31	0.019	0.0058	24.6	1075	360	13	52.28	60.48	1.000	21	315	2369	178.5	136.5	2772	2928	198	562.5
32	0.028	0.0042	26.6	644	489	5	52.82	59.92	0.644	19	285	1617	218.5	66.5	2000	2397	125	224.2
33	0.166	0.0095	27.9	1033	130	24	49.21	61.76	0.707	20	300	1729	70	230	912	2611	114	186.5
34	0.142	0.0089	5.7	1271	334	19	53.90	60.43	0.732	18	270	1894	153	117	1870	2004	187	501.7
35	0.070	0.0060	7.8	1690	265	22	50.26	60.95	0.882	14	210	1909	91	119	1112	2328	139	277.2
36	0.191	0.0066	26.9	241	223	24	51.85	61.59	0.909	18	270	1137	99	171	1344	3507	168	405.0
37	0.017	0.0063	17.8	1702	205	2	53.83	60.73	0.550	14	210	1154	77	133	2736	3124	152	331.5
38	0.093	0.0029	15.1	896	403	28	50.52	61.71	0.589	14	210	2097	133	77	1110	2149	185	491.1
39	0.082	0.0037	18.4	800	498	15	50.90	60.83	0.680	30	450	1761	345	105	2136	3197	178	454.6

	Φ_m	Φ_f	k_m	k_{hf}	k_{hf}	d_f	r_o	r_w	μ_w	h	h_t	p_{sf}	d_{top}	d_{owc}	l_{wp}	p_i	wd	$acre$
40	0.155	0.0052	24.6	805	174	22	54.17	61.58	0.528	14	210	1588	63	147	1376	2106	172	424.5
41	0.161	0.0031	16.0	547	412	22	50.65	61.63	0.761	10	150	3213	105	45	1104	3300	138	273.2
42	0.046	0.0086	6.1	2873	178	25	56.24	60.95	0.668	25	375	2581	112.5	262.5	1480	3255	185	491.1
43	0.169	0.0037	0.7	2905	270	8	54.06	61.96	0.965	15	225	2711	172.5	52.5	2880	3179	180	464.9
44	0.095	0.0030	12.8	2474	420	14	55.30	60.66	0.604	10	150	2203	105	45	1248	2921	104	155.2
45	0.133	0.0025	29.0	2211	269	18	51.44	60.90	0.953	20	300	2317	130	170	1030	3339	103	152.2
46	0.145	0.0030	18.6	609	391	28	53.84	60.50	0.838	12	180	2208	114	66	894	3618	149	318.5
47	0.153	0.0049	20.9	1145	299	25	49.08	60.31	0.734	28	420	2314	210	210	1584	3338	198	562.5
48	0.062	0.0038	21.6	647	423	26	57.06	61.94	0.956	15	225	2456	157.5	67.5	708	2511	118	199.8
49	0.139	0.0093	10.4	103	242	17	56.80	60.92	0.552	15	225	2374	97.5	127.5	1090	2842	109	170.5
50	0.134	0.0049	15.5	1017	129	17	56.18	62.11	0.873	22	330	2280	77	253	1840	3581	184	485.8
51	0.041	0.0027	16.7	2128	336	25	50.61	60.82	0.868	13	195	2107	110.5	84.5	1152	3643	144	297.5
52	0.033	0.0091	4.7	1913	464	2	53.94	61.80	0.781	18	270	1464	207	63	2952	3873	164	385.9
53	0.105	0.0098	16.9	1674	177	26	48.23	60.83	0.592	27	405	1008	121.5	283.5	1104	2960	184	485.8
54	0.192	0.0049	20.8	1373	272	12	52.25	61.90	0.799	24	360	1107	156	204	2604	2282	186	496.4
55	0.078	0.0061	10.5	809	148	13	50.80	61.49	0.504	23	345	1794	218.5	126.5	3348	3857	186	496.4
56	0.121	0.0033	25.1	1554	115	22	49.61	60.78	0.567	19	285	2271	66.5	218.5	928	2366	116	193.1
57	0.153	0.0064	10.8	2310	405	5	52.23	61.86	0.947	16	240	2315	152	88	2160	3454	135	261.5
58	0.058	0.0034	13.6	1770	323	18	48.94	62.27	0.536	23	345	1744	195.5	149.5	1890	3551	189	512.5
59	0.106	0.0064	11.6	2268	173	8	53.99	60.65	0.621	20	300	2007	90	210	1792	3726	112	180.0
60	0.143	0.0074	23.3	1972	299	10	52.71	61.55	0.527	21	315	1111	157.5	157.5	1596	2375	114	186.5
61	0.179	0.0030	22.0	457	307	12	54.96	60.94	0.721	22	330	2495	165	165	1988	2621	142	289.3
62	0.114	0.0037	20.8	1107	441	12	54.39	61.80	0.949	10	150	2007	105	45	2702	3174	193	534.4

	Φ_m	Φ_f	k_m	k_{hf}	k_{hf}	d_f	r_o	r_w	μ_w	h	h_t	p_{sf}	d_{top}	d_{owc}	l_{wp}	p_i	wd	$acre$
63	0.036	0.0039	28.4	367	484	18	48.34	60.23	0.598	30	450	1991	345	105	1250	3278	125	224.2
64	0.038	0.0048	23.5	528	371	5	48.69	62.04	0.547	27	405	3309	256.5	148.5	2448	3590	153	335.9
65	0.059	0.0056	21.2	674	261	6	51.20	62.37	0.654	17	255	1964	110.5	144.5	2720	2068	170	414.7
66	0.058	0.0034	11.7	1351	291	10	54.54	62.10	0.551	25	375	2571	187.5	187.5	1960	3133	140	281.2
67	0.165	0.0082	17.7	2113	192	23	52.08	61.33	0.998	13	195	1802	71.5	123.5	1120	2401	140	281.2
68	0.187	0.0094	1.5	128	382	22	55.18	60.32	0.649	30	450	1753	285	165	840	2979	105	158.2
69	0.096	0.0077	15.9	2972	148	18	55.92	61.52	0.914	14	210	3370	119	91	1460	3885	146	305.8
70	0.047	0.0054	25.0	910	402	24	53.31	61.75	0.649	17	255	2848	161.5	93.5	1304	3724	163	381.2
71	0.058	0.0062	0.5	2844	498	25	51.25	61.95	0.523	29	435	1122	333.5	101.5	1344	2543	168	405.0
72	0.127	0.0031	25.9	2728	484	9	49.06	61.85	0.753	24	360	2376	276	84	2800	3002	200	573.9
73	0.100	0.0051	2.4	1238	314	9	54.11	60.63	0.881	15	225	1899	112.5	112.5	2240	3906	160	367.3
74	0.077	0.0097	20.1	172	485	16	55.79	61.19	0.816	17	255	1768	195.5	59.5	2316	2053	193	534.4
75	0.168	0.0059	15.0	2047	146	10	52.23	60.03	0.545	26	390	2668	117	273	2576	3926	184	485.8
76	0.121	0.0057	6.5	2527	120	25	48.91	60.09	0.540	25	375	1975	87.5	287.5	1224	3785	153	335.9
77	0.114	0.0031	17.2	2917	221	24	50.66	60.15	0.889	20	300	1313	110	190	1040	2008	130	242.5
78	0.184	0.0054	3.7	265	332	17	49.54	61.56	0.953	24	360	3010	204	156	1848	3737	154	340.3
79	0.064	0.0066	20.1	1405	312	8	50.81	61.09	0.767	18	270	3656	135	135	2464	3767	154	340.3
80	0.154	0.0071	18.0	1789	460	20	52.40	60.29	0.555	18	270	1346	207	63	1160	2958	116	193.1
81	0.153	0.0046	1.7	2091	316	7	53.27	61.09	0.913	13	195	2073	97.5	97.5	1936	2793	121	210.1
82	0.082	0.0043	1.7	2186	272	14	52.57	60.18	0.669	10	150	1405	65	85	1620	3289	135	261.5
83	0.024	0.0013	0.6	2208	384	16	53.18	62.01	0.873	30	450	1547	285	165	2388	2092	199	568.2
84	0.020	0.0090	13.1	1184	106	29	57.44	61.26	0.505	30	450	1294	105	345	708	2121	118	199.8
85	0.111	0.0092	25.0	1786	420	22	54.38	62.22	0.524	15	225	3104	157.5	67.5	1264	3144	158	358.2

	Φ_m	Φ_f	k_m	k_{hf}	k_{hf}	d_f	r_o	r_w	μ_w	h	h_t	p_{sf}	d_{top}	d_{owc}	l_{wp}	p_i	wd	$acre$
86	0.187	0.0019	15.6	267	291	7	50.41	61.32	0.802	22	330	1066	165	165	2960	2743	185	491.1
87	0.035	0.0034	25.9	2941	202	16	54.76	61.92	0.763	28	420	1248	154	266	1344	3055	112	180.0
88	0.118	0.0040	2.9	925	247	2	50.89	62.09	0.865	24	360	2584	156	204	1800	3251	100	143.5
89	0.099	0.0071	27.2	1825	364	22	54.72	62.37	0.854	17	255	1340	144.5	110.5	1304	2255	163	381.2
90	0.012	0.0022	3.2	2890	167	18	54.95	59.80	0.891	29	435	1490	130.5	304.5	2000	2324	200	573.9
91	0.074	0.0075	15.5	638	211	25	48.68	62.05	0.644	25	375	1178	137.5	237.5	846	3165	141	285.3
92	0.041	0.0020	4.3	659	179	29	50.55	61.39	0.846	11	165	1390	49.5	115.5	732	3354	122	213.6
93	0.161	0.0069	16.8	1090	178	27	50.24	62.37	0.778	14	210	1750	63	147	702	2200	117	196.4
94	0.069	0.0054	0.1	2805	230	12	54.68	61.17	0.698	29	435	1509	159.5	275.5	2800	2299	200	573.9
95	0.110	0.0080	23.0	1232	452	1	56.44	61.05	0.531	22	330	3237	231	99	3060	3612	170	414.7
96	0.041	0.0074	25.5	892	288	16	51.44	61.88	0.890	29	435	1411	217.5	217.5	1380	2009	115	189.8
97	0.124	0.0091	27.5	540	261	7	55.81	60.39	0.669	28	420	3164	182	238	2176	3333	136	265.4
98	0.060	0.0090	29.6	1251	171	7	54.75	61.10	0.804	15	225	2267	67.5	157.5	1648	3016	103	152.2
99	0.147	0.0046	29.5	1913	155	12	56.49	61.53	0.808	25	375	1982	287.5	87.5	2646	3750	189	512.5
100	0.141	0.0073	8.1	480	262	3	54.02	61.29	0.552	13	195	1796	84.5	110.5	2394	3563	133	253.8
101	0.152	0.0028	3.0	1361	437	22	51.87	62.00	0.564	19	285	2247	199.5	85.5	1456	2635	182	475.3
102	0.096	0.0013	15.2	365	346	22	57.16	61.72	0.775	25	375	1835	212.5	162.5	1368	3353	171	419.6
103	0.026	0.0077	17.6	1882	250	16	48.01	61.32	0.743	29	435	1646	188.5	246.5	2376	2616	198	562.5
104	0.054	0.0055	22.9	131	450	10	52.62	60.44	0.945	26	390	3777	273	117	2408	3886	172	424.5
105	0.184	0.0053	2.5	1762	413	25	52.24	61.53	0.899	24	360	1988	252	108	1600	2748	200	573.9
106	0.039	0.0091	19.9	2390	285	17	52.61	60.02	0.867	13	195	1868	97.5	97.5	1884	2762	157	353.7
107	0.167	0.0065	15.5	782	425	28	55.70	61.43	0.526	20	300	1130	210	90	834	2281	139	277.2
108	0.112	0.0066	5.1	1399	459	26	51.22	61.52	0.536	21	315	2721	241.5	73.5	702	3442	117	196.4

	Φ_m	Φ_f	k_m	k_{hf}	k_{hf}	d_f	r_o	r_w	μ_w	h	h_t	p_{sf}	d_{top}	d_{owc}	l_{wp}	p_i	wd	$acre$
109	0.199	0.0087	28.2	1751	271	11	55.85	61.70	0.544	14	210	1966	91	119	1946	3489	139	277.2
110	0.025	0.0082	17.7	278	233	16	52.71	62.12	0.899	13	195	3538	84.5	110.5	2220	3912	185	491.1
111	0.094	0.0062	13.2	1539	338	11	48.36	62.35	0.972	16	240	1571	136	104	2422	2067	173	429.4
112	0.193	0.0032	19.7	741	380	24	55.22	61.31	0.566	19	285	2635	180.5	104.5	896	3079	112	180.0
113	0.011	0.0090	13.6	2527	250	22	52.73	62.21	0.861	29	435	1123	188.5	246.5	1080	2064	135	261.5
114	0.026	0.0073	26.9	801	352	29	49.89	61.89	0.824	30	450	2703	285	165	2754	3422	153	335.9
115	0.165	0.0054	16.0	2554	481	24	51.41	59.84	0.559	27	405	1112	310.5	94.5	1520	3841	190	518.0
116	0.183	0.0020	6.5	926	163	27	51.65	61.43	0.901	28	420	1151	210	210	1800	3299	100	143.5
117	0.026	0.0098	20.4	908	316	13	49.92	62.04	0.664	23	345	3016	172.5	172.5	1960	3764	140	281.2
118	0.086	0.0074	11.0	2265	224	22	55.38	61.06	0.827	12	180	2496	66	114	856	3404	107	164.3
119	0.059	0.0055	7.2	787	128	23	50.43	62.00	0.875	22	330	1953	77	253	1448	2186	181	470.1
120	0.092	0.0015	26.0	1898	137	22	50.69	61.24	0.870	17	255	1506	59.5	195.5	872	2778	109	170.5
121	0.183	0.0071	12.2	1840	285	26	55.66	61.44	0.617	28	420	2933	210	210	1158	3954	193	534.4
122	0.045	0.0014	3.4	600	103	8	49.89	59.88	0.867	15	225	1078	52.5	172.5	2864	3172	179	459.7
123	0.038	0.0057	9.0	840	357	7	48.91	60.74	0.933	12	180	1379	102	78	2224	2105	139	277.2
124	0.036	0.0019	12.0	2589	100	11	53.76	59.93	0.543	15	225	1010	52.5	172.5	2212	3016	158	358.2
125	0.175	0.0084	25.0	2742	112	9	54.83	61.07	0.683	23	345	2428	80.5	264.5	2562	2999	183	480.5
126	0.120	0.0084	12.1	2128	183	27	53.47	60.30	0.685	10	150	1805	45	105	690	3090	115	189.8
127	0.148	0.0095	22.0	2487	311	24	55.79	61.64	0.794	27	405	2067	202.5	202.5	2610	2933	145	301.7
128	0.038	0.0023	10.8	766	150	18	54.44	60.33	0.799	26	390	1283	117	273	1410	2958	141	285.3
129	0.172	0.0069	4.2	1770	103	5	54.48	60.18	0.895	25	375	1602	87.5	287.5	2032	2227	127	231.4
130	0.128	0.0057	7.8	2450	390	25	54.79	60.29	0.684	13	195	1948	123.5	71.5	1008	2708	126	227.8
131	0.077	0.0098	2.6	1271	241	5	54.36	59.91	0.603	26	390	2550	169	221	1600	3718	100	143.5

	Φ_m	Φ_f	k_m	k_{hf}	k_{hf}	d_f	r_o	r_w	μ_w	h	h_t	p_{sf}	d_{top}	d_{owc}	l_{wp}	p_i	wd	$acre$
132	0.086	0.0082	7.7	360	274	29	50.09	60.53	0.886	24	360	1519	156	204	906	3294	151	327.1
133	0.024	0.0051	8.9	1030	274	11	55.09	61.20	0.603	10	150	2339	65	85	2030	2681	145	301.7
134	0.183	0.0100	13.1	372	360	2	56.11	61.24	0.791	18	270	3753	63	207	2970	3992	165	390.6
135	0.033	0.0084	3.6	275	119	7	49.19	61.10	0.776	23	345	3192	80.5	264.5	2976	3371	186	496.4
136	0.026	0.0080	12.0	2941	411	28	52.98	60.46	0.761	29	435	1478	101.5	333.5	2800	3386	200	573.9
137	0.096	0.0059	9.5	1515	210	17	54.64	62.24	0.679	17	255	2911	144.5	110.5	1400	3616	100	143.5
138	0.115	0.0054	26.5	923	300	28	49.01	61.33	0.983	11	165	1049	60.5	104.5	1888	3456	118	199.8
139	0.019	0.0045	23.6	2506	436	28	54.62	61.07	0.576	17	255	3398	178.5	76.5	828	3691	138	273.2
140	0.182	0.0085	2.2	2590	442	20	55.70	62.02	0.891	23	345	2175	241.5	103.5	1310	3358	131	246.2
141	0.190	0.0082	11.8	2388	485	28	51.50	62.07	0.550	19	285	1349	218.5	66.5	810	3876	135	261.5
142	0.103	0.0015	0.1	1021	295	13	54.62	60.50	0.647	14	210	1044	105	105	2376	2536	198	562.5
143	0.103	0.0046	6.6	1411	188	28	52.16	60.34	0.619	17	255	1066	76.5	178.5	726	3818	121	210.1
144	0.074	0.0057	0.0	2281	190	1	56.42	61.27	0.765	21	315	1486	115.5	199.5	3582	3364	199	568.2
145	0.181	0.0048	5.7	418	314	18	56.33	61.46	0.546	13	195	2422	97.5	97.5	1940	2464	194	540.0
146	0.080	0.0069	4.3	418	404	24	50.56	60.88	0.703	18	270	2342	171	99	896	2746	112	180.0
147	0.031	0.0067	8.0	882	239	7	54.13	60.34	0.552	22	330	1446	143	187	2752	3847	172	424.5
148	0.158	0.0036	5.3	1621	284	28	53.82	62.26	0.556	18	270	1706	135	135	1116	3913	186	496.4
149	0.084	0.0049	4.2	2920	355	23	53.41	60.01	0.892	30	450	3233	255	195	1280	3930	160	367.3
150	0.085	0.0062	28.0	344	239	16	56.36	61.33	0.589	22	330	1918	253	77	1184	2692	148	314.3
151	0.087	0.0099	27.0	1004	164	17	50.65	60.17	0.802	23	345	1792	103.5	241.5	1280	3694	128	235.1
152	0.028	0.0025	28.2	945	386	23	51.18	60.23	0.982	26	390	1710	247	143	960	2214	120	206.6
153	0.140	0.0022	28.3	2614	294	23	49.36	61.55	0.591	21	315	1719	178.5	136.5	2660	2781	190	518.0
154	0.189	0.0044	14.5	2743	273	7	57.40	61.29	0.847	29	435	2770	188.5	246.5	1664	2948	104	155.2

	Φ_m	Φ_f	k_m	k_{hf}	k_{hf}	d_f	r_o	r_w	μ_w	h	h_t	p_{sf}	d_{top}	d_{owc}	l_{wp}	p_i	wd	$acre$
155	0.192	0.0028	11.3	1953	453	10	54.46	59.94	0.879	22	330	1395	231	99	1932	3389	138	273.2
156	0.119	0.0054	15.7	840	257	17	52.79	62.22	0.716	17	255	2244	110.5	144.5	1850	3052	185	491.1
157	0.021	0.0041	8.0	357	171	25	54.39	61.69	0.828	22	330	1446	99	231	920	2121	115	189.8
158	0.087	0.0090	18.1	306	232	8	56.56	60.79	0.799	26	390	2234	221	169	1998	2445	111	176.8
159	0.043	0.0031	10.9	1518	281	19	57.00	62.15	0.715	15	225	2099	97.5	127.5	2400	3605	200	573.9
160	0.119	0.0088	4.1	2564	394	22	50.18	61.57	0.865	17	255	1177	76.5	178.5	1120	2568	140	281.2
161	0.125	0.0074	27.4	2991	303	15	48.77	60.78	0.631	30	450	1161	345	105	1146	3758	191	523.4
162	0.051	0.0089	19.2	112	253	25	52.74	61.44	0.547	16	240	1424	136	104	2484	3728	138	273.2
163	0.067	0.0052	28.5	187	144	18	56.58	61.33	0.780	27	405	1807	256.5	148.5	762	2599	127	231.4
164	0.124	0.0077	3.2	2306	466	29	48.19	61.19	0.813	20	300	1485	190	110	1146	3080	191	523.4
165	0.142	0.0098	25.3	2551	152	5	53.03	62.01	0.726	13	195	2556	136.5	58.5	824	3170	103	152.2
166	0.088	0.0068	15.5	2648	347	16	49.25	60.54	0.826	20	300	1299	150	150	864	2570	144	297.5
167	0.017	0.0091	4.6	2263	253	15	49.32	61.57	0.913	22	330	1970	99	231	1344	2055	168	405.0
168	0.066	0.0053	11.4	440	496	12	56.70	60.73	0.654	15	225	2358	97.5	127.5	2664	2402	148	314.3
169	0.048	0.0071	1.7	2698	273	17	55.28	61.03	0.515	29	435	2186	304.5	130.5	2028	3659	169	409.8
170	0.076	0.0066	5.1	589	382	1	50.65	60.02	0.942	26	390	1063	117	273	2592	2959	162	376.5
171	0.107	0.0057	29.0	2791	177	19	48.58	61.91	0.621	10	150	2897	115	35	816	3277	136	265.4
172	0.080	0.0075	24.2	591	375	14	52.58	60.02	0.880	23	345	1833	241.5	103.5	1936	2872	121	210.1
173	0.151	0.0065	6.7	2662	120	8	55.22	61.18	0.645	30	450	1654	135	315	924	2169	154	340.3
174	0.110	0.0063	30.0	1224	173	24	51.39	61.88	0.639	10	150	3357	115	35	2492	3535	178	454.6
175	0.163	0.0049	1.9	1209	118	24	52.01	61.72	0.503	11	165	2456	38.5	126.5	2604	2815	186	496.4
176	0.165	0.0032	12.8	887	454	25	53.27	60.17	0.687	21	315	1753	136.5	178.5	1744	3042	109	170.5
177	0.034	0.0011	12.0	2250	147	29	55.78	60.71	0.652	23	345	2179	149.5	195.5	1216	3901	152	331.5

	Φ_m	Φ_f	k_m	k_{hf}	k_{hf}	d_f	r_o	r_w	μ_w	h	h_t	p_{sf}	d_{top}	d_{owc}	l_{wp}	p_i	wd	$acre$
178	0.166	0.0065	3.4	1398	264	25	48.69	61.04	0.645	14	210	1820	63	147	1368	3317	114	186.5
179	0.131	0.0096	12.7	2157	148	3	50.79	61.33	0.621	24	360	1920	156	204	1780	2456	178	454.6
180	0.108	0.0090	6.6	809	202	12	52.20	61.46	0.699	10	150	1598	45	105	2928	2307	183	480.5
181	0.113	0.0032	10.6	1958	495	14	50.40	60.22	0.740	14	210	1718	91	119	1670	2293	167	400.2
182	0.125	0.0011	8.0	2444	239	28	53.98	61.27	0.782	15	225	3541	82.5	142.5	1224	3631	153	335.9
183	0.154	0.0083	8.8	2574	183	28	52.79	62.22	0.745	28	420	1668	154	266	856	3071	107	164.3
184	0.173	0.0023	5.7	1254	366	23	56.99	61.84	0.635	13	195	2141	58.5	136.5	2282	2481	163	381.2
185	0.083	0.0089	0.7	434	489	17	57.35	61.58	0.995	13	195	1916	45.5	149.5	2340	2038	130	242.5
186	0.149	0.0042	7.3	1145	125	15	55.09	60.48	0.931	28	420	1143	154	266	2268	2185	162	376.5
187	0.135	0.0089	4.9	1894	270	15	56.17	60.64	0.821	26	390	2298	273	117	1312	2624	164	385.9
188	0.193	0.0073	23.1	1056	318	27	53.60	59.85	0.975	20	300	2173	150	150	1664	2769	104	155.2
189	0.143	0.0078	15.8	2190	111	8	49.16	60.92	0.919	10	150	2086	115	35	1456	2335	182	475.3
190	0.167	0.0068	29.2	1998	120	17	51.36	62.17	0.822	27	405	1647	310.5	94.5	1620	2611	162	376.5
191	0.019	0.0044	13.4	635	340	26	56.28	61.13	0.657	14	210	2189	119	91	3438	3671	191	523.4
192	0.097	0.0066	2.1	1445	304	6	52.89	61.79	0.698	19	285	1884	85.5	199.5	1160	3253	145	301.7
193	0.040	0.0035	0.3	2300	485	15	51.47	62.39	0.719	12	180	2089	138	42	672	2495	112	180.0
194	0.018	0.0032	17.8	1527	432	28	51.66	60.26	0.626	22	330	2733	187	143	1824	3007	152	331.5
195	0.140	0.0069	26.5	2518	401	24	50.27	61.15	0.789	19	285	1273	199.5	85.5	1360	3752	170	414.7
196	0.149	0.0087	12.7	480	348	21	53.35	61.43	0.958	21	315	1989	136.5	178.5	3312	2058	184	485.8
197	0.093	0.0018	18.2	2303	257	29	50.89	62.17	0.948	23	345	3848	195.5	149.5	1272	3933	159	362.7
198	0.082	0.0097	2.1	2784	243	29	48.68	61.53	0.741	23	345	1609	80.5	264.5	840	3036	140	281.2
199	0.196	0.0013	27.7	2514	135	29	48.85	60.81	0.721	10	150	2010	115	35	1424	2862	178	454.6
200	0.086	0.0085	19.3	852	236	5	48.68	61.72	0.656	11	165	1836	93.5	71.5	1920	2716	120	206.6

	Φ_m	Φ_f	k_m	k_{hf}	k_{hf}	d_f	r_o	r_w	μ_w	h	h_t	p_{sf}	d_{top}	d_{owc}	l_{wp}	p_i	wd	$acre$
201	0.094	0.0085	3.1	717	319	28	52.10	61.93	0.528	29	435	1156	101.5	333.5	2960	3699	185	491.1
202	0.040	0.0014	21.0	1614	284	16	49.23	61.36	0.877	17	255	1262	161.5	93.5	1344	2776	112	180.0
203	0.090	0.0040	2.8	120	210	21	55.74	60.49	0.542	12	180	1865	78	102	2352	2367	168	405.0
204	0.070	0.0095	2.6	1489	305	10	56.99	62.20	0.678	17	255	1852	59.5	195.5	1464	2425	122	213.6
205	0.180	0.0039	6.4	2982	425	26	51.54	59.94	0.698	20	300	1557	90	210	1116	3733	186	496.4
206	0.057	0.0083	7.5	1852	138	25	49.20	61.17	0.943	15	225	2143	82.5	142.5	1060	2975	106	161.2
207	0.123	0.0085	18.2	661	397	29	50.85	61.86	0.791	13	195	2231	71.5	123.5	642	3834	107	164.3
208	0.088	0.0081	21.1	1522	335	19	56.75	60.79	0.922	16	240	2132	152	88	1920	2563	160	367.3
209	0.145	0.0082	22.6	1370	174	24	51.49	61.91	0.644	27	405	2140	256.5	148.5	1560	2962	130	242.5
210	0.176	0.0035	16.6	2257	120	2	49.42	62.10	0.744	26	390	2342	195	195	1008	3811	126	227.8
211	0.026	0.0069	18.9	1384	330	8	48.77	61.65	0.865	26	390	1516	221	169	2232	2165	186	496.4
212	0.098	0.0054	29.6	253	436	3	55.41	60.78	0.601	18	270	1160	207	63	2718	2394	151	327.1
213	0.016	0.0098	19.0	354	299	15	52.57	60.45	0.608	20	300	2606	170	130	2862	3690	159	362.7
214	0.153	0.0077	18.0	2414	275	13	54.68	60.46	0.988	27	405	2045	229.5	175.5	1408	2617	176	444.4
215	0.143	0.0061	27.3	2001	159	12	54.99	61.79	0.797	12	180	1088	138	42	1040	3363	104	155.2
216	0.051	0.0037	17.1	193	111	26	53.71	59.93	0.652	13	195	2775	110.5	84.5	2052	3160	114	186.5
217	0.139	0.0033	10.1	1715	402	13	54.29	61.58	0.984	23	345	1820	149.5	195.5	2244	2911	187	501.7
218	0.116	0.0090	28.7	2187	418	9	56.78	61.41	0.948	29	435	2181	333.5	101.5	888	2983	111	176.8
219	0.172	0.0050	13.2	420	217	2	54.62	61.74	0.595	20	300	1011	130	170	2160	2421	120	206.6
220	0.116	0.0083	18.1	728	146	7	56.75	62.34	0.501	28	420	1495	238	182	2448	3217	153	335.9
221	0.181	0.0019	21.6	2451	250	7	52.68	60.80	0.856	20	300	1296	190	110	952	2496	119	203.2
222	0.090	0.0087	20.4	502	431	1	49.41	60.48	0.934	15	225	2780	142.5	82.5	2646	3574	147	310.0
223	0.078	0.0012	6.4	2657	436	21	48.68	62.08	0.559	26	390	1069	117	273	756	3547	126	227.8

	Φ_m	Φ_f	k_m	k_{hf}	k_{hf}	d_f	r_o	r_w	μ_w	h	h_t	p_{sf}	d_{top}	d_{owc}	l_{wp}	p_i	wd	$acre$
224	0.103	0.0091	2.5	2778	366	1	55.14	61.90	0.520	16	240	2103	56	184	1170	2425	195	545.6
225	0.059	0.0091	8.2	136	484	18	51.08	61.00	0.799	23	345	1648	126.5	218.5	3078	3557	171	419.6
226	0.187	0.0057	26.0	1193	477	12	54.71	60.04	0.802	20	300	1293	210	90	1568	2036	112	180.0
227	0.099	0.0021	16.8	586	145	8	54.52	61.27	0.758	21	315	2332	178.5	136.5	2288	3761	143	293.4
228	0.058	0.0026	13.9	1666	359	19	53.31	60.29	0.504	10	150	2611	75	75	1320	2646	110	173.6
229	0.092	0.0074	12.9	394	292	10	55.15	61.18	0.844	16	240	3352	104	136	2304	3415	128	235.1
230	0.143	0.0085	23.2	213	126	4	53.05	60.72	0.973	26	390	2340	247	143	3006	3914	167	400.2
231	0.086	0.0013	19.6	2806	459	16	52.88	60.62	0.937	17	255	2979	144.5	110.5	708	3177	118	199.8
232	0.045	0.0078	19.7	2917	298	5	52.98	61.69	0.557	16	240	1467	136	104	804	2225	134	257.6
233	0.121	0.0041	13.0	1968	124	20	51.89	61.86	0.621	24	360	3582	156	204	1440	3615	144	297.5
234	0.081	0.0067	15.2	297	204	25	49.17	60.33	0.780	19	285	1837	142.5	142.5	2178	3735	121	210.1
235	0.052	0.0041	11.3	702	360	23	50.40	61.56	0.806	10	150	3579	65	85	2960	3657	185	491.1
236	0.052	0.0029	14.4	214	153	24	54.85	59.94	0.650	22	330	2597	165	165	2502	2610	139	277.2
237	0.109	0.0081	10.3	1461	355	19	56.39	61.88	0.899	12	180	1474	78	102	2328	2786	194	540.0
238	0.151	0.0035	11.5	2974	406	20	50.15	62.26	0.891	11	165	1571	71.5	93.5	648	2862	108	167.4
239	0.171	0.0048	14.4	2870	252	16	53.84	62.16	0.527	16	240	1239	120	120	876	2731	146	305.8
240	0.139	0.0018	21.9	2200	220	26	52.03	61.13	0.854	16	240	1927	152	88	1040	3745	130	242.5
241	0.089	0.0050	0.5	1971	342	7	57.09	61.61	0.821	19	285	1161	218.5	66.5	1360	2144	136	265.4
242	0.173	0.0054	15.5	1666	467	15	52.96	60.62	0.581	15	225	1897	112.5	112.5	1368	3602	114	186.5
243	0.048	0.0035	27.1	2145	282	13	54.51	60.00	0.557	11	165	2438	126.5	38.5	1950	3464	195	545.6
244	0.125	0.0041	6.6	114	276	27	55.44	62.01	0.956	24	360	1645	108	252	2430	2790	135	261.5
245	0.113	0.0036	26.2	2369	281	19	51.02	60.18	0.741	17	255	3109	178.5	76.5	832	3515	104	155.2
246	0.041	0.0025	2.5	2787	478	29	48.90	60.76	0.926	12	180	1275	42	138	624	2811	104	155.2

	Φ_m	Φ_f	k_m	k_{hf}	k_{hf}	d_f	r_o	r_w	μ_w	h	h_t	p_{sf}	d_{top}	d_{owc}	l_{wp}	p_i	wd	$acre$
247	0.011	0.0046	14.0	124	187	17	56.26	61.42	0.905	24	360	2003	180	180	2268	2999	126	227.8
248	0.157	0.0073	0.7	2491	452	25	51.90	62.39	0.593	29	435	3431	101.5	333.5	1464	3435	183	480.5
249	0.155	0.0028	24.3	2325	107	14	55.75	61.15	0.624	14	210	3505	147	63	1600	3663	200	573.9
250	0.090	0.0070	5.4	2991	236	16	49.79	62.38	0.527	18	270	1954	81	189	708	2799	118	199.8
251	0.021	0.0050	5.0	760	406	6	49.09	60.39	0.804	12	180	3306	54	126	2400	3504	150	322.8
252	0.043	0.0026	20.7	1961	347	28	56.76	61.61	0.756	18	270	2715	171	99	1100	3148	110	173.6
253	0.012	0.0082	12.1	878	150	20	48.01	61.98	0.600	12	180	2085	54	126	2016	2349	112	180.0
254	0.112	0.0065	9.0	877	104	14	56.64	61.74	0.995	25	375	1578	137.5	237.5	1952	2312	122	213.6
255	0.058	0.0034	23.1	2315	339	24	48.37	60.89	0.750	11	165	1245	104.5	60.5	952	2097	119	203.2
256	0.184	0.0060	15.0	2435	340	3	53.45	61.91	0.666	30	450	3083	225	225	1384	3207	173	429.4
257	0.086	0.0087	21.5	726	132	15	50.51	60.10	0.609	20	300	1646	230	70	2646	3207	147	310.0
258	0.179	0.0074	1.7	1462	237	1	53.11	60.63	0.813	17	255	2550	59.5	195.5	1992	3035	166	395.4
259	0.023	0.0071	13.1	735	297	15	56.74	62.36	0.788	22	330	2028	143	187	2112	3944	132	250.0
260	0.045	0.0096	17.2	2775	380	20	48.70	61.67	0.875	20	300	1221	170	130	1032	2270	172	424.5
261	0.103	0.0021	14.4	2324	215	19	52.32	61.99	0.504	12	180	2948	102	78	2646	3487	189	512.5
262	0.127	0.0069	13.2	1158	370	3	52.31	60.68	0.650	15	225	3303	157.5	67.5	678	3928	113	183.2
263	0.158	0.0095	3.8	853	139	10	53.64	61.71	0.572	23	345	1844	103.5	241.5	2592	2202	162	376.5
264	0.105	0.0015	9.0	2646	359	18	52.31	61.46	0.925	25	375	1622	137.5	237.5	780	2323	130	242.5
265	0.091	0.0034	0.1	645	405	27	51.38	59.99	0.669	17	255	2476	59.5	195.5	2480	3176	155	344.7
266	0.126	0.0099	28.5	2301	495	20	55.21	60.11	0.638	12	180	2352	138	42	1480	3117	185	491.1
267	0.173	0.0079	23.0	191	150	28	48.14	62.35	0.503	28	420	1535	266	154	3132	3403	174	434.4
268	0.137	0.0053	22.5	1962	245	3	51.74	61.09	0.901	18	270	2115	171	99	1130	3354	113	183.2
269	0.067	0.0048	10.5	1191	250	4	53.46	59.94	0.769	26	390	1881	169	221	1848	3014	132	250.0

	Φ_m	Φ_f	k_m	k_{hf}	k_{hf}	d_f	r_o	r_w	μ_w	h	h_t	p_{sf}	d_{top}	d_{owc}	l_{wp}	p_i	wd	$acre$
270	0.144	0.0044	4.5	716	445	16	52.74	60.17	0.935	15	225	1180	67.5	157.5	2928	2026	183	480.5
271	0.083	0.0029	14.9	2397	216	20	52.97	62.12	0.861	21	315	3098	157.5	157.5	1072	3508	134	257.6
272	0.118	0.0044	24.3	521	153	5	51.09	61.01	0.834	12	180	1894	126	54	2672	2242	167	400.2
273	0.181	0.0040	19.2	641	447	27	53.14	59.98	0.980	25	375	1139	212.5	162.5	2752	3558	172	424.5
274	0.188	0.0098	21.9	1507	400	9	57.93	62.13	0.798	28	420	2059	266	154	1812	2823	151	327.1
275	0.165	0.0060	25.8	2530	267	2	52.56	60.55	0.904	14	210	1501	147	63	984	3215	123	217.1
276	0.010	0.0086	18.8	509	100	7	52.26	60.50	0.992	20	300	2148	170	130	2070	2513	115	189.8
277	0.011	0.0047	5.4	2223	159	3	50.13	61.34	0.943	20	300	1645	90	210	920	2059	115	189.8
278	0.027	0.0052	17.2	2104	209	28	49.93	61.04	0.607	26	390	2386	221	169	1510	2512	151	327.1
279	0.060	0.0084	4.9	200	448	1	56.33	60.76	0.517	25	375	1496	112.5	262.5	3006	2487	167	400.2
280	0.014	0.0099	27.2	1517	340	4	55.27	61.50	0.726	16	240	2360	184	56	1584	2601	132	250.0
281	0.091	0.0057	2.3	2917	228	1	53.30	62.24	0.507	24	360	2648	84	276	864	3950	144	297.5
282	0.075	0.0093	10.2	426	213	7	56.29	61.41	0.737	29	435	2680	188.5	246.5	1854	3916	103	152.2
283	0.113	0.0077	17.4	2255	274	1	53.12	60.54	0.976	27	405	1169	229.5	175.5	1040	2004	130	242.5
284	0.186	0.0061	14.3	1951	461	19	53.52	60.33	0.624	24	360	1085	180	180	1820	2146	182	475.3
285	0.067	0.0097	24.2	1823	470	15	50.13	60.94	0.693	20	300	2561	210	90	1460	3780	146	305.8
286	0.074	0.0084	15.9	1546	302	8	53.88	59.87	0.716	14	210	1730	105	105	1464	2591	122	213.6
287	0.173	0.0096	6.8	1746	351	6	49.43	62.08	0.915	14	210	2107	77	133	2040	2454	170	414.7
288	0.075	0.0068	21.3	1336	387	3	48.52	61.39	0.912	23	345	1121	218.5	126.5	2478	2851	177	449.5
289	0.036	0.0044	4.5	321	109	11	54.83	60.33	0.726	18	270	1165	81	189	2610	3394	145	301.7
290	0.106	0.0053	19.7	942	329	1	54.09	61.15	0.690	29	435	1764	246.5	188.5	2002	3441	143	293.4
291	0.173	0.0092	19.0	1727	118	18	50.20	59.94	0.963	18	270	1156	153	117	1860	2474	155	344.7
292	0.083	0.0011	6.9	1936	269	14	52.06	62.04	0.870	28	420	2597	154	266	1500	2886	150	322.8

	Φ_m	Φ_f	k_m	k_{hf}	k_{hf}	d_f	r_o	r_w	μ_w	h	h_t	p_{sf}	d_{top}	d_{owc}	l_{wp}	p_i	wd	$acre$
293	0.142	0.0024	5.5	2799	287	9	54.30	60.95	0.869	14	210	1951	63	147	912	3762	152	331.5
294	0.129	0.0052	5.0	2935	109	22	53.55	61.22	0.973	16	240	1582	72	168	930	3231	155	344.7
295	0.096	0.0059	4.5	371	126	25	49.28	61.27	0.755	20	300	1424	90	210	1854	2563	103	152.2
296	0.100	0.0015	6.1	2019	469	8	49.69	61.57	0.896	20	300	3437	90	210	1360	3874	136	265.4
297	0.190	0.0069	28.6	1848	313	15	48.01	60.77	0.726	24	360	1201	276	84	1490	2190	149	318.5
298	0.026	0.0090	0.5	1474	246	13	52.18	60.00	0.925	30	450	1252	105	345	1332	3080	111	176.8
299	0.063	0.0020	28.7	1133	245	10	52.88	60.99	0.695	16	240	1842	184	56	1400	2241	100	143.5
300	0.095	0.0049	0.8	1479	160	25	49.60	59.92	0.869	18	270	1995	63	207	1632	3184	136	265.4
301	0.122	0.0035	29.1	2045	159	29	54.67	61.72	0.988	28	420	1915	322	98	1920	2179	192	528.9
302	0.177	0.0099	8.9	2882	240	19	48.18	59.90	0.762	30	450	2533	165	285	648	3564	108	167.4
303	0.099	0.0065	15.8	358	234	6	49.20	62.28	0.715	26	390	2161	195	195	2880	3484	160	367.3
304	0.093	0.0033	25.9	2413	413	4	57.52	61.73	0.604	25	375	2988	262.5	112.5	888	3241	111	176.8
305	0.152	0.0022	26.9	1813	294	17	57.76	62.24	0.662	30	450	1182	345	105	1050	2018	105	158.2
306	0.099	0.0059	5.7	2745	285	10	48.31	61.13	0.555	28	420	1986	126	294	690	2764	115	189.8
307	0.174	0.0085	19.8	393	152	8	52.94	60.43	0.688	30	450	1694	255	195	2754	3135	153	335.9
308	0.037	0.0073	17.4	578	299	22	48.68	61.86	0.793	11	165	1881	126.5	38.5	2632	2610	188	507.1
309	0.105	0.0085	29.3	249	369	6	50.43	61.77	0.671	10	150	1126	115	35	2412	2465	134	257.6
310	0.103	0.0028	3.2	1561	434	20	56.34	62.38	0.909	28	420	3199	98	322	1728	3238	144	297.5
311	0.054	0.0059	5.4	2328	362	2	56.14	60.73	0.766	26	390	2349	117	273	1024	3644	128	235.1
312	0.026	0.0089	22.4	920	493	1	54.29	61.76	0.761	23	345	2956	218.5	126.5	3168	3014	198	562.5
313	0.023	0.0021	1.5	753	491	9	48.02	60.09	0.887	30	450	1592	105	345	2528	2101	158	358.2
314	0.034	0.0020	28.2	2953	113	25	49.31	61.85	0.903	19	285	1794	66.5	218.5	1890	3908	135	261.5
315	0.153	0.0020	7.3	2897	412	19	48.51	62.32	0.912	17	255	1629	76.5	178.5	930	3020	155	344.7

	Φ_m	Φ_f	k_m	k_{hf}	k_{hf}	d_f	r_o	r_w	μ_w	h	h_t	p_{sf}	d_{top}	d_{owc}	l_{wp}	p_i	wd	$acre$
316	0.167	0.0043	28.7	2032	230	8	54.28	60.27	0.595	16	240	1413	152	88	810	2543	135	261.5
317	0.158	0.0032	15.3	2205	426	27	48.29	62.22	0.513	26	390	1383	221	169	2682	3811	149	318.5
318	0.046	0.0041	16.9	1068	169	23	49.36	59.92	0.528	12	180	1411	54	126	1120	2878	112	180.0
319	0.091	0.0032	29.8	1616	370	17	54.95	60.43	0.571	12	180	1747	126	54	2296	3592	164	385.9
320	0.013	0.0045	23.1	892	450	27	53.16	59.82	0.586	11	165	2644	71.5	93.5	1040	2877	130	242.5
321	0.072	0.0048	9.4	2183	402	11	53.43	61.55	0.813	15	225	1693	112.5	112.5	1272	2071	106	161.2
322	0.036	0.0068	1.7	2356	191	10	56.08	62.15	0.515	25	375	1591	187.5	187.5	1824	3978	114	186.5
323	0.096	0.0081	1.3	335	243	18	55.94	61.29	0.736	12	180	2119	54	126	2208	3644	184	485.8
324	0.119	0.0034	24.4	742	245	3	53.02	60.20	0.839	20	300	2925	70	230	1024	3024	128	235.1
325	0.160	0.0086	12.4	691	206	11	50.77	61.11	0.557	28	420	1853	210	210	1376	2904	172	424.5
326	0.090	0.0077	11.5	1909	234	6	49.20	61.28	0.618	27	405	2138	94.5	310.5	3072	2183	192	528.9
327	0.134	0.0064	23.5	2690	123	10	51.40	60.17	0.698	20	300	2110	130	170	2016	3429	126	227.8
328	0.168	0.0017	19.7	587	407	7	49.73	59.89	0.603	18	270	1079	153	117	2394	2073	171	419.6
329	0.114	0.0065	18.1	686	111	27	54.38	61.24	0.901	21	315	1113	73.5	241.5	1920	2220	192	528.9
330	0.181	0.0073	2.9	1460	354	24	48.91	60.17	0.650	20	300	2027	190	110	1270	2551	127	231.4
331	0.020	0.0020	10.1	1197	123	16	48.75	60.79	0.888	20	300	1579	90	210	2358	2219	131	246.2
332	0.074	0.0064	7.4	285	373	3	48.32	61.30	0.777	30	450	2064	255	195	636	3392	106	161.2
333	0.053	0.0083	11.4	2307	321	15	55.25	59.85	0.865	18	270	1093	171	99	1750	2637	125	224.2
334	0.166	0.0083	8.1	1267	102	28	49.44	61.30	0.887	25	375	2176	87.5	287.5	2352	2952	196	551.2
335	0.076	0.0018	6.5	2055	215	25	54.36	62.22	0.950	27	405	1905	283.5	121.5	1848	2105	154	340.3
336	0.015	0.0091	24.0	249	158	29	53.66	61.70	0.897	27	405	1052	175.5	229.5	2672	3188	167	400.2
337	0.192	0.0051	6.3	991	129	11	51.77	62.32	0.595	25	375	2646	137.5	237.5	2240	3334	140	281.2
338	0.139	0.0016	26.9	2899	284	10	56.22	61.38	0.514	27	405	1597	202.5	202.5	912	2619	152	331.5

	Φ_m	Φ_f	k_m	k_{hf}	k_{hf}	d_f	r_o	r_w	μ_w	h	h_t	p_{sf}	d_{top}	d_{owc}	l_{wp}	p_i	wd	$acre$
339	0.174	0.0032	22.4	2801	248	23	51.05	61.67	0.564	19	285	1280	104.5	180.5	654	2286	109	170.5
340	0.188	0.0076	16.1	1196	429	7	51.19	60.59	0.567	13	195	2797	84.5	110.5	1700	3243	170	414.7
341	0.139	0.0014	29.1	1891	315	28	55.85	60.99	0.564	19	285	2069	123.5	161.5	2142	2942	153	335.9
342	0.184	0.0048	17.0	1731	427	27	53.04	59.92	0.968	24	360	3784	204	156	1590	3913	159	362.7
343	0.059	0.0059	6.5	2508	284	11	50.61	60.80	0.637	23	345	1431	195.5	149.5	1260	2352	126	227.8
344	0.178	0.0096	25.7	2877	105	11	55.32	60.74	0.971	22	330	3398	253	77	840	3447	140	281.2
345	0.185	0.0029	25.9	318	101	21	49.63	60.55	0.819	20	300	1752	230	70	2736	3310	152	331.5
346	0.067	0.0020	9.4	2675	166	21	57.21	61.92	0.936	23	345	1512	149.5	195.5	2064	2988	172	424.5
347	0.024	0.0068	9.8	1731	246	24	50.22	60.97	0.684	12	180	1362	54	126	1442	3675	103	152.2
348	0.156	0.0020	25.2	663	387	18	48.84	61.90	0.618	25	375	2002	287.5	87.5	1270	3080	127	231.4
349	0.026	0.0099	14.8	742	163	3	48.74	61.85	0.594	17	255	2064	93.5	161.5	2184	2771	182	475.3
350	0.148	0.0032	1.6	2146	211	17	55.70	60.54	0.773	12	180	1465	90	90	1600	3314	100	143.5
351	0.134	0.0084	12.8	1800	214	22	55.40	59.94	0.653	18	270	1023	63	207	2268	2177	126	227.8
352	0.042	0.0085	8.4	2908	228	20	55.58	61.46	0.508	17	255	2674	93.5	161.5	1926	2895	107	164.3
353	0.033	0.0028	4.3	1600	235	27	50.46	62.22	0.696	28	420	1679	182	238	2576	2381	184	485.8
354	0.130	0.0078	11.0	389	255	7	52.66	62.15	0.981	12	180	2412	102	78	1216	3631	152	331.5
355	0.013	0.0092	23.8	583	458	21	55.87	60.89	0.925	27	405	1363	310.5	94.5	2576	2373	184	485.8
356	0.099	0.0091	1.2	396	455	22	52.23	60.20	0.504	13	195	1729	58.5	136.5	1460	2952	146	305.8
357	0.148	0.0056	20.5	2584	287	24	55.05	61.35	0.781	17	255	1299	110.5	144.5	1480	2187	148	314.3
358	0.094	0.0081	8.6	1955	200	25	57.81	61.52	0.557	26	390	2051	273	117	2100	2120	175	439.4
359	0.135	0.0027	19.7	1180	479	23	53.70	60.83	0.770	22	330	2606	165	165	2176	2697	136	265.4
360	0.066	0.0077	7.0	572	349	15	51.46	60.47	0.708	27	405	2445	148.5	256.5	912	3240	114	186.5
361	0.191	0.0053	18.7	1229	182	21	53.58	62.00	0.759	14	210	1554	91	119	960	2327	160	367.3

	Φ_m	Φ_f	k_m	k_{hf}	k_{hf}	d_f	r_o	r_w	μ_w	h	h_t	p_{sf}	d_{top}	d_{owc}	l_{wp}	p_i	wd	$acre$
362	0.142	0.0062	2.3	2419	143	23	51.00	62.26	0.943	22	330	2822	209	121	768	2847	128	235.1
363	0.049	0.0033	29.0	1259	326	10	49.59	60.78	0.575	26	390	2155	299	91	1630	2295	163	381.2
364	0.115	0.0018	18.3	2289	209	27	54.65	59.97	0.717	21	315	3497	241.5	73.5	1430	3937	143	293.4
365	0.177	0.0037	11.5	956	128	17	54.84	60.27	0.530	16	240	2081	72	168	846	2328	141	285.3
366	0.116	0.0093	0.9	1956	163	9	55.92	61.30	0.691	10	150	2095	45	105	2292	3497	191	523.4
367	0.153	0.0052	25.7	2666	119	8	51.49	60.28	0.861	12	180	2823	138	42	2058	2897	147	310.0
368	0.180	0.0034	18.1	707	372	26	50.50	60.56	0.548	18	270	2048	153	117	1480	2190	148	314.3
369	0.170	0.0079	25.4	1493	412	11	51.45	61.00	0.834	25	375	2624	87.5	287.5	2716	3245	194	540.0
370	0.035	0.0079	15.1	427	422	5	51.29	60.70	0.648	20	300	1350	150	150	1480	2814	148	314.3
371	0.046	0.0012	0.2	483	206	28	57.27	60.63	0.799	11	165	1923	126.5	38.5	2070	2112	115	189.8
372	0.039	0.0089	27.6	285	458	19	55.56	61.00	0.576	20	300	1359	130	170	936	2658	156	349.2
373	0.015	0.0082	12.3	329	343	29	50.88	60.41	0.718	22	330	2065	121	209	2752	2807	172	424.5
374	0.012	0.0039	22.0	1918	105	6	54.06	59.87	0.506	12	180	2211	66	114	1130	2648	113	183.2
375	0.123	0.0070	4.5	1292	237	25	55.66	61.51	0.615	14	210	1787	63	147	2002	2526	143	293.4
376	0.185	0.0094	27.3	2584	351	18	57.02	61.89	0.756	13	195	2141	110.5	84.5	3096	3228	172	424.5
377	0.149	0.0035	23.3	2314	278	2	53.96	60.86	0.608	16	240	2473	88	152	3258	2582	181	470.1
378	0.067	0.0025	22.7	2930	424	17	48.69	60.65	0.673	28	420	2166	238	182	1080	3726	180	464.9
379	0.104	0.0077	12.2	2366	157	19	50.18	61.74	0.874	21	315	1269	220.5	94.5	2952	2023	164	385.9
380	0.059	0.0053	21.1	2813	489	15	56.69	61.74	0.707	16	240	2058	56	184	2604	2114	186	496.4
381	0.149	0.0069	17.0	2243	433	2	52.14	60.25	0.528	28	420	1073	266	154	2148	2551	179	459.7
382	0.032	0.0097	17.5	835	236	15	54.61	60.11	0.695	26	390	1623	221	169	2464	2361	154	340.3
383	0.152	0.0038	10.4	2185	346	2	55.83	60.25	0.737	16	240	2172	120	120	2256	2266	188	507.1
384	0.164	0.0017	21.1	2111	221	25	50.48	61.43	0.913	13	195	1487	149.5	45.5	928	2813	116	193.1

	Φ_m	Φ_f	k_m	k_{hf}	k_{hf}	d_f	r_o	r_w	μ_w	h	h_t	p_{sf}	d_{top}	d_{owc}	l_{wp}	p_i	wd	$acre$
385	0.152	0.0081	4.8	2342	135	18	53.54	61.99	0.652	23	345	1488	80.5	264.5	1728	2611	144	297.5
386	0.074	0.0043	0.1	2266	308	21	50.30	61.13	0.911	17	255	1360	144.5	110.5	618	3283	103	152.2
387	0.121	0.0063	16.9	1023	430	19	48.07	60.23	0.783	29	435	2708	159.5	275.5	3168	2871	198	562.5
388	0.099	0.0027	16.4	1580	405	19	55.67	61.66	0.527	14	210	2055	49	161	1876	2751	134	257.6
389	0.027	0.0017	16.5	2341	479	28	48.22	62.16	0.630	21	315	2033	178.5	136.5	2688	3353	168	405.0
390	0.167	0.0024	20.8	1761	233	6	51.93	60.37	0.795	29	435	3567	304.5	130.5	1690	3663	169	409.8
391	0.140	0.0084	27.8	2866	255	14	50.53	62.06	0.740	22	330	2410	187	143	3114	3868	173	429.4
392	0.061	0.0037	28.3	597	160	25	50.04	60.35	0.599	21	315	1749	220.5	94.5	2466	3062	137	269.3
393	0.194	0.0045	27.1	2730	233	15	54.62	61.98	0.620	12	180	2602	54	126	2016	2897	144	297.5
394	0.067	0.0084	27.8	929	320	6	48.07	61.16	0.809	22	330	1971	99	231	3104	3044	194	540.0
395	0.088	0.0079	3.5	1919	164	21	55.46	61.04	0.572	15	225	2345	82.5	142.5	1596	3285	114	186.5
396	0.055	0.0044	10.2	1442	146	27	56.00	62.11	0.858	19	285	2667	66.5	218.5	2862	2805	159	362.7
397	0.018	0.0040	20.8	153	234	2	55.28	61.45	0.577	28	420	1565	266	154	1700	2443	170	414.7
398	0.109	0.0035	5.4	1382	300	7	53.19	61.71	0.701	21	315	2065	199.5	115.5	2574	2143	143	293.4
399	0.066	0.0067	12.8	1813	150	20	56.22	60.40	0.507	17	255	1760	127.5	127.5	1708	2628	122	213.6
400	0.098	0.0063	3.0	421	445	26	54.37	59.86	0.537	25	375	2310	137.5	237.5	1416	2526	118	199.8
401	0.041	0.0068	11.8	1315	493	2	50.88	59.92	0.916	10	150	1099	55	95	2560	2692	160	367.3
402	0.051	0.0099	23.4	572	325	1	57.47	61.80	0.723	27	405	1837	148.5	256.5	1140	3023	190	518.0
403	0.010	0.0021	16.1	206	255	27	57.67	62.32	0.963	25	375	1667	287.5	87.5	1660	2635	166	395.4
404	0.182	0.0076	23.1	890	296	14	48.67	60.81	0.547	14	210	1034	77	133	3024	3752	168	405.0
405	0.139	0.0024	19.2	767	454	27	52.38	62.38	0.688	22	330	1404	165	165	732	2320	122	213.6
406	0.108	0.0049	26.8	1139	462	10	51.21	60.65	0.773	28	420	1095	126	294	2172	2318	181	470.1
407	0.109	0.0085	1.8	489	299	21	49.34	60.16	0.556	19	285	1021	123.5	161.5	3276	2046	182	475.3

	Φ_m	Φ_f	k_m	k_{hf}	k_{hf}	d_f	r_o	r_w	μ_w	h	h_t	p_{sf}	d_{top}	d_{owc}	l_{wp}	p_i	wd	$acre$
408	0.030	0.0042	5.3	2995	311	1	49.35	60.80	0.952	27	405	1526	121.5	283.5	2502	3766	139	277.2
409	0.199	0.0017	12.5	1589	463	15	56.06	61.26	0.817	20	300	3274	130	170	804	3864	134	257.6
410	0.078	0.0060	22.2	1224	331	10	53.25	61.45	0.953	16	240	1408	168	72	792	2943	132	250.0
411	0.011	0.0073	4.1	1257	287	22	52.10	60.21	0.658	27	405	1312	202.5	202.5	2702	3322	193	534.4
412	0.114	0.0054	12.7	2786	187	10	51.71	60.20	0.556	12	180	1286	126	54	1224	2088	102	149.3
413	0.107	0.0026	22.9	1536	341	19	50.27	60.16	0.815	23	345	1472	218.5	126.5	3276	2048	182	475.3
414	0.057	0.0019	15.7	1866	173	13	52.46	61.65	0.530	15	225	1313	52.5	172.5	2136	2554	178	454.6
415	0.019	0.0028	22.6	113	179	17	50.66	61.01	0.837	13	195	2252	58.5	136.5	2632	3465	188	507.1
416	0.170	0.0022	5.1	1804	444	28	52.59	60.09	0.739	12	180	1118	66	114	2352	3050	196	551.2
417	0.019	0.0039	20.2	2354	150	18	52.33	61.62	0.653	18	270	1147	99	171	1150	3145	115	189.8
418	0.070	0.0096	18.6	2005	358	5	50.60	60.27	0.758	17	255	2044	76.5	178.5	2556	3890	142	289.3
419	0.159	0.0058	0.2	1632	274	25	49.34	61.89	0.854	13	195	2796	71.5	123.5	3492	3455	194	540.0
420	0.195	0.0032	22.2	2494	345	22	52.19	61.14	0.907	23	345	1874	126.5	218.5	1568	2078	112	180.0
421	0.121	0.0049	29.8	2891	394	4	53.07	61.23	0.658	30	450	2966	345	105	1356	3327	113	183.2
422	0.158	0.0070	3.9	1009	221	5	51.24	60.34	0.656	25	375	2324	162.5	212.5	1704	2445	142	289.3
423	0.148	0.0059	10.8	2411	117	9	54.85	61.84	0.672	22	330	1973	121	209	2640	3206	165	390.6
424	0.134	0.0065	5.7	927	434	13	52.43	61.17	0.833	25	375	1105	162.5	212.5	1110	2181	185	491.1
425	0.136	0.0088	21.4	143	247	16	52.36	61.28	0.931	21	315	2765	115.5	199.5	1016	3848	127	231.4
426	0.188	0.0044	5.3	373	364	8	55.93	60.90	0.881	26	390	1685	247	143	2196	2080	183	480.5
427	0.112	0.0077	29.6	1053	458	25	56.16	61.68	0.938	30	450	1874	195	255	630	2110	105	158.2
428	0.086	0.0024	0.5	986	209	23	55.52	59.99	0.936	14	210	2567	63	147	1150	3750	115	189.8
429	0.137	0.0015	1.2	152	499	8	55.89	61.35	0.586	16	240	1412	136	104	3072	3732	192	528.9
430	0.094	0.0041	24.1	570	433	18	53.01	62.04	0.925	20	300	1216	130	170	1072	2204	134	257.6

	Φ_m	Φ_f	k_m	k_{hf}	k_{hf}	d_f	r_o	r_w	μ_w	h	h_t	p_{sf}	d_{top}	d_{owc}	l_{wp}	p_i	wd	$acre$
431	0.035	0.0084	25.8	1387	416	3	53.55	60.97	0.980	19	285	2772	123.5	161.5	1380	3178	115	189.8
432	0.093	0.0044	17.0	2323	362	20	54.31	61.50	0.885	14	210	1514	49	161	2464	2629	154	340.3
433	0.114	0.0098	22.6	2075	317	11	48.98	60.59	0.938	16	240	2373	168	72	1050	3430	175	439.4
434	0.085	0.0064	15.6	2172	254	20	50.46	61.38	0.534	19	285	1584	142.5	142.5	2286	2677	127	231.4
435	0.086	0.0040	17.6	1433	428	9	54.16	60.53	0.823	30	450	3620	105	345	1404	3922	117	196.4
436	0.153	0.0094	5.7	2765	338	20	51.05	61.88	0.662	21	315	1278	241.5	73.5	1068	3781	178	454.6
437	0.109	0.0091	15.1	2967	412	12	55.67	61.87	0.820	28	420	1594	154	266	1990	2979	199	568.2
438	0.103	0.0087	1.5	2804	495	12	50.67	62.28	0.940	26	390	2738	221	169	1060	3572	106	161.2
439	0.027	0.0033	1.7	1438	415	7	48.40	60.96	0.687	20	300	2143	170	130	1788	2860	149	318.5
440	0.058	0.0036	10.1	2724	441	22	50.97	60.99	0.883	23	345	2947	103.5	241.5	1560	3314	156	349.2
441	0.095	0.0080	18.9	1220	294	24	53.56	61.36	0.584	24	360	2233	276	84	912	3282	152	331.5
442	0.145	0.0054	20.2	1724	233	15	54.89	59.88	0.814	22	330	2356	165	165	1936	2845	121	210.1
443	0.199	0.0097	20.6	2552	182	6	55.18	60.29	0.857	13	195	1949	136.5	58.5	1624	3109	116	193.1
444	0.187	0.0053	20.9	925	297	18	53.59	62.25	0.653	20	300	2694	170	130	1632	2710	102	149.3
445	0.028	0.0100	24.0	2023	112	6	53.33	62.26	0.632	27	405	1024	94.5	310.5	1488	2738	124	220.6
446	0.191	0.0054	19.8	1846	431	12	56.76	60.98	0.958	25	375	2256	187.5	187.5	1330	3095	133	253.8
447	0.041	0.0055	15.6	2003	205	25	51.93	61.91	0.808	15	225	1688	157.5	67.5	1704	3851	142	289.3
448	0.194	0.0079	10.0	998	370	13	52.58	62.22	0.547	20	300	1894	190	110	1428	2668	102	149.3
449	0.123	0.0045	28.0	1061	417	27	50.08	61.55	0.814	18	270	2282	153	117	900	2854	150	322.8
450	0.056	0.0051	7.4	645	372	11	55.57	60.77	0.596	29	435	1114	101.5	333.5	2632	2774	188	507.1
451	0.023	0.0022	15.3	391	360	21	53.47	60.85	0.888	16	240	1353	152	88	2184	3754	156	349.2
452	0.067	0.0078	22.2	931	194	18	51.57	60.94	0.932	12	180	1915	90	90	1836	3822	153	335.9
453	0.165	0.0061	7.6	1128	290	3	55.01	61.56	0.667	14	210	1514	119	91	1890	2272	105	158.2

	Φ_m	Φ_f	k_m	k_{hf}	k_{hf}	d_f	r_o	r_w	μ_w	h	h_t	p_{sf}	d_{top}	d_{owc}	l_{wp}	p_i	wd	$acre$
454	0.025	0.0068	25.4	1653	474	12	49.09	61.01	0.568	29	435	2302	275.5	159.5	2272	2454	142	289.3
455	0.077	0.0082	16.1	2973	196	27	48.07	62.28	0.883	26	390	2770	273	117	3600	3026	200	573.9
456	0.035	0.0030	27.3	181	183	2	53.97	60.72	0.659	30	450	2782	105	345	3312	3769	184	485.8
457	0.040	0.0087	10.5	2157	208	12	54.59	60.68	0.626	10	150	1783	105	45	702	2827	117	196.4
458	0.022	0.0091	28.1	2724	410	7	53.80	62.13	0.600	13	195	2362	110.5	84.5	2268	2592	126	227.8
459	0.143	0.0036	27.8	2610	232	7	57.10	61.22	0.535	27	405	1208	94.5	310.5	1144	2495	143	293.4
460	0.026	0.0075	17.6	445	341	11	54.36	61.75	0.776	26	390	1597	143	247	1512	2660	126	227.8
461	0.127	0.0041	3.1	2870	173	27	53.26	60.12	0.702	29	435	2538	130.5	304.5	3204	3792	178	454.6
462	0.043	0.0035	11.0	1378	134	15	50.60	60.98	0.875	28	420	2299	238	182	2376	2498	198	562.5
463	0.134	0.0025	8.3	2639	223	24	48.51	59.99	0.744	21	315	2682	157.5	157.5	1010	2748	101	146.4
464	0.105	0.0070	8.0	2608	192	11	55.32	61.52	0.692	24	360	2122	84	276	3600	2378	200	573.9
465	0.064	0.0058	6.8	1129	463	14	49.64	61.63	0.531	21	315	1505	241.5	73.5	912	2340	152	331.5
466	0.168	0.0085	0.0	1930	474	28	50.80	62.19	0.607	12	180	1183	66	114	1300	3296	130	242.5
467	0.165	0.0034	26.8	2607	112	4	50.59	61.52	0.772	14	210	1939	77	133	1224	2986	102	149.3
468	0.188	0.0026	13.6	160	337	3	53.47	61.59	0.705	21	315	1079	115.5	199.5	936	2410	156	349.2
469	0.010	0.0049	17.4	322	117	21	53.41	62.02	0.950	14	210	2685	49	161	1760	3994	110	173.6
470	0.132	0.0053	9.5	1192	269	28	55.88	61.02	0.528	16	240	2253	120	120	1216	3721	152	331.5
471	0.120	0.0077	12.0	1097	488	9	50.19	60.62	0.660	14	210	1086	77	133	2178	3338	121	210.1
472	0.058	0.0049	2.2	2563	316	3	57.26	61.26	0.594	17	255	2764	161.5	93.5	1904	2802	119	203.2
473	0.107	0.0030	3.8	454	400	17	50.37	61.62	0.575	19	285	2594	104.5	180.5	1670	3187	167	400.2
474	0.086	0.0029	11.8	2458	151	20	51.09	60.57	0.562	24	360	1448	108	252	1776	2135	148	314.3
475	0.036	0.0060	3.6	349	162	29	57.46	62.16	0.757	27	405	2929	202.5	202.5	738	3217	123	217.1
476	0.191	0.0070	29.4	657	207	8	52.11	61.08	0.694	16	240	1344	104	136	1192	3873	149	318.5

	Φ_m	Φ_f	k_m	k_{hf}	k_{hf}	d_f	r_o	r_w	μ_w	h	h_t	p_{sf}	d_{top}	d_{owc}	l_{wp}	p_i	wd	$acre$
477	0.078	0.0095	15.6	1925	273	18	48.10	60.34	0.989	24	360	3431	276	84	1872	3959	104	155.2
478	0.169	0.0014	15.2	285	258	29	51.10	59.87	0.646	28	420	1693	154	266	996	3125	166	395.4
479	0.018	0.0025	9.8	2254	270	15	49.55	60.24	0.796	24	360	1729	204	156	1352	2562	169	409.8
480	0.175	0.0017	19.2	2860	358	13	49.40	60.47	0.840	28	420	1111	238	182	2538	3804	141	285.3
481	0.024	0.0039	25.9	2415	278	18	52.50	62.30	0.808	24	360	1096	204	156	1360	3770	136	265.4
482	0.070	0.0018	8.0	565	104	16	53.45	61.84	0.780	26	390	3327	221	169	1344	3909	112	180.0
483	0.190	0.0083	16.2	2239	113	4	50.62	61.55	0.640	11	165	1650	60.5	104.5	2466	2251	137	269.3
484	0.172	0.0046	16.5	2295	259	17	56.83	61.99	0.576	29	435	2402	130.5	304.5	2916	3762	162	376.5
485	0.043	0.0069	28.9	2655	491	5	49.03	60.89	0.867	18	270	2102	171	99	1854	2624	103	152.2
486	0.112	0.0061	8.1	1344	317	8	56.24	61.63	0.520	20	300	1044	70	230	1650	3246	165	390.6
487	0.066	0.0010	8.0	643	464	16	52.27	61.05	0.901	22	330	2479	231	99	1840	3565	115	189.8
488	0.182	0.0069	9.3	978	229	24	57.20	61.93	0.703	24	360	3267	156	204	2268	3843	126	227.8
489	0.025	0.0039	16.7	1030	216	21	53.28	60.94	0.915	13	195	1476	136.5	58.5	1368	2258	114	186.5
490	0.160	0.0034	11.4	1381	451	15	56.71	62.04	0.986	12	180	1027	138	42	690	2761	115	189.8
491	0.043	0.0051	7.4	1149	411	26	51.53	59.82	0.711	21	315	1395	136.5	178.5	1430	2456	143	293.4
492	0.147	0.0066	20.3	1914	257	28	52.00	62.39	0.527	13	195	2076	45.5	149.5	1300	3004	130	242.5
493	0.054	0.0082	7.8	2822	452	14	53.98	60.52	0.894	20	300	2347	210	90	3184	2927	199	568.2
494	0.156	0.0098	14.9	883	453	1	50.21	61.60	0.875	16	240	3147	136	104	2048	3454	128	235.1
495	0.051	0.0012	14.9	809	286	27	49.33	60.20	0.754	14	210	3007	105	105	2448	3195	136	265.4
496	0.196	0.0081	12.8	2770	269	15	48.42	61.05	0.784	30	450	1444	255	195	1930	2706	193	534.4
497	0.083	0.0035	17.0	2786	282	26	52.01	62.11	0.655	18	270	1345	99	171	2220	2845	185	491.1
498	0.131	0.0084	18.4	998	378	7	53.96	60.54	0.874	12	180	3198	114	66	1392	3686	116	193.1
499	0.019	0.0072	24.2	321	138	4	57.20	61.84	0.668	17	255	3715	110.5	144.5	1128	3933	188	507.1

	Φ_m	Φ_f	k_m	k_{hf}	k_{hf}	d_f	r_o	r_w	μ_w	h	h_t	p_{sf}	d_{top}	d_{owc}	l_{wp}	p_i	wd	$acre$
500	0.054	0.0064	26.4	2364	393	4	50.94	60.24	0.942	21	315	3523	220.5	94.5	642	3580	107	164.3
501	0.176	0.0045	4.8	479	152	17	53.45	61.70	0.667	17	255	2705	110.5	144.5	1416	2803	177	449.5
502	0.097	0.0016	2.7	1438	298	14	55.82	60.44	0.898	22	330	1744	231	99	3120	2494	195	545.6
503	0.011	0.0100	9.4	1376	203	11	51.27	60.01	0.902	23	345	1901	241.5	103.5	1620	2637	162	376.5
504	0.098	0.0069	18.2	1854	336	22	48.95	62.02	0.525	26	390	2916	91	299	1152	3233	144	297.5
505	0.167	0.0031	11.4	468	191	14	52.42	61.59	0.701	20	300	1953	130	170	1000	2384	100	143.5
506	0.176	0.0018	27.8	1837	482	21	48.29	62.29	0.983	19	285	3444	218.5	66.5	880	3484	110	173.6
507	0.067	0.0032	1.7	483	125	27	54.75	62.36	0.707	14	210	1499	91	119	1146	2413	191	523.4
508	0.055	0.0091	29.8	434	173	24	49.12	61.19	0.665	14	210	1125	77	133	1580	2379	158	358.2
509	0.188	0.0025	7.3	498	167	19	49.91	60.40	0.834	22	330	2471	187	143	2790	2490	155	344.7
510	0.093	0.0053	18.5	886	216	29	53.30	61.04	0.929	15	225	1871	157.5	67.5	1936	2121	121	210.1
511	0.106	0.0092	4.4	2837	154	26	54.27	62.11	0.894	28	420	2183	294	126	3564	3209	198	562.5
512	0.045	0.0027	0.9	1598	175	19	51.74	59.86	0.769	18	270	2497	135	135	894	2956	149	318.5
513	0.039	0.0050	17.2	1391	482	1	54.06	60.13	0.871	30	450	1339	285	165	1980	3765	165	390.6
514	0.182	0.0066	0.9	994	218	29	56.46	61.73	0.870	19	285	1107	180.5	104.5	1376	2837	172	424.5
515	0.199	0.0063	21.3	1461	194	12	55.02	60.82	0.722	16	240	1406	120	120	1656	2815	138	273.2
516	0.084	0.0070	6.4	2360	364	12	51.93	60.82	0.925	27	405	1126	283.5	121.5	1248	2752	104	155.2
517	0.167	0.0034	7.7	589	101	15	53.72	61.36	0.747	21	315	2566	157.5	157.5	1498	3166	107	164.3
518	0.191	0.0048	28.8	165	131	16	50.50	59.86	0.974	30	450	1092	345	105	900	2081	150	322.8
519	0.180	0.0082	5.5	2155	223	28	55.27	60.81	0.899	12	180	1053	126	54	864	2987	144	297.5
520	0.170	0.0094	24.0	1854	189	25	51.43	59.95	0.567	18	270	1008	81	189	1140	2675	114	186.5
521	0.140	0.0052	1.2	1299	378	14	48.79	61.59	0.619	20	300	1226	110	190	1498	3370	107	164.3
522	0.043	0.0038	9.3	2752	380	26	51.02	61.15	0.564	19	285	2295	85.5	199.5	2338	3725	167	400.2

	Φ_m	Φ_f	k_m	k_{hf}	k_{hf}	d_f	r_o	r_w	μ_w	h	h_t	p_{sf}	d_{top}	d_{owc}	l_{wp}	p_i	wd	$acre$
523	0.055	0.0050	29.0	1483	440	12	51.00	60.00	0.767	28	420	1964	210	210	2800	2471	175	439.4
524	0.134	0.0010	10.5	2016	472	11	48.50	60.18	0.866	20	300	2773	70	230	1700	3656	170	414.7
525	0.015	0.0035	3.7	1541	328	9	49.76	60.92	0.734	24	360	2577	180	180	1416	2893	177	449.5
526	0.061	0.0022	18.2	2789	312	10	56.61	61.51	0.991	15	225	2638	172.5	52.5	1264	2645	158	358.2
527	0.196	0.0025	19.4	2140	443	14	54.56	60.37	0.841	23	345	1797	218.5	126.5	1456	2218	182	475.3
528	0.153	0.0069	3.8	211	183	26	53.48	61.56	0.816	26	390	2124	273	117	1680	2180	105	158.2
529	0.119	0.0018	26.9	113	253	21	50.71	61.02	0.748	10	150	2225	75	75	1000	3177	125	224.2
530	0.126	0.0093	1.6	1666	338	11	56.96	61.69	0.644	30	450	1566	165	285	1670	3038	167	400.2

2. Input variables for testing in dual porosity system

	Φ_m	Φ_f	k_m	k_{hf}	k_{hf}	d_f	r_o	r_w	μ_w	h	h_t	p_{sf}	d_{top}	d_{owc}	l_{wp}	p_i	wd	$acre$
1	0.181	0.0023	22.8	1297	222	28	50.09	61.40	0.592	28	420	2469	126	294	1872	2621	117	196.4
2	0.085	0.0024	25.8	1921	140	8	57.64	62.14	0.981	12	180	2371	138	42	2408	2995	172	424.5
3	0.142	0.0075	14.5	1676	248	22	52.14	60.46	0.878	12	180	1510	114	66	2136	3300	178	454.6
4	0.049	0.0071	2.3	726	188	27	50.30	60.37	0.975	23	345	2171	264.5	80.5	2100	2510	175	439.4
5	0.128	0.0018	6.0	2601	410	27	51.60	61.91	0.593	14	210	1881	63	147	2632	3122	188	507.1
6	0.141	0.0011	23.4	114	272	2	53.02	61.63	0.645	11	165	1417	60.5	104.5	1764	3828	126	227.8
7	0.066	0.0044	12.2	462	348	17	55.48	62.08	0.529	21	315	2001	73.5	241.5	1860	3454	186	496.4
8	0.119	0.0081	24.8	2347	211	1	56.32	61.65	0.522	24	360	1760	84	276	642	3037	107	164.3

	Φ_m	Φ_f	k_m	k_{hf}	k_{hf}	d_f	r_o	r_w	μ_w	h	h_t	p_{sf}	d_{top}	d_{owc}	l_{wp}	p_i	wd	$acre$
9	0.070	0.0050	4.4	159	291	5	51.94	61.52	0.640	28	420	2444	154	266	1380	2743	138	273.2
10	0.164	0.0019	22.0	513	225	12	48.97	60.94	0.585	10	150	1157	45	105	1640	3265	164	385.9
11	0.079	0.0083	4.5	1029	430	7	50.65	61.26	0.839	11	165	3114	104.5	60.5	888	3616	111	176.8
12	0.143	0.0069	25.2	2723	397	16	55.92	62.37	0.951	20	300	1674	230	70	2772	2634	198	562.5
13	0.130	0.0051	16.4	1881	157	10	57.37	62.29	0.676	11	165	1348	71.5	93.5	1224	2160	102	149.3
14	0.193	0.0058	28.8	146	127	21	53.68	60.68	0.550	22	330	1803	77	253	1560	3360	130	242.5
15	0.022	0.0098	15.7	2696	250	7	51.78	61.21	0.571	27	405	3680	283.5	121.5	984	3884	164	385.9
16	0.124	0.0067	28.0	659	397	7	53.97	60.88	0.734	15	225	1170	112.5	112.5	1428	3889	119	203.2
17	0.138	0.0065	9.4	2349	453	4	54.66	60.38	0.515	14	210	2089	133	77	1940	3846	194	540.0
18	0.113	0.0027	2.0	177	388	1	55.62	59.88	0.842	29	435	1553	275.5	159.5	2304	2754	192	528.9
19	0.171	0.0082	29.0	2508	455	6	49.86	62.05	0.711	21	315	2314	136.5	178.5	1632	3576	136	265.4
20	0.018	0.0028	19.5	2316	165	15	53.17	62.13	0.830	12	180	1397	102	78	2556	2267	142	289.3
21	0.073	0.0047	12.6	2191	180	18	54.40	61.09	0.817	23	345	1302	195.5	149.5	1184	3580	148	314.3
22	0.102	0.0032	25.6	2735	198	19	57.36	62.15	0.904	22	330	1296	165	165	1240	3645	124	220.6
23	0.173	0.0034	10.4	2317	284	4	54.00	61.68	0.596	18	270	1046	81	189	2128	2455	133	253.8
24	0.104	0.0057	0.3	148	165	14	52.26	60.77	0.524	16	240	1364	120	120	2394	2033	133	253.8
25	0.199	0.0094	1.1	1214	389	3	49.29	61.00	0.874	13	195	1623	123.5	71.5	1048	2964	131	246.2
26	0.091	0.0057	4.6	180	453	12	50.93	60.24	0.710	27	405	1957	175.5	229.5	2160	2937	180	464.9
27	0.061	0.0052	11.2	103	419	9	52.77	61.87	0.869	21	315	2384	199.5	115.5	1270	2771	127	231.4
28	0.100	0.0057	26.3	120	437	19	49.30	62.11	0.843	17	255	2077	161.5	93.5	1840	2642	184	485.8
29	0.041	0.0040	13.2	586	315	7	50.28	60.17	0.978	18	270	1826	207	63	1264	3018	158	358.2
30	0.040	0.0040	19.1	536	183	19	49.81	62.24	0.654	16	240	2950	88	152	1134	3635	189	512.5

3. IMEX, CMG codes for multiple simulation runs (train case #1)

```
RESULTS SIMULATOR IMEX 2001200
 *TITLE1
 '25 x 25 x 15 rectangle grid '
 *TITLE2
 'Two Phase, Dual Porosity'

 INUNIT FIELD
 WSRF WELL 1
 WSRF GRID TIME
 WSRF SECTOR TIME
 OUTSRF WELL LAYER NONE
 OUTSRF RES ALL
 OUTSRF GRID SO SG SW PRES OILPOT BPP SSPRES WINFLUX
 WPRN GRID 0
 OUTPRN GRID NONE
 OUTPRN RES NONE
 **$  Distance units: ft
 RESULTS XOFFSET           0.0000
 RESULTS YOFFSET           0.0000
 RESULTS ROTATION           0.0000  **$  (DEGREES)
 RESULTS AXES-DIRECTIONS 1.0 -1.0 1.0
 **$ ************************************************************
 **$ Definition of fundamental cartesian grid
 **$ ************************************************************
 GRID VARI 25 25 15
 KDIR DOWN
 DI IVAR
 25*100
 DJ JVAR
 25*100
 DK ALL
 9375*24
 DTOP
 625*5000

 DUALPOR
 SHAPE GK
 NULL MATRIX CON            1
 NULL FRACTURE CON            1

 *DIFRAC *CON 19
 *DJFRAC *CON 19
 *DKFRAC *CON 19

  PINCHOUTARRAY CON            1

  *POR *MATRIX     *CON         1.647975e-01
```

```
*POR *FRACTURE   *CON         3.113019e-03

*PRPOR *MATRIX 15.0
*CPOR  *MATRIX 3.0E-6
*PRPOR *FRACTURE 15.0
*CPOR  *FRACTURE 3.0E-6

*PERMI *MATRIX *CON  1.546586e+01
*PERMJ *MATRIX *CON  1.546586e+01
*PERMK *MATRIX *CON  1.546586e+01

*PERMI *FRACTURE *CON  435
*PERMJ *FRACTURE *CON  435
*PERMK *FRACTURE *CON  298

AQUIFER BOTTOM
*AQPROP
**$thickness   porosity     permeability  radius       angle
  -99999       -99999       -99999        -99999       -99999
*AQLEAK  OFF
*AQMETHOD  CARTER-TRACY

**********************************************************************
** Component Properties section
**********************************************************************
MODEL OILWATER
 PVT
 **$          p        Rs        Bo        Eg      viso      visg
           15.0      100.0     1.036   100.0        1.04    0.008
         4800.0      550.0     1.41    1300.0      1.04     0.0081

 *DENSITY *OIL   5.751631e+01
 *DENSITY *GAS   0.0647
 *DENSITY *WATER 6.121626e+01
 *CO       9.28E-6
 *CVO      4.60E-5
 *BWI      1.0
 *CW       3.50E-6
 *REFPW    14.73
 *VWI      8.689208e-01
 *CVW      0.0
 PTYPE MATRIX   CON           1
 PTYPE FRACTURE CON           1

**********************************************************************
** Rock-fluid Properties Section
**********************************************************************
ROCKFLUID
**FRACTURE
RPT 1
SWT
**  Sw       krw      krow
  0.05      0.00      1.00
```

```
  0.25      0.25      0.75
  0.50      0.50      0.50
  0.75      0.75      0.25
  0.95      0.95      0.05
     1         1         0


**MATRIX
RPT 2
SWT
**  Sw    krw       krow      Pcow
  0.20    0.0000    1.0000    5.0
  0.25    0.0004    0.6027    4.0
  0.30    0.0024    0.4490    3.0
  0.35    0.0075    0.3242    2.5
  0.40    0.0167    0.2253    2.0
  0.45    0.0310    0.1492    1.8
  0.50    0.0515    0.0927    1.6
  0.60    0.1146    0.0265    1.4
  0.70    0.2133    0.0031    1.2
  0.80    0.3542    0.0010    1.0
  0.90    0.5438    0.0005    0.5
  1.00    0.7885    0.0000    0.0

*RTYPE *FRACTURE *CON  1
*RTYPE *MATRIX   *CON  2


**********************************************************************
** Initial Condition Section
**********************************************************************
*INITIAL
*VERTICAL *BLOCK_CENTER *WATER_OIL
*REFPRES  2305
*REFDEPTH 5000
*DWOC     5410
*PB       *MATRIX   *CON  0.0
*PB       *FRACTURE *CON  0.0

************************************************************
** Numerical Methods Control Section
************************************************************
*NUMERICAL
*MAXSTEPS    2999
NORM PRESS 500
NORM SATUR 0.1
AIM OFF

RUN
DATE 2014 1 1
DTWELL 1
*DTMAX  100.00
**$
```

```
WELL  'Well-1'
PRODUCER 'Well-1'
OPERATE  MIN  BHP  2215.  CONT
**$          rad  geofac  wfrac  skin
GEOMETRY  K  0.25  0.37  1.  0.
PERF  GEOA  'Well-1'
**$ UBA      ff  Status  Connection
    8 13 11   1.  OPEN    FLOW-TO  'SURFACE' REFLAYER
    9 13 11   1.  OPEN    FLOW-TO  1
    10 13 11   1.  OPEN    FLOW-TO  2
    11 13 11   1.  OPEN    FLOW-TO  3
    12 13 11   1.  OPEN    FLOW-TO  4
    13 13 11   1.  OPEN    FLOW-TO  5
    14 13 11   1.  OPEN    FLOW-TO  6
    15 13 11   1.  OPEN    FLOW-TO  7
    16 13 11   1.  OPEN    FLOW-TO  8
    17 13 11   1.  OPEN    FLOW-TO  9
    18 13 11   1.  OPEN    FLOW-TO  10
*AIMSET *FRACTURE *CON 1        ** Set all blocks implicit
*AIMSET *MATRIX   *CON 1

DATE 2014 1  31.00000
DATE 2014 3  2.00000
DATE 2014 4  1.00000
DATE 2014 5  1.00000
DATE 2014 5  31.00000
DATE 2014 6  30.00000
DATE 2014 7  30.00000
DATE 2014 8  29.00000
DATE 2014 9  28.00000
DATE 2014 10 28.00000
DATE 2015 2  5.00000
DATE 2015 5 16.00000
DATE 2015 8 24.00000
DATE 2015 12  2.00000
DATE 2016 3 11.00000
DATE 2016 6 19.00000
DATE 2016 9  27.00000
STOP
```

References

1. Al-Bulushi, N., Araujo, M., Kraaijveld, M., & Jing, X. D. 2007. Predicting Water Saturation Using Artificial Neural Networks. Society of Petrophysicists and Well-Log Analysts.
2. Alrumah, M. 2011. A Study on the Analysis of the Formation of High Water Saturation Zones around Well Perforations. Ph.D. dissertation. The Pennsylvania State University, University Park, Pennsylvania.
3. Anietie Ndarake Okon. 2012. Water Coning in a Fractured Reservoir: A Simulation Study. MS. Thesis. Norwegian University of Science and Technology.
4. Beale, M. H. 2014. Neural Network Toolbox User's Guide. October 2014. http://www.mathworks.com/help/pdf_doc/nnet/nnet_ug.pdf
5. Broomhead, D. S., Lowe, D., & ROYAL SIGNALS AND RADAR ESTABLISHMENT MALVERN (UNITED KINGDOM). 1988. Radial basis functions, multi-variable functional interpolation and adaptive networks.
6. Chaperon, I. 1986. Theoretical Study of Coning Toward Horizontal and Vertical Wells in Anisotropic Formations: Subcritical and Critical Rates. Presented at SPE Annual Technical Conference and Exhibition, 5-8 October, New Orleans. SPE-15377-MS. http://dx.doi.org/10.2118/15377-MS
7. Graupe, D. 2007. Principles of artificial neural networks. Hackensack, N.J; Singapore: World Scientific.
8. Joshi, S. D. 1991. Horizontal Well Technology. First edition. Tulsa, Ok: PennWell Corp.
9. Mohaghegh, S. 2000. Virtual-intelligence applications in petroleum engineering: Part I - artificial neural networks. Journal of Petroleum Technology, 52(9), 64-64.

10. Muskat, M., & Wycokoff, R. D. 1935. An Approximate Theory of Water-coning in Oil Production. SPE J. SPE-935144-G http://dx.doi.org/10.2118/935144-G
11. Mcewen, C. R. 1962. Material Balance Calculations with Water Influx in the Presence of Uncertainty in Pressures. SPE-J. SPE-225-PA http://dx.doi.org/10.2118/225-PA
12. Petri Hodju & Jokko Halme, 1999 Introduction, Neural Networks Information Homepage.1999 http://koti.mbnet.fi/~phodju/nenet/index.html
13. PetroWiki, 2014.Water and gas coning. October 30 2013. http://petrowiki.org/Water_and_gas_coning
14. Rosenblatt, F. 1958. The perceptron: A probabilistic model for information storage and organization in the brain. Psychological Review, 65(6), 386-408. doi:10.1037/h0042519
15. Saad, S. E.-D. M., Darwich, T. D., & Asaad, Y. (1995, January 1). Water Coning in Fractured Basement Reservoirs. Presented at Middle East Oil Show, 11-14 March, Bahrain. SPE-29808-MS. http://dx.doi.org/10.2118/29808-MS
16. Van Golf-Racht, T. D. 1994. Water-Coning in a Fractured Reservoir. Presented at SPE Annual Technical Conference and Exhibition, 25-28 September, New Orleans, Louisiana. SPE-28572-MS. http://dx.doi.org/10.2118/28572-MS
17. Warren, J.E. and Root, P.J. 1963. The Behavior of Naturally Fractured Reservoirs. SPE J. 3 (3): 245–255. SPE-426-PA. http://dx.doi.org/10.2118/426-PA
18. Yang, W., & Wattenbarger, R. A. 1991. Water Coning Calculations for Vertical and Horizontal Wells. Presented at SPE Annual Technical Conference and Exhibition, 6-9 October, Dallas, Texas. SPE-22931-MS. http://dx.doi.org/10.2118/22931-MS
19. Yegnanarayana, B. 1999. Artificial neural network. India: Prentice-Hall of India Pvt. Ltd.
20. Zhanshou, Yu. 2000. Feed-Forward Neural Networks and Their Applications in Forecasting. MS thesis. University of Houston, Houston, Texas.

Bibliography

1. Learnfast For Schools . (2014, 1 1). *The Science*. Retrieved from LEARNFAST: http://www.learnfastforschools.com.au/wp-content/uploads/2014/03/neuron-images.jpg
2. Creative Commons license. (2012, December 3). *Machine Learning: Introduction to the Artificial Neural Network*. Retrieved from DUROFY: http://www.durofy.com/machine-learning-introduction-to-the-artificial-neural-network/
3. Geology.com. (2015, April 2). *Horizontal Drilling & Directional Drilling: Natural Gas Wells*. Retrieved April 2, 2015, from Geology.com: News and Information for Geology & Earth Science: http://geology.com/articles/horizontal-drilling/
4. Joshi, S. (2001). *Horizontal Well Technology.* PennWell Corporatioin.
5. Joshi.S.D. (2011). *Horizontal Well Technology.* PennWell Pub. Co.
6. Teng, Y. (2014, March 9). *Thinking and Computing*. Retrieved from Training neural networks: back-propagation vs. genetic algorithms: http://thinkingandcomputing.com/2014/03/09/genetic-algorithms-neural-networks/
7. Warren, R. (1963). The Behavior of Naturally Fractured Reservoirs. *Society of Petroleum Engineers Journal*, 246.